RATIONAL DEVELOPMENT OF PROTEIN FORMULATIONS IN SOLID AND SOLUTION STATES

By

MAYA S. SALNIKOVA

M.S., University of Kansas, 2006

M.S., University of Iowa, 2004

B.S., Tashkent Pharmaceutical Institute, 2000

Submitted to the Department of Pharmaceutical Chemistry and the faculty of the Graduate School of the University of Kansas in partial fulfillment of the requirements for the degree of Doctor of Philosophy.

Dissertation Committee:

_____

Chairperson

_____

_____

_____

_____

Dissertation defended on June 4th, 2007

The Dissertation Committee for Maya S. Salnikova certifies that this is the approved version of the following dissertation:

RATIONAL DEVELOPMENT OF PROTEIN FORMULATIONS IN SOLID AND SOLUTION STATES

Dissertation Committee:

_____
Chairperson

_____

_____

_____

_____

Dissertation approved: June 4, 2007

ABSTRACT

Development of protein formulations in the solid and solution state involves stability studies during long-term storage (2-3 years). A long-term study of a protein under conditions leading to its rapid physical and chemical degradation often results in excessive use of resources and severe time constraints. To minimize these problems, a thorough preformulation study of protein behavior under different conditions is necessary. An in depth understanding of the properties of proteins in both the solution and solid state may subsequently result in selection of conditions leading to adequate stability during storage.

Preformulation studies of a protein in solution often involve a three step approach. In this method a protein is first characterized under a range of conditions (*e.g.* pH, temperature, *etc.*), and the data is then summarized in the form of an empirical phase diagram. This information is then used to design a high throughput screening approach to identify stabilizing compounds. This approach was employed for preformulation studies of vaccines against *Clostridium difficile* (*C. difficile*) - associated disease. Such vaccines contain formaldehyde treated toxoids A and B in free or adjuvant bound form. Studies of *C. difficile* toxins and toxoids under a range of conditions revealed a stabilizing effect of formaldehyde crosslinking on the thermal stability of the toxoids. Furthermore, screening for stabilizing compounds resulted in the identification of conditions and specific compounds that lead to enhanced thermal stability of free and bound to adjuvant toxoids.

Preformulation studies of proteins in the solid state usually involve characterization of an amorphous solid in general (*e.g.* moisture content, crystallinity, structural relaxation, *etc.*) and specific protein properties (*e.g.* extent of protein structure preservation). Unfortunately, these characteristics of the solid and protein cannot usually predict protein stability during storage. Therefore, a more in depth understanding of amorphous matrices is needed. To understand the role of interactions between protein and expient as well as the homogeneity of protein/excipient mixtures, a study of a model system containing human Growth Hormone (hGH) and sugars (sucrose and trehalose) was performed. This study revealed that the extent of protein/excipient interaction can be used to describe the degree of homogeneity of a lyophilized mixture which can be related to the cryo- and lyo- protecting properties of the excipients. Additionally, it was seen that the rate of structural relaxation is proportional to the rate of insoluble aggregate formation.

These studies of proteins in solution and the solid state allowed for the identification of conditions for long term stability studies of *C. difficile* vaccines and contributed to our understanding of the role of interactions between protein and excipient in lyophilized solids.

Dedicated to:

My mother,
Zinaida Nikolaevna Salnikova

and

My husband,
Dushyant B. Varshney

ACKNOWLEDGEMENTS

I would like to thank Professors J. Howard Rytting and C. Russell Middaugh, my research advisors, for their constant support and encouragement. Their guidance not only helped me to learn pharmaceutical chemistry but also elucidated its logical application in variety of projects. I consider myself very fortunate for the opportunity to work under their guidance. I appreciate Dr. Rytting's guidance in the lyophilization project. I admire his patience and wisdom. I thank Dr. Middaugh for giving me an opportunity to work on vaccine formulation project under his direct supervision. I cannot stop admiring his experiences and knowledge. Especially, I want to thank Dr. Middaugh for guiding me in my career choices.

I would like to extend my thanks to the past and present members of the Rytting and Middaugh research groups for their valuable advice and support. Specially, I would like to thank Sangeeta Joshi for her friendship, guidance, long discussions about my projects and endless support. I appreciate her guidance and collaborations on *C. difficile* projects.

I would like to thank Dr. Michel Warny from Acambis Inc. for the collaborations on the *C. difficile* project. I appreciate the opportunity to work and contribute in this project. Additionally, I acknowledge that Acambis Inc. provided material for the *C. difficile* studies as well as financial support for the project. I thank Genentech Inc. for providing human Growth Hormone used in lyophilization studies.

I thank Dr. Siahaan, Dr. Picking and Dr. Laurence, my dissertation committee members for their valuable comments and suggestions. Especially, I want to thank my dissertation readers Dr. Siahaan and Dr. Picking.

I want to extend my sincere thanks to all professors at the pharmaceutical chemistry department for providing an outstanding curriculum and for training students to face industrial challenges. I enjoyed each and every class I took at the department.

I thank past and present students and postdocs at the pharmaceutical chemistry department. I appreciate an opportunity to know them. I thank all staff at the department. Especially, I thank Nancy Helm for her ability to always listen and provide support, her encouragements and promptness.

Financial support for my graduate studies was provided by the pharmaceutical chemistry department, Siegfried Lindenbaum scholarship and Merck predoctoral fellowship.

Special thanks to my mother, Zinaida Salnikova, for giving me an example of dedication and strength. Her endless love and encouragements kept me motivated to achieve my goals and tought me not to give up. I would not have become the person that I am today without her presence in my life. I want to thank my husband, Dushyant Varshney, for his love, understanding, patience and never ending support.

With sincerest gratitude,

Maya

TABLE OF CONTENTS

Chapter 1: Introduction ……..1

1.1. Overview ……... 2

1.2. Formulation of proteins…….. 3

1.2.1. Vaccine formulations ……. 3

1.2.2. Solid protein formulations ……..… 9

1.3. Specific aims and chapters summaries ……...14

1.3.1. Physical characterization of *Clostridium difficile* toxins and toxoids - effect of formaldehyde crosslinking on thermal stability……....14

1.3.2. Preformulation studies of Clostridium difficile toxoids A and B…….16

1.3.3. Stability of Growth Hormone in lyophilized formulation - effect of protein-excipient interactions and molecular mobility…….……..……17

1.4. Bibliography ……..……..19

Chapter 2: Physical characterization of *Clostridium difficile* toxins and toxoids - effect of the formaldehyde crosslinking on thermal stability …....40

2.1. Introduction ……..… 41

2.2. Experimental methods ……43

2.2.1. Materials ……43

2.2.2. Characterization of physical stability ……43

2.2.2.1. Sample preparation ……43

2.2.2.2 High-resolution UV absorbance spectroscopy ……..44

2.2.2.3. Far-UV Circular Dichroism Spectroscopy ……45

2.2.2.4. Intrinsic Trp fluorescence spectroscopy ……45

2.2.2.5. ANS fluorescence spectroscopy ……46

2.2.2.6. Dynamic Light Scattering ……..46

2.2.2.7. Empirical phase diagrams ……..47

2.3. Results ……48

2.3.1 High-resolution UV absorbance spectroscopy ……..48

2.3.2. Far-UV Circular Dichroism Spectroscopy ……51

2.3.3. Intrinsic Trp fluorescence spectroscopy ……53

2.3.4. ANS fluorescence spectroscopy ……54

2.3.5. Dynamic Light Scattering ……..55

2.3.6. Empirical phase diagrams ……...55

2.4. Discussion ……...57

2.5. Conclusion ……60

2.5. Bibliography ……...61

Chapter 3: Preformulation studies of *Clostridium difficile* toxoids A and B…82

3.1. Introduction …… 83

3.2. Experimental methods ……84

3.2.1. Materials …….. 84

3.2.2. Excipient screening studies ……...85

3.2.2.1. Aggregation assay ……... 85

3.2.2.2. Structural stability studies ……86

3.2.2.2.1. Far-UV Circular Dichroism Spectroscopy ……..86

3.2.2.2.2. ANS fluorescence spectroscopy ……..….... 87

3.2.2.2.3. High-resolution UV absorbance spectroscopy ….87

3.2.2.2.4. Dynamic Light Scattering ……....……87

3.2.2.2.5. Differential Scanning Calorimetry …..…….88

3.2.2.2.6. Agitation studies ……..…….88

3.2.3. Adjuvant studies ……89

3.2.3.1. Adsorption to aluminum hydroxide ……..….89

3.2.3.2. Desorption of toxoids from Alhydrogel® ……...89

3.2.3.3. Stability of toxoids bound to Alhydrogel® …….90

3.3. Results and discussion …….…..…90

3.3.1. Excipient screening studies …….…….90

3.3.1.1. Agitation studies ….…….…….95

3.2.3. Adjuvant studies …….…….95

3.4. Conclusions …….……..96

3.5. Bibliography …….…….97

Chapter 4: Stability of human growth hormone in lyophilized formulations – The effect of protein-excipient interactions and molecular mobility …….…….116

4.1. Introduction ……..117

4.2. Experimental methods …….....118

4.2.1. Materials ……118

4.2.1.1. Lyophilization procedure ……...119

4.2.2. Extent of protein-excipient interactions ……..120

4.2.2.1. Isoperibol solution calorimetry ……..120

4.2.2.2. Water sorption analysis …….….121

4.2.2.3. Differential scanning calorimetry ……...121

4.2.2.4. Fourier Transform Infrared Spectroscopy …….…..122

4.2.3. Conformational characterization of freeze-dried protein …. 123

4.2.4. Structural mobility measurements …… 124

4.2.5. Stability studies ……..… 125

4.2.6. Studies of solution protein formulations before lyophilization……126

4.2.6.1. High-resolution UV absorbance spectroscopy …….....126

4.2.6.2. Dynamic Light Scattering ……...……...126

4.2.6.3. Differential Scanning Calorimetry …….126

4.3. Results and discussion ……..……..127

4.3.1. Extent of protein-excipient interactions ……...127

4.3.2. Structural mobility measurements ……..……..…129

4.3.3. Conformational characterization of freeze-dried protein … 129

4.3.4. Stability studies …….……...….130

4.3.4. Studies of solution protein formulations before lyophilization……130

4.4.Summary and conclusions ……...…….131

4.5. Bibliography …….133

Chapter 5: Summary, conclusions and future directions ……...148

5.1. Solution protein formulations ……...149

5.1.1. Summary and conclusions ……....….149

5.1.2. Future directions …….……..……..155

5.2. Solid protein formulations ……..…..……157

5.2.1. Summary and conclusions ……...…157

5.2.2. Future directions ……....…159

5.3. Bibliography ……...……..161

INDEX OF FIGURES

Figure	Page	Caption
1.1	34	*Clostridium difficile* endospores (from reference 47).
1.2	35	Structure of *C. difficile* toxins A and B. Toxins A and B consist of three major domains: N-terminus (responsible for enzymatic activity), C-terminus (involved in receptor binding) and middle part (potentially involved in the translocation of the toxin into the cytosol). (from reference 58)
1.3	36	Model of the uptake of *C. difficile* toxins. The uptake of the toxins involves binding to receptors on the surface of target cells, subsequent endocytocis, cleavage of N-terminal catalytic domain with subsequent translocation from an acidic endosomal compartment into the cytosol. In the cytosol, the toxins glucosylate Rho proteins by using UDP-glucose as a cosubstrate. (from reference 63)
1.4	37	Stereoview of the N-terminal catalytic portion of toxin B. Structure is depicted as a ribbon plot with α-helices and ß-strands. (from reference 64)
1.5	38	Stereoview of solenoid structure of C-therminal domain of toxin A. (A) ribbon representation and (B) schematic representation with rectangles. (from reference 59)
2.1	68	Second derivative near-UV absorbance spectrum for toxin/toxoid A and B at 10°C.

2.2	69	Shifts in second derivative UV absorption peak position as a function of temperature for toxin A (a) and toxoid A (b) at pH 5.5 (□), 6.0 (■), 6.5 (○), 7.0 (●), 7.5 (Δ), 8.0 (▲).The figures represent the following negative peaks: (1) 260 nm, Phe; (2) 266 nm, Phe/Tyr; (3) 277 nm, Tyr; (4) 285 nm, Tyr/Trp; (5) 293 nm, Trp. The thermal traces represent an average of two measurements, where each data point had standard error of less than 0.5. Peak position scale was adjusted to reflect the changes.
2.3	70	Shifts in second derivative UV absorption peak position as a function of temperature for toxin B (a) and toxoid B (b) at pH 5.0 (□), 5.5 (■), 6.0 (○), 6.5 (●), 7.0 (Δ), 7.5 (▲).The figures represent the following negative peaks: (1) 260 nm, Phe; (2) 266 nm, Phe/Tyr; (3) 277 nm, Tyr; (4) 285 nm, Tyr/Trp; (5) 293 nm, Trp. The thermal traces represent an average of two measurements, where each data point had standard error of less than 0.5. Peak position scale was adjusted to reflect the changes.
2.4	71	High resolution second derivative near UV spectroscopy peak positions based empirical phase diagrams for toxin/toxoid A and toxin/toxoid B (the data for the corresponding toxin and toxoid was normalized simultaneously).
2.5	72	Traces of optical density at 350 nm as a function of temperature for toxin A (a) and toxoid A (b) at pH 5.5 (□), 6.0 (■), 6.5 (○), 7.0 (●), 7.5 (Δ), 8.0 (▲); and toxin B (c) and toxoid B (d) at pH 5.0 (□), 5.5 (■), 6.0 (○), 6.5 (●), 7.0 (Δ), 7.5 (▲).The thermal traces represent an average of two measurements, where each data point had standard error of less than 0.05. Onset of precipitation (e), where the temperature is encoded by rhomb for toxin A, filled rhomb for toxoid A, square for toxin B and filled square for toxoid B.
2.6	73	CD spectra at 10°C for toxin A (a) and toxoid A (b) at pH 5.5 (□), 6.0 (■), 6.5 (○), 7.0 (●), 7.5 (Δ), 8.0 (▲); and toxin B (c) and toxoid B (d) at pH 5.0 (□), 5.5 (■), 6.0 (○), 6.5 (●), 7.0 (Δ), 7.5 (▲).The thermal traces represent an average of two measurements, where each data point had standard error of less than 0.05.

2.7	74	CD trace at 208 nm over the temperature range for toxin A (a) and toxoid A (b) at pH 5.5 (□), 6.0 (■), 6.5 (○), 7.0 (●), 7.5 (Δ), 8.0 (▲); and toxin B (c) and toxoid B (d) at pH 5.0 (□), 5.5 (■), 6.0 (○), 6.5 (●), 7.0 (Δ), 7.5 (▲).The thermal traces represent an average of two measurements, where each data point had standard error of less than 0.25. Midpoints of thermal transitions (e), where the temperature is encoded by rhomb for toxin A, filled rhomb for toxoid A, square for toxin B and filled square for toxoid B.
2.8	75	CD spectra at 10°C for toxin B (a) and toxoid B (b) at pH 7.0: before melt (□), after melt (■). Each spectrum represents an average of two measurements, where each data point had standard error of less than 0.05.
2.9	76	Trp fluorescence as a function of temperature: (a-d) normalized emission peak intensity change and (e-h) emission peak position change for toxin A (a,e) and toxoid A (b,f) at pH 5.5 (□), 6.0 (■), 6.5 (○), 7.0 (●), 7.5 (Δ), 8.0 (▲); and toxin B (c,g) and toxoid B (d,h) at pH 5.0 (□), 5.5 (■), 6.0 (○), 6.5 (●), 7.0 (Δ), 7.5 (▲). The thermal traces represent an average of two measurements, where each data point had standard error of less than 0.5.
2.10	77	ANS fluorescence as a function of temperature: (a-d) emission peak intensity change and (e-h) emission peak position change for toxin A (a,e) and toxoid A (b,f) at pH 5.5 (□), 6.0 (■), 6.5 (○), 7.0 (●), 7.5 (Δ), 8.0 (▲); and toxin B (c,g) and toxoid B (d,h) at pH 5.0 (□), 5.5 (■), 6.0 (○), 6.5 (●), 7.0 (Δ), 7.5 (▲). The thermal traces represent an average of two measurements where each data point has standard error of less than 0.5. Onsets of thermal transitions (i), where the temperature is encoded by rhomb for toxin A, filled rhomb for toxoid A, square for toxin B and filled square for toxoid B.
2.11	78	Hydrodynamic diameter as a function of temperature: for toxin A (a), toxoid A (b), toxin B (c) and toxoid B (d); MSD Number based(■) and Lognormal Number based (◊). The thermal traces represent an average of two measurements where each data point has standard error of less than 1.0. Note that in figure A and B sizes estimated above 1000 nm are not reliable.

2.12	79	Empirical phase diagram created using OD 350, Trp and ANS fluorescence, and CD data for toxins/toxoids A and B (p.unfolded stands for partially unfolded). Data was normalized simultaneously for the corresponding toxin and toxoid.
3.1	101	Studies of solute effects on the structural stability of toxoid A (x) in presence of 20% trehalose (□), 20% sucrose (■), 10% sorbitol (○), 10% dextrose (●), 20% glycerol (Δ), 0.05% tween 80 (▲), 0.1% pluronic F68 (◊): (a) CD signal at 208 nm; (c) ANS emission intensity (d) ANS emission peak position and (b) DSC thermogram. The thermal traces represent an average of 2 measurements, where each data point had a standard error of less than 0.5.
3.2	102	Studies of solute effects on the structural stability of toxoid B (x) in presence of 20% trehalose (□), 20% sucrose (■), 10% sorbitol (○), 10% dextrose (●), 20% glycerol (Δ), 0.05% tween 80 (▲), 0.1% pluronic F68 (◊): (a) CD signal at 208 nm; (c) ANS emission intensity (d) ANS emission peak position and (b) DSC thermograms. The thermal traces represent an average of 2 measurements. Each data point had a standard error of less than 0.5.
3.3	103	Studies of the effect of combinations of solutes on the thermal stability of toxoid A (x) in presence of 10% sorbitol and 0.05% tween 80 (□), 10% dextrose and 0.05% tween 80 (■), 10% sorbitol, 10% dextrose and 0.05% tween 80 (○), 10% dextrose and 10% sorbitol (●): (a) monitored by the CD signal at 208 nm and (b) OD 350 nm. The thermal traces represent an average of 2 measurements, in which each data point had a standard error of less than 0.05.
3.4	104	Studies of combinations of solutes and their effect on the thermal stability of toxoid B (x) in presence of 10% sorbitol and 0.05% tween 80 (□), 10% dextrose and 0.05% tween 80 (■), 10% sorbitol, 10% dextrose and 0.05% tween 80 (○), 10% dextrose and 10% sorbitol (●): (a) monitored by CD signal at 208 nm and (b) OD 350 nm. The thermal traces represent an average of 2 measurements, where each data point had standard error of less than 0.05.

3.5	105	Studies of the properties of the tween 80 (□) in presence of 10% dextrose (■), 10% sorbitol (○), 10% dextrose and 10% sorbitol (●) as a function of temperature: 208 nm CD signal of 0.05% tween 80 (a) and 0.1% tween 80 (b); OD 350 nm for 0.05% tween 80 (c) and 0.1% tween 80 (d); hydrodynamic diameter MSD Number based (filled square) and Lognormal Number based (filled rhomb) for 0.05% tween 80 (e) and 0.1% tween 80 (f). Sizes of > 1μm are not accurate given the nature of DLS measurements. The thermal traces represent an average of 2 measurements, where each data point had standard error of less than 0.5.
3.6	106	Studies of the effect of solute concentration on the midpoint of the thermal transition (Tm) monitored with CD 208 nm signal for toxoid A (a) and toxoid B (b) in presence of sorbitol and 0.05% tween 80 (♦), dextrose and 0.05% tween 80 (■), sorbitol, dextrose and 0.05% tween 80 (▲), sorbitol, dextrose and 0.1% tween 80 (x), sorbitol and dextrose (◊).
3.7	107	The hydrodynamic diameter as a function of temperature for toxoid A (a-c) and toxoid B (d-f) where the filled squares represent MSD number based diameter and filled rhomboids represent the lognormal number based diameter. Sizes of > 1 μm are not accurate given the nature of DLS measurements. (a,d) protein alone; (b,e) protein in presence of 10% sorbitol and 10% dextrose; (c,f) protein in presence of 10% sorbitol, 10% dextrose and 0.05% tween 80. The thermal traces represent an average of 2 measurements, where each data point had a standard error of less than 0.5.
3.8	108	Alhydrogel® binding studies: (a) sorption isotherm and (b) desorption isotherm in presence of 2M NaCl for toxoid A (◊) and toxoid B (▲).
4.1	137	Tg values of colyophilized a) hGH/sucrose, and b) hGH/trehalose formulations as a function of composition. Measured Tg values are represented as symbols and the prediction by Gordon-Taylor equation is represented by the dotted line. Each measurement was conducted in duplicate and has a s.d. of 0.5.
4.2	138	Enthalpy of dissolution for colyophilized (dark bars) and physical (white bars) mixtures of hGH in the presence of sugars.

4.3	139	WSA-based interaction parameters for colyophilized hGH/sucrose (■) and hGH/trehalose (♦) mixtures as a function of RH.
4.4	140	Second derivative amide I FTIR spectra of native hGH in solution (1), hGH in a lyophilized formulation with sucrose (2), trehalose (3) and dried protein alone (4).
4.5	141	The kinetics of hGH deamidation in lyophilized formulations containing hGH alone (▲ and dotted line), hGH with sucrose (♦ and solid black line) and hGH with trehalose (■and solid grey line).
4.6	142	The kinetics of soluble aggregate formation in lyophilized formulations containing hGH alone (▲and dotted line), hGH with sucrose (♦ and solid black line) and hGH with trehalose (■ and solid grey line).
4.7	143	The kinetics of insoluble aggregate formation in lyophilized mixtures containing hGH with sucrose (♦ and solid black line) and hGH with trehalose (■ and solid grey line).

INDEX OF SCHEMES

Scheme	Page	Caption
1.1	39	Crosslinking of side chains containing primary amines with formaldehyde to form methylene bridges.

INDEX OF TABLES

Table	Page	Caption
2.1	80	Secondary structure assignment with DICHROWEB (estimated error is ±2-3%). Note that CD measurements were performed on protein in 5 mM sodium phosphate buffer pH 7.0. *Assignment of secondary structure in previously heated protein.
2.2	81	Lognormal Number based mean hydrodynamic diameter and polydispersity for toxins/toxoids A and B.
3.1	109	Effect of GRAS excipients on toxoid A aggregation. Compounds which delay/prevent aggregation have positive % of aggregation inhibition values; compounds which induce aggregation have negative % of aggregation inhibition values.
3.2	110	Effect of GRAS excipients on toxoid B aggregation. Compounds which delay/prevent aggregation have positive % of aggregation inhibition values; compounds which induce aggregation have negative % of aggregation inhibition values.
3.3	111	Effect of solutes (detergents) on the thermal stability of toxoid A and B. The thermal stability (Tm) was monitored by DSC. The Tm is the temperature corresponding to the maximum peak position of the thermal transition.
3.4	112	Effect of excipients on the toxoid A midpoint of the thermal transition temperature (Tm). The thermal transition was monitored by the CD signal at 208 nm as a function of temperature. Each measurement was conducted in duplicate and has ~0.5°C of uncertainty.
3.5	113	Effect of excipients on the toxoid B midpoint of thermal transition temperature (Tm). The thermal transition was monitored by the CD signal at 208 nm as a function of temperature. Each measurement was conducted in duplicate and has ~0.5°C of uncertainty.

3.6	114	Thermal stability of toxoid A bound to Alhydrogel in the presence and absence of excipient(s) (unless specified otherwise). The thermal stability (Tm) was monitored by DSC, with the Tm indicating the temperature corresponding to the peak position of the thermal transition. The percent of toxoid bound to adjuvant was measured in each condition with an uncertainty of 1%. Each condition was studied in duplicate.
3.7	115	The thermal stability of toxoid B bound to Alhydrogel in the presence and absence of solute(s) (unless specified otherwise). The thermal stability (Tm) was monitored by DSC. The Tm indicates the temperature corresponding to the peak position of the thermal transition. The percent of protein bound to adjuvant was measured under each condition with an uncertainty of 1%. Each condition was studied in duplicate.
4.1	144	Predicted and actual moisture content for hGH/excipient formulations. The prediction of moisture content was based on the area of the carboxilate band at 1580 cm^{-1} from FTIR measurements.
4.2	145	Degradation rate constants for lyophilized hGH formulations.
4.3	146	Percent insoluble aggregate formed immediately after lyophilization and after 28 weeks of storage at 50°C.
4.4	147	Midpoint transition temperature (Tm) for hGH in solutions with and without sugar. The Tm was monitored with solution DSC. The midpoint of the temperature of thermal aggregation was monitored by the OD at 350 nm.

LIST OF ABBREVIATIONS

ANS	8-Anilino-1-naphthalene sulfonate
ATR	Attenuated total reflectance
CD	Circular Dichroism
DSC	Differential scanning calorimetry
FTIR	Fourier transform infrared spectroscopy
GRAS	Generally regarded as safe
h	Hour(s)
HPLC	High performance liquid chromatography
min	Minute(s)
MOPS	3-(N-morpholino)propanesulfonic acid
MW	Molecular weight
OD 350 nm	Optical density at 350 nm
Phe	Phenylalanine
pI	Isoelectric point
PTI	Photon technology International
s	Second(s)
s.d.	Standard deviation
SEC	Size exclusion chromatography
Tm	Thermal transition temperature
Trp	Tryptophan
Tyr	Tyrosine

UV	Ultraviolet
Vis	Visible

Chapter 1:

Introduction.

1.1. Overview

The role of biopharmaceuticals containing proteins and nucleic acids in the treatment of various chronic and severe diseases, as well as in preventing infectious diseases, is growing rapidly. Currently, over 350 biopharmaceuticals are in clinical trials.[1] Unfortunately, biotechnology-based approaches suffer drawbacks due to the unique characteristics of biomolecules which lead to their decreased stability during storage. For example, proteins usually have well defined secondary and tertiary structure, preservation of which is typically required for biological activity. Moreover, the loss of native characteristics, *i.e.* unfolding of proteins due to physical (*e.g.* aggregation) and chemical (*e.g.* deamidation, oxidation and isomerization) degradation during storage, can lead to immunogenicity and toxicity, as well as loss of potency.[2-4] Thus, the development of biopharmaceuticals still remains a challenge and requires an in depth understanding of protein behavior in solution and solid states to achieve stable products.

The studies described here are directed towards preformulation of a *Clostridium difficile* vaccine in solution state and an investigation of the role of protein-excipient interactions on the stability of lyophilized protein formulations.

1.2. Formulation of proteins

1.2.1. Vaccine formulations

Infectious diseases play a tremendous effect on survival of individuals, groups and nations throughout the human history. Increased human population and domestication of cattle led to adaptation of some of the animal pathogens to humans and ultimately increase of human pathogens. For example, the animal-originated pathogens include smallpox, influenza, tuberculosis, malaria, plague, measles and cholera. Human pathogens are divided into four classes which include bacteria, viruses, parasites and fungi. Among these pathogens viruses and bacteria are the most prominent as they lead to various diseases including cancer.[5-9]

To prevent infectious diseases more than 70 vaccines have been developed. Most of these vaccines contain live attenuated organisms, inactivated / killed whole organisms, subunit conjugates and inactivated toxins (toxoids).[6] Live attenuated vaccines (*e. g.* polio, yellow fever, measles, mumps, rubella, varicella, rotavirus, CA influenza, *salmonella typhi*, *vibrio cholerae* and adenovirus) are obtained by one of the four available approaches.[5,10] These approaches involve usage of natural pathogens from another mammal, passage of wild-type viruses in tissue culture until virulence is greatly reduced, usage of mutants that are able to grow only at low temperatures (cold-adapted strains) and selective deletion or inactivation of genes in bacteria.[5,10-14] Vaccines containing inactivated / killed whole organisms (*e.g.* polio,

rabies, Japanese encephalitis, hepatitis A and *bacilus antracis*) are obtained by inactivation of organisms which leads to their death and loss of infectivity. Subunit and conjugate vaccines (hepatitis B, *salmonella typhi*) contain polysaccharides, proteins or polysaccharide/protein conjugates which represent epitopes on the organism's surface.[5,15-17]

Many pathogenic bacteria produce toxins that are responsible for various diseases such as botulism, diphtheria and etc. There are two types of bacterial toxins: the lipopolysaccharides (endotoxins) and proteins (exotoxins). Lipopolysaccharides are usually associated with bacterial cell walls, whereas proteins are often released from bacteria during their exponential growth. The exotoxins may act at sites removed from the site of bacterial growth. Some exotoxins (tetanus, *shigella* neurotoxin and diphtheria) are considered to be very powerful and potent human poisons that can lead to lethality comparable to snake venom.[18]

Treatment of the toxins with formaldehyde leads to reaction with the N-terminal amino acid residues and the side chains of arginine, cysteine, histidine and lysine residues, and the subsequent formation of methylol groups and Schiff-bases as well as intramolecular methylene bridges with amine, phenol, imidazole or indole groups.[19-25] The reaction of formaldehyde with primary amine-containing side chains is represented in Scheme 1. The intramolecular crosslinking of toxins with formaldehyde leads to their complete inactivation with at least partial retention of their immunogenicity. In addition, the crosslinking may result in changes in the toxin's shape and overall stabilization of their structure.[26-29]

Live vaccines are usually very effective, however, they carry a risk of reverting to virulent forms and subsequent disease in patients. On the other hand, killed organisms and toxoids are safer, but they typically produce weaker immune responses and require multiple doses.[5-11] The immunogenicity of vaccines is usually increased by introducing adjuvants to the formulation. Adjuvants, typically aluminum-containing salts, tend to adsorb antigens and lead to higher immune responses through a variety of still poorly understood mechanisms.[30-33]

To be effective as vaccines, antigens must be stable during storage. Most vaccine instability and failure to initiate immune responses originates from physical and chemical degradation.[34-38] Thus, studies directed towards characterization of antigens under different conditions and screening for stabilizing compounds is of a great importance and in many cases is a central key to the development of an effective vaccine.

A systematic approach to preformulation development has been initiated in our group. The approach consists of the following consecutive steps: biophysical characterization of protein/virus under different conditions (*e.g.* pH, temperature, concentration, ionic strength and *etc*), visualization of the data in the form of an empirical phase diagram and screening for stabilizing compounds. Identification of the condition(s) leading to natively-folded protein as well as stabilizing compound(s) allows rapid selection of formulation(s) for accelerated and long-term stability studies. This approach has been applied in several protein and viral systems and has been shown to be very effective.[35,39-48]

The approach described above was utilized for preformulation studies of a proposed *Clostridium difficile* (*C. difficile*) vaccines. *C. difficile* vaccines contain toxoids A and B, which are derived from corresponding toxins by crosslinking with formaldehyde.

C. difficile is a gram-positive, endospore forming, rod-shaped bacterium (Figure 1).[18] *C. difficile* has more than 150 ribotypes, 24 toxinotypes and produces two large toxins designated A (308 kDa, 2,710 amino acids) and B (260 kDa, 2,366 amino acids). The toxins are responsible for *C. difficile*-associated disease (CDAD), which manifests itself as nosocomial diarrhea and pseudomembranous colitis.[49-53] Emerging strains of *C. difficile* lead to severe CDAD outbreaks in North America and Europe and therefore require preventive vaccination.[51]

C. difficile toxins A and B exhibit 49% amino acid identity and belong to the large clostrodial cytotoxin (LCT) family, which includes the *Clostridium sordelii* toxins and *Clostridium novyi* alpha toxin. Toxins A and B possess high molecular weight, an N-terminal enzymatic domain (*e.g.* residues 1-543), a central hydrophobic region (*e.g.* residues 900-1,200) and a C-terminal domain carrying carbohydrate recognition sequence repeats (*e.g.* residues 1,750-2,710 or 2,366).[51,54-58] A schematic representation of toxins' structure is illustrated in Figure 2 (adapted from reference 58). It is thought that the C-terminal part binds to cell surface carbohydrate containing receptors which leads to endocytosis of the toxin.[59,60] The central hydrophobic region then undergoes pH-induced conformational changes, which mediate formation of pores and translocation of the amino-terminal fragment from

early endosomes to the cytoplasm.[61-63] In the cytosol, the N-terminal enzymatic fragment catalyzes glycosylation of Rho/Ras proteins at Thr37/35, which leads to shutdown of essential cellular processes.[59,64] The proposed mechanism of toxins' action is represented in Figure 3 (please note that the model was adapted from reference 63). The structure of the N-terminal domain of toxin B (Figure 4, adapted from reference 64) and the C-terminus domain of toxin A (Figure 5, adapted from reference 59) are well characterized although the complete structure of the toxins is not yet available. The role of the hydrophobic region is especially poorly understood.[64] The N-terminal catalytic portion of toxin B consists of 543 residues, which are arranged in a mixed α/ß-structure of 11 ß-strands in the core and 21 α-helices on the periphery.[65] The 39 repeats in the C-terminal domain (960 residues) from toxin A are arranged in the form of a ß-selenoid fold.[60] The toxins possess differences in structure as well as in degree of the enzymatic activity. The cell-surface carbohydrate receptor binding C-terminal domain in toxin A contains 39 repeats (861 residues) whereas toxin B has 19 repeats (515 residues). It was observed that only toxin A is capable of entering into enterocytes in animals while both toxins are enterotoxic in humans. In addition, the enzymatic activity of toxin B is approximately 100-fold greater than that for toxin A.[58]

Unfortunately, treatment of CDAD with antimicrobial agents (metrnidazole and vancomycin) leads to recurrence of the disease.[66-68] To induce immunity against CDAD a vaccination employing the administration of formaldehyde crosslinked (inactivated) toxoids A and B is envisioned, and the formulation of a stable vaccine is

required.[69,70,71-74] The preformulation studies of *C. difficile* toxins and toxoids conducted in our study can potentially assist in the development of a commercial vaccine.

1.2.2. Solid protein formulations

To achieve stability of biopharmaceuticals in solution, various additives (*i.e.* excipients) have been employed. It has been found that in solution, excipients can stabilize the native structure of proteins by preferential exclusion. The preferential hydration of a protein in presence of certain compounds increases the chemical potential of the system and forces the protein to attain compactly folded state(s).[75,76]

Simple empirical testing of well established stabilizers is often, however, not adequate. For many proteins, it remains a challenge to find appropriate conditions for stabilization and improvement of a shelf life. To overcome these difficulties, lyophilization (freeze-drying) and spray-drying methods have provided alternatives to solution stabilized proteins. An optimal shelf life of 18-24 months can often be achieved by these methods. To protect proteins during the process of lyophilization (freezing, primary and secondary drying) and spray-drying, a variety of different excipients have been employed.[77,78]

There are two main proposed mechanisms, which attempt to explain the protection of proteins by certain compounds during lyophilization and subsequent storage. According to the "vitrification" (kinetic) theory, excipients form rigid glassy matrices, which slow down internal macromolecular motions thus providing reduced chemical reactivity and physical changes.[79] The "water substitution" (thermodynamic) hypothesis suggests that the excipients replace water during drying by hydrogen bonding to the protein, which leads to the stabilization of protein

secondary structure.[80] Numerous empirical observations have shown that neither of the above theories can explain the behavior of protein in solid formulation by themselves. Although degradation of a protein in lyophilized formulation (containing excipients) is significantly decreased compared to solution formulation, the protein in a lyophilized state still has a tendency to degrade physically (e.g. aggregation, unfolding) and chemically (*e.g.* deamidation, oxidation) during long term storage.[77,78,81-83]

To better understand the characteristics of lyophilized formulation that influence stability of a protein, amorphous matrices are studied in a great detail. Amorphous matrices (glasses) are very complex in nature as they possess characteristics of a solid and a liquid at the same time. Amorphous solids are unordered like liquids and have high viscosity like solids.[84] Amorphous solids are metastable (possess high free energy) and therefore have increased molecular mobility of the matrix compared to crystals. The high mobility (structural relaxation) of matrix is related to its tendency to attain more compact state with lower free energy over the storage (annealing).[85,86] Molecular mobility of components in amorphous matrix can be described by long range (translation and rotation) and short range (vibration) motions. The long range movements are called α-motions whereas short range movements are often referred as ß-motions.[87] Additionally, proteins in solution and solid state demonstrate numerous molecular motions by themselves. The motions can be categorized as small-scale molecular vibrations, local rotations of individual side chains and large scale motions of entire protein.[88-91] The mixture

containing protein and excipient represents "molecular dispersion" or "solid solution".[92] Complex interplay between the properties of amorphous matrix such as mobility of components in a mixture, local motions of protein alone and stability of protein during storage is still unclear and remains under investigation.[93-95]

The indirect assessment of strength of an amorphous matrix can be performed with differential scanning calorimetry (DSC) which measures temperature at which rigid "glassy" state of an amorphous solid transforms into flexible "rubbery" state. This temperature is called a glass transition temperature (Tg) and is usually related to stability of the protein in amorphous matrix. It is believed that if protein formulation is stored at temperature which is 50°C below the Tg, then the formulation will have higher stability during storage. This estimation of optimum storage temperature by this approach is often accurate, however, it can not allow prediction of protein stability during storage at different temperatures.[96] Alternatively, indirect measurements of structural relaxation times of an amorphous matrix can be performed by variety of techniques such as DSC, dielectric relaxation spectroscopy (DRS), thermostimulated current (TSC), isothermal microcalorimetry, thermomechanical analysis (TMA), neutron scattering and solid state NMR.[80] Estimated, employing DSC and TAM measurements, time of structural relaxation at different temperatures has shown to be useful in prediction of protein stability at different temperatures for some proteins.[81] However, the predicted with DSC and TAM measurements structural relaxation time describes mostly α-motions and may not always be related to protein stability during storage.[97] An attempt to relate ß-

motions that are measured by employing neutron scattering has shown to be effective in predicting preservation of protein activity during storage.[87,98] On the other hand, for some protein formulations a preservation of protein native structure in solid state is a better parameter for describing protein stability during storage.[97,99]

It was hypothesized that interactions between protein and excipient play an important role not only in protection of protein from lyophilization induced stresses (e.g. cold induced and drying induced denaturation) but also play a significant role in stabilization of protein during storage.[80] The protein/excipient interactions can be measured with variety of techniques such as isoperibol solution calorimetry (ISC), water sorption analysis (WSA), differential scanning calorimetry (DSC) and Fourier transform infrared spectroscopy (FTIR).[92,96,100-104] Recent studies of lyophilized protein formulations have demonstrated that excipients that are able to more extensively hydrogen bond (H-bond) with proteins do, in fact, enhance protein stability.[100] Excipients usually H-bond to proteins during secondary drying which leads to the preservation of protein structure through favorable solute/protein surface interactions. This, in turn, leads to enhanced stability during long term storage.[105] Although studies have shown that some H-bonding excipients (*e.g.* sucrose) produce better protein stability than others (*e.g.* trehalose),[106] there has been no systematic study of any protein that establishes a direct relationship between the magnitude of such protein-excipient interactions (e.g. homogeneity of mixture) and the stability of proteins.

Understanding of such relationships that are characteristic of amorphous matrices and the stability of proteins in solid formulations are the primary focus of a major aspect of this work.

1.3. Specific aims and chapters summaries

1.3.1. Physical characterization of Clostridium difficile toxins and toxoids - effect of formaldehyde crosslinking on thermal stability

The specific aims of Chapter 2 involve the biophysical characterization of *C. difficile* toxins and toxoids and investigation of the effect of formaldehyde crosslinking on toxoids' thermal stability.

Nosocomial diarrhea and pseudomembranous colitis causing toxins A and B from *Clostridium difficile* were studied at pH 5-8 and over the temperature range of 10-85°C. The proteins were crosslinked with formaldehyde to inactivate them to toxoid forms and permit their use as vaccines. Structural changes and aggregation behavior were monitored using circular dichroism, intrinsic and extrinsic (ANS) fluorescence spectroscopy, turbidity measurements, high resolution UV absorbance spectroscopy and dynamic light scattering. The combined results were then summarized in empirical phase diagrams. Toxins A and B had similar secondary structure with a combination of helical, ß-sheet and unordered character and were partially unfolded at pH 5-5.5. Upon heating, toxin A at all pH values partially unfolded at ~45°C and formed insoluble aggregates at ~50°C. Toxin B partially unfolded at ~40°C, and upon heating to ~50°C precipitated at pH 5.0-6.0 and formed soluble aggregates at pH 6.5-7.5. The thermal stability of the toxins was pH

dependent with the proteins more thermally stable at higher pH. Similar studies of formaldehyde crosslinked toxoids A and B revealed enhanced thermal stability, in which secondary and tertiary structure changes, as well aggregation, were delayed by about 10°C. These studies reveal both similarities and differences between *C. difficile* toxins A and B and demonstrate the stabilizing effect of formaldehyde crosslinking on the thermal stability of their corresponding toxoids.

1.3.2. Preformulation studies of Clostridium difficile toxoids A and B

The specific aim of Chapter 3 is directed toward identification of stabilizing compound(s) of free and adjuvant bound C. *difficile* toxoids.

To enhance the physical stability of *Clostridium difficile* toxoids A and B, screening for stabilizing compounds was performed. The screening of 30 GRAS compounds at various concentrations and in several combinations was performed in two parts. First, a high-throughput aggregation assay was used to screen for compounds that delayed or prevented aggregation of toxoids under stress conditions (toxoids at pH 5-5.5 were incubated at 55°C for 55 or 75 min). Compounds which stabilized both proteins were further studied for their ability to delay unfolding under conditions leading to a presumably native-like folded state (pH 6.5). The thermal stability of the toxoids on the surface of Alhydrogel® was monitored with DSC and also showed significant improvement in the presence of certain excipients. In conclusion, this study has generated information concerning the free and adjuvant bound toxoids behavior under a range of conditions (temperature, solutes) that can be used to design pharmaceutical formulations of enhanced physical stability.

1.3.3. Stability of Growth Hormone in lyophilized formulations - effect of protein-excipient interactions and molecular mobility

The specific aim of Chapter 4 is to understand the relationship between the extent of protein-excipient interactions, structural relaxation of amorphous matrix and physico-chemical stability of a protein.

For this human Growth Hormone (hGH) was lyophilized with sucrose and trehalose in a 1:2 weight ratio. Potential protein-excipient interactions were analyzed immediately after lyophilization with Isoperibol Solution Calorimetry, Water Sorption Analysis, Differential Scanning Calorimetry (DSC) and FTIR. Fragility of the amorphous matrix was determined from the dependence of the glass transition temperature on scanning rate (with DSC). The initial relaxation time of the amorphous formulations was calculated by the Vogel–Tammann–Fulcher (VTF) equation. The physical and chemical stability of the hGH during storage at 50°C was monitored by RP-HPLC, SEC-HPLC and UV absorbance. The hGH formulations containing sucrose demonstrated greater protein-excipient interactions and faster initial relaxation time compared to trehalose formulations. Although both formulations had similar chemical stability (deamidation), their physical stabilities (aggregation) were different. The hGH/sucrose formulation showed a higher rate and lower extent of the formation of insoluble aggregates. The decreased amount of high order aggregates in the sucrose formulations could be correlated with the greater

extent of protein-excipient interaction. In contrast, the higher rate of aggregation seen in the sucrose formulations could be correlated with the higher molecular mobility of the matrix.

1.4. Bibliography

1. Crommelin DJA, Storm G, Verrijk R, de Leede L, Jiskoot W, Hennink WE 2003. Shifting paradigms: biopharmaceuticals versus low molecular weight drugs. Int. J. Pharm. 266(1-2):3-16.

2. Ahern TJ, Manning MC, Editors. 1992. Stability of Protein Pharmaceuticals, Part A: Chemical and Physical Pathways of Protein Degradation. [In: Pharm. Biotechnol., 1992; 2]. ed. p 434 pp.

3. Cleland JL, Powell MF, Shire SJ 1993. The development of stable protein formulations: a close look at protein aggregation, deamidation, and oxidation. Crit Rev Ther Drug Carrier Syst 10(4):307-377.

4. Fagain CO 1995. Understanding and increasing protein stability. Biochimica et Biophysica Acta, Protein Structure and Molecular Enzymology 1252(1):1-14.

5. Ada G 2001. Vaccines and vaccination. N Engl J Med 345(14):1042-1053.

6. Ada G 2005. Overview of vaccines and vaccination. Mol Biotechnol 29(3):255-271.

7. Ada G, Karupiah G 1997. Overview of host defense mechanisms with special reference to viral infections. Gamma Interferon in Antiviral Defense:1-18.

8. Diamond B 2005. Global polio campaign doomed to fail, experts warn. Nat. Med. (N. Y., NY, U. S.) 11(12):1260.

9. Morens DM, Folkers GK, Fauci AS 2004. The challenge of emerging and re-emerging infectious diseases. Nature (London, U. K.) 430(6996):242-249.

10. Pringle CR 2003. Temperature-sensitive mutant vaccines. Methods Mol Med 87(Vaccine Protocols (2nd Edition)):19-36.

11. Ada G 2007. The importance of vaccination. Front Biosci 12:1278-1290.

12. Ada GL 1992. Vaccine antigens. Struct. Antigens 1:367-391.

13. Ada GL 1994. Vaccination strategies to control infections: An overview. Strategies Vaccine Des.:1-16.

14. Ada GL. 1994. Strategies in Vaccine Design. ed. p 217 pp.

15. Avery OT, Goebel WF 1929. Chemo-immunological studies on conjugated carbohydrate-proteins. II. Immunological specificity of synthetic sugar-protein antigens. J Exp Med 50:533-550.

16. Egea E, Iglesias A, Salazar M, Morimoto C, Kruskall MS, Awdeh Z, Schlossman SF, Alper CA, Yunis EJ 1991. The cellular basis for lack of antibody response to hepatitis B vaccine in humans. J Exp Med 173(3):531-538.

17. Griffiths E, Knezevic I 2003. Assuring the quality and safety of vaccines: regulatory expectations for licensing and batch release. Methods Mol Med 87(Vaccine Protocols (2nd Edition)):353-376.

18. Todar K. 2005. Todar's online textbook of bacteriology. ed.: University of Wisconsin-Madison Department of Bacteriology.

19. Metz B, Kersten GFA, Hoogerhout P, Brugghe HF, Timmermans HAM, de Jong A, Meiring H, ten Hove J, Hennink WE, Crommelin DJA, Jiskoot W 2004. Identification of Formaldehyde-induced Modifications in Proteins: Reactions with model peptides. J Biol Chem 279(8):6235-6243.

20. Fraenkel-Conrat HL, Cooper M, Olcott HS 1945. Reaction of CH2O with proteins. J Am Chem Soc 67:950-954.

21. Fraenkel-Conrat H, Brandon BA, Olcott HS 1947. The reaction of formaldehyde with proteins. IV. Participation of indole groups. Gramicidin. J Biol Chem 168:99-118.

22. Fraenkel-Conrat H, Olcott HS 1948. Reaction of formaldehyde with proteins. V. Cross-linking between amino and primary amide or guanidyl groups. J Am Chem Soc 70:2673-2684.

23. Fraenkel-Conrat H, Olcott HS 1948. Reaction of formaldehyde with proteins. VI. Cross-linking of amino groups with phenol, imidazole, or indole groups. J Biol Chem 174:827-843.

24. Martin CJ, Lam DP, Marini MA 1975. Reaction of formaldehyde with the histidine residues of proteins. Bioorg Chem 4(1):22-29.

25. Thaysen-Andersen M, Jorgensen SB, Wilhelmsen ES, Petersen JW, Hojrup P 2007. Investigation of the detoxification mechanism of formaldehyde-treated tetanus toxin. Vaccine 25(12):2213-2227.

26. Paliwal R, London E 1996. Comparison of the conformation, hydrophobicity, and model membrane interactions of diphtheria toxin to those of formaldehyde-treated toxin (diphtheria toxoid): formaldehyde stabilization of the native conformation inhibits changes that allow membrane insertion. Biochemistry 35(7):2374-2379.

27. Rappuoli R, Douce G, Dougan G, Pizza M 1995. Genetic detoxification of bacterial toxins: a new approach to vaccine development. Int Arch Allergy Immunol 108(4):327-333.

28. Rappuoli R 1994. Toxin inactivation and antigen stabilization: Two different uses of formaldehyde. Vaccine 12(7):579-581.

29. Kersten G, Jiskoot W, Hazendonk T, Spiekstra A, Westdijk J, Beuvery C 1999. Characterization of diphtheria toxoid. Pharmacy and Pharmacology Communications 5(1):27-31.

30. Gupta RK 1998. Aluminum compounds as vaccine adjuvants. Adv Drug Delivery Rev 32(3):155-172.

31. Gupta RK, Rost BE 2000. Aluminum compounds as vaccine adjuvants. Methods Mol Med 42(Vaccine Adjuvants):65-89.

32. Gupta RK, Rost BE, Relyveld E, Siber GR 1995. Adjuvant properties of aluminum and calcium compounds. Pharm. Biotechnol. 6:229-248.

33. O'Hagan DT, MacKichan ML, Singh M 2001. Recent developments in adjuvants for vaccines against infectious diseases. Biomol Eng 18(3):69-85.

34. Liu L, Xie B, Li S, Wang W, Wang Y, Wang X, Liu J 2005. Stability of HAV-MV vaccine. Zhongguo Shengwu Zhipinxue Zazhi 18(5):403-404.

35. Peek LJ, Brandau DT, Jones LS, Joshi SB, Middaugh CR 2006. A systematic approach to stabilizing EBA-175 RII-NG for use as a malaria vaccine. Vaccine 24(31-32):5839-5851.

36. Shi L, Evans RK, Burke CJ 2004. Improving vaccine stability, potency, and delivery. American Pharmaceutical Review 7(5):100,102, 104-107.

37. Volkin DB, Burke CJ, Sanyal G, Middaugh CR 1996. Analysis of vaccine stability. Dev. Biol. Stand. 87(New Approaches to Stabilisation of Vaccines Potency):135-142.

38. Volkin DB, Burke CJ, Sanyal G, Middaugh CR 1997. Characterization of vaccine stability. Book of Abstracts, 213th ACS National Meeting, San Francisco, April 13-17:BIOC-025.

39. Kueltzo LA, Ersoy B, Ralston JP, Middaugh CR 2003. Derivative absorbance spectroscopy and protein phase diagrams as tools for comprehensive protein characterization: A bGCSF case study. J. Pharm. Sci. 92(9):1805-1820.

40. Peek LJ, Brey RN, Middaugh CR 2006. A rapid, three-step process for the preformulation of a recombinant ricin toxin A-chain vaccine. J. Pharm. Sci. 96(1):44-60.

41. Fan H, Vitharana SN, Chen T, O'Keefe D, Middaugh CR 2007. Effects of pH and Polyanions on the Thermal Stability of Fibroblast Growth Factor 20. Mol. Pharm. 4(2):232-240.

42. Rexroad J, Martin TT, McNeilly D, Godwin S, Middaugh CR 2006. Thermal stability of adenovirus type 2 as a function of pH. J. Pharm. Sci. 95(7):1469-1479.

43. Fan H, Kashi RS, Middaugh CR 2006. Conformational lability of two molecular chaperones Hsc70 and gp96: Effects of pH and temperature. Arch Biochem Biophys 447(1):34-45.

44. Rexroad J, Evans RK, Middaugh CR 2005. Effect of pH and ionic strength on the physical stability of adenovirus type 5. J. Pharm. Sci. 95(2):237-247.

45. Jiang G, Joshi SB, Peek LJ, Brandau DT, Huang J, Ferriter MS, Woodley WD, Ford BM, Mar KD, Mikszta JA, Hwang CR, Ulrich R, Harvey NG, Middaugh CR, Sullivan VJ 2005. Anthrax vaccine powder formulations for nasal mucosal delivery. J. Pharm. Sci. 95(1):80-96.

46. Ausar SF, Rexroad J, Frolov VG, Look JL, Konar N, Middaugh CR 2005. Analysis of the Thermal and pH Stability of Human Respiratory Syncytial Virus. Mol. Pharm. 2(6):491-499.

47. Fan H, Ralston J, Dibiase M, Faulkner E, Middaugh CR 2005. Solution behavior of IFN-b-1a: An empirical phase diagram based approach. J. Pharm. Sci. 94(9):1893-1911.

48. Choosakoonkriang S, Lobo BA, Koe GS, Koe JG, Middaugh CR 2003. Biophysical characterization of PEI/DNA complexes. J. Pharm. Sci. 92(8):1710-1722.

49. Kuijper EJ, Coignard B, Tull P 2006. Emergence of Clostridium difficile-associated disease in North America and Europe. Clinical Microbiology and Infection 12(Suppl. 6):2-18.

50. Drudy D, Fanning S, Kyne L 2007. Toxin A-negative, toxin B-positive Clostridium difficile. Int. J. Infect. Dis. 11(1):5-10.

51. Warny M, Pepin J, Fang A, Killgore G, Thompson A, Brazier J, Frost E, McDonald LC 2005. Toxin production by an emerging strain of Clostridium difficile associated with outbreaks of severe disease in North America and Europe. Lancet 366(9491):1079-1084.

52. Dove CH, Wang SZ, Price SB, Phelps CJ, Lyerly DM, Wilkins TD, Johnson JL 1990. Molecular characterization of the Clostridium difficile toxin A gene. Infect Immun 58(2):480-488.

53. Barroso LA, Wang SZ, Phelps CJ, Johnson JL, Wilkins TD 1990. Nucleotide sequence of Clostridium difficile toxin B gene. Nucleic Acids Res 18(13):4004.

54. Just I, Gerhard R 2004. Large clostridial cytotoxins. Rev. Physiol. Biochem. Pharmacol. 152:23-47.

55. Just I, Gerhard R 2006. Clostridium difficile toxins A and B: modulation of intracellular signal cascades. Crossroads between Bacterial Protein Toxins and Host Cell Defences:43-56.

56. Just I, Selzer J, Wilm M, von Eichel-Streiber C, Mann M, Aktories K 1995. Glucosylation of Rho proteins by Clostridium difficile toxin B. Nature (Lond) 375(6531):500-503.

57. von Eichel-Streiber C, Boquet P, Sauerborn M, Thelestam M 1996. Large clostridial cytotoxins--a family of glycosyltransferases modifying small GTP-binding proteins. Trends Microbiol 4(10):375-382.

58. Warny M, Kelly CP 2003. Pathogenicity of Clostridium difficile toxins. Microbial Pathogenesis and the Intestinal Epithelial Cell:503-524.

59. Greco A, Ho JGS, Lin S-J, Palcic MM, Rupnik M, Ng KKS 2006. Carbohydrate recognition by Clostridium difficile toxin A. Nat. Struct. Mol. Biol. 13(5):460-461.

60. Ho JGS, Greco A, Rupnik M, Ng KKS 2005. Crystal structure of receptor-binding C-terminal repeats from Clostridium difficile toxin A. Proc Natl Acad Sci U S A 102(51):18373-18378.

61. Walev I, Bhakdi SC, Hofmann F, Djonder N, Valeva A, Aktories K, Bhakdi S 2001. Delivery of proteins into living cells by reversible membrane

permeabilization with streptolysin-O. Proc Natl Acad Sci U S A 98(6):3185-3190.

62. Barth H, Pfeifer G, Hofmann F, Maier E, Benz R, Aktories K 2001. Low pH-induced formation of ion channels by Clostridium difficile toxin B in target cells. J Biol Chem 276(14):10670-10676.

63. Qa'Dan M, Spyres LM, Ballard JD 2000. pH-induced conformational changes in Clostridium difficile toxin B. Infect Immun 68(5):2470-2474.

64. Jank T, Giesemann T, Aktories K 2007. Rho-glucosylating Clostridium difficile toxins A and B: new insights into structure and function. Glycobiology 17(4):15-22R.

65. Reinert DJ, Jank T, Aktories K, Schulz GE 2005. Structural Basis for the Function of Clostridium difficile Toxin B. J Mol Biol 351(5):973-981.

66. Jodlowski TZ, Oehler R, Kam LW, Melnychuk I 2006. Emerging therapies in the treatment of Clostridium difficile-associated disease. Ann Pharmacother 40(12):2164-2169.

67. Pepin J 2006. Improving the treatment of Clostridium difficile-associated disease: where should we start? Clin Infect Dis 43(5):553-555.

68. Kyne L, Kelly CP 2001. Recurrent Clostridium difficile diarrhoea. Gut 49(1):152-153.

69. Giannasca PJ, Warny M 2004. Active and passive immunisation against Clostridium difficile diarrhoea and colitis. Old Herborn University Seminar Monograph 17(Possibilities for Active and Passive Vaccination Against Opportunistic Infections):91-105.

70. Lyerly DM, Bostwick EF, Binion SB, Wilkins TD 1991. Passive immunization of hamsters against disease caused by Clostridium difficile by use of bovine immunoglobulin G concentrate. Infect Immun 59(6):2215-2218.

71. Sougioultzis S, Kyne L, Drudy D, Keates S, Maroo S, Pothoulakis C, Giannasca Paul J, Lee Cynthia K, Warny M, Monath Thomas P, Kelly Ciaran P. 2005. Clostridium difficile toxoid vaccine in recurrent C. difficile-associated diarrhea. ed., United States: Gastroenterology Division, Beth Israel Deaconess Medical Center, Harvard Medical School, Boston, Massachusetts, 02215,USA. p 764-770.

72. Torres JF, Thomas WD, Jr., Lyerly DM, Giel MA, Hill JE, Monath TP 1996. Clostridium difficile vaccine: influence of different adjuvants and routes of immunization on protective immunity in hamsters. Vaccine Research 5(3):149-162.

73. Torres JF, Lyerly DM, Hill JE, Monath TP 1995. Evaluation of formalin-inactivated Clostridium difficile vaccines administered by parenteral and

mucosal routes of immunization in hamsters. Infect Immun 63(12):4619-4627.

74. Kotloff KL, Wasserman SS, Losonsky GA, Thomas W, Jr., Nichols R, Edelman R, Bridwell M, Monath TP 2001. Safety and immunogenicity of increasing doses of a Clostridium difficile toxoid vaccine administered to healthy adults. Infect Immun 69(2):988-995.

75. Arakawa T, Timasheff SN 1982. Stabilization of protein structure by sugars. Biochemistry 21(25):6536-6544.

76. Arakawa T, Timasheff SN 1982. Preferential interactions of proteins with salts in concentrated solutions. Biochemistry FIELD Full Journal Title:Biochemistry 21(25):6545-6552.

77. Carpenter JF, Crowe JH 1988. The mechanism of cryoprotection of proteins by solutes. Cryobiology 25(3):244-255.

78. Carpenter JF, Izutsu K-I, Randolph TW 1999. Freezing- and drying-induced perturbations of protein structure and mechanisms of protein protection by stabilizing additives. Drugs Pharm Sci 96(Freeze-Drying/Lyophilization of Pharmaceutical and Biological Products):123-160.

79. Wang W 2000. Lyophilization and development of solid protein pharmaceuticals. Int. J. Pharm. 203(1-2):1-60.

80. Hill JJ, Shalaev EY, Zografi G 2005. Thermodynamic and dynamic factors involved in the stability of native protein structure in amorphous solids in relation to levels of hydration. J. Pharm. Sci. 94(8):1636-1667.

81. Duddu SP, Zhang G, Dal Monte PR 1997. The relationship between protein aggregation and molecular mobility below the glass transition temperature of lyophilized formulations containing a monoclonal antibody. Pharm. Res. 14(5):596-600.

82. Pikal MJ 1994. Freeze-drying of proteins: process, formulation, and stability. ACS Symp Ser 567(Formulation and Delivery of Proteins and Peptides):120-133.

83. Pikal MJ, Dellerman KM, Roy ML, Riggin RM 1991. The effects of formulation variables on the stability of freeze-dried human growth hormone. Pharm. Res. 8(4):427-436.

84. Angell CA 2002. Liquid Fragility and the Glass Transition in Water and Aqueous Solutions. Chem. Rev. (Washington, DC, U. S.) 102(8):2627-2649.

85. Martinez LM, Angell CA 2001. A thermodynamic connection to the fragility of glass-forming liquids. Nature (London, U. K.) 410(6829):663-667.

86. Sastry S 2001. The relationship between fragility, configurational entropy and the potential energy landscape of glass-forming liquids. Nature (Lond) 409(6817):164-167.

87. Cicerone MT, Soles CL 2004. Fast dynamics and stabilization of proteins: Binary glasses of trehalose and glycerol. Biophys J 86(6):3836-3845.

88. Barth A, Zscherp C 2002. What vibrations tell about proteins. Q Rev Biophys 35(4):369-430.

89. Bicout DJ, Zaccai G 2001. Protein flexibility from the dynamical transition: a force constant analysis. Biophys J 80(3):1115-1123.

90. Daniel RM, Finney JL, Reat V, Dunn R, Ferrand M, Smith JC 1999. Enzyme dynamics and activity: time-scale dependence of dynamical transitions in glutamate dehydrogenase solution. Biophys J 77(4):2184-2190.

91. Fenimore PW, Frauenfelder H, McMahon BH, Parak FG 2002. Slaving: solvent fluctuations dominate protein dynamics and functions. Proc Natl Acad Sci U S A 99(25):16047-16051.

92. Shamblin SL, Taylor LS, Zografi G 1998. Mixing Behavior of Colyophilized Binary Systems. J. Pharm. Sci. 87(6):694-701.

93. Gabel F, Bicout D, Lehnert U, Tehei M, Weik M, Zaccai G 2002. Protein dynamics studied by neutron scattering. Q Rev Biophys 35(4):327-367.

94. Giuffrida S, Cottone G, Cordone L 2004. Structure-dynamics coupling between protein and external matrix in sucrose-coated and in trehalose-coated MbCO: An FTIR study. J. Phys. Chem. B 108(39):15415-15421.

95. Scopigno T, Ruocco G, Sette F, Monaco G 2003. Is the Fragility of a Liquid Embedded in the Properties of Its Glass? Science (Washington, DC, U. S.) 302(5646):849-852.

96. Shamblin SL, Tang X, Chang L, Hancock BC, Pikal MJ 1999. Characterization of the Time Scales of Molecular Motion in Pharmaceutically Important Glasses. J. Phys. Chem. B 103(20):4113-4121.

97. Chang L, Shepherd D, Sun J, Ouellette D, Grant KL, Tang X, Pikal MJ 2005. Mechanism of protein stabilization by sugars during freeze-drying and storage: Native structure preservation, specific interaction, and/or immobilization in a glassy matrix? J. Pharm. Sci. 94(7):1427-1444.

98. Tsai AM, Neumann DA, Bell LN 2000. Molecular dynamics of solid-state lysozyme as affected by glycerol and water: a neutron scattering study. Biophys J 79(5):2728-2732.

99. Griebenow K, Santos AM, Carrasquillo KG 1999. Secondary structure of proteins in the amorphous dehydrated state probed by FTIR spectroscopy. Dehydration-induced structural changes and their prevention. Internet Journal of Vibrational Spectroscopy 3(1).

100. Allison SD, Chang B, Randolph TW, Carpenter JF 1999. Hydrogen bonding between sugar and protein is responsible for inhibition of dehydration-induced protein unfolding. Arch Biochem Biophys 365(2):289-298.

101. Lopez-Diez EC, Bone S 2000. An investigation of the water-binding properties of protein + sugar systems. Phys Med Biol 45(12):3577-3588.

102. Lopez-Diez EC, Bone S 2004. The interaction of trypsin with trehalose: an investigation of protein preservation mechanisms. Biochim Biophys Acta 1673(3):139-148.

103. Souillac PO, Costantino HR, Middaugh CR, Rytting JH 2002. Investigation of protein/carbohydrate interactions in the dried state. 1. Calorimetric studies. J. Pharm. Sci. 91(1):206-216.

104. Taylor LS, Zografi G 1998. Sugar-Polymer Hydrogen Bond Interactions in Lyophilized Amorphous Mixtures. J. Pharm. Sci. 87(12):1615-1621.

105. Liao Y-H, Brown MB, Quader A, Martin GP 2002. Protective Mechanism of Stabilizing Excipients Against Dehydration in the Freeze-Drying of Proteins. Pharm. Res. 19(12):1854-1861.

106. Allison SD, Chang B, Randolph TW, Carpenter JF 1999. Hydrogen bonding between sugar and protein is responsible for inhibition of dehydration-induced protein unfolding. Arch Biochem Biophys 365(2):289-298.

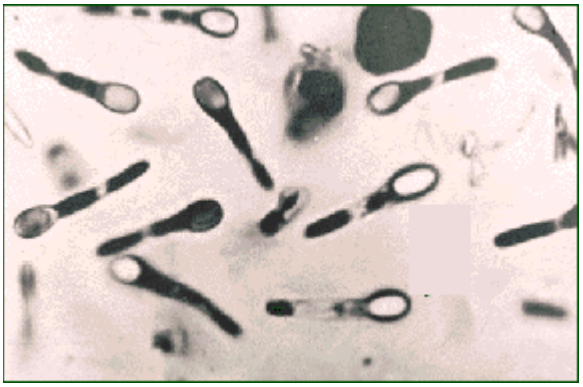

Figure 1.1. *Clostridium difficile* endospores (from reference 47)

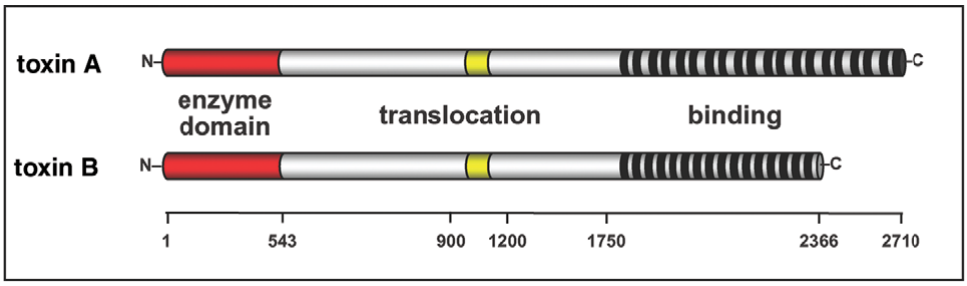

Figure 1.2. Structure of *C. difficile* toxins A and B. Toxins A and B consist of three major domains: N-terminus (responsible for enzymatic activity), C-terminus (involved in receptor binding) and middle part (potentially involved in the translocation of the toxin into the cytosol). (from reference 58)

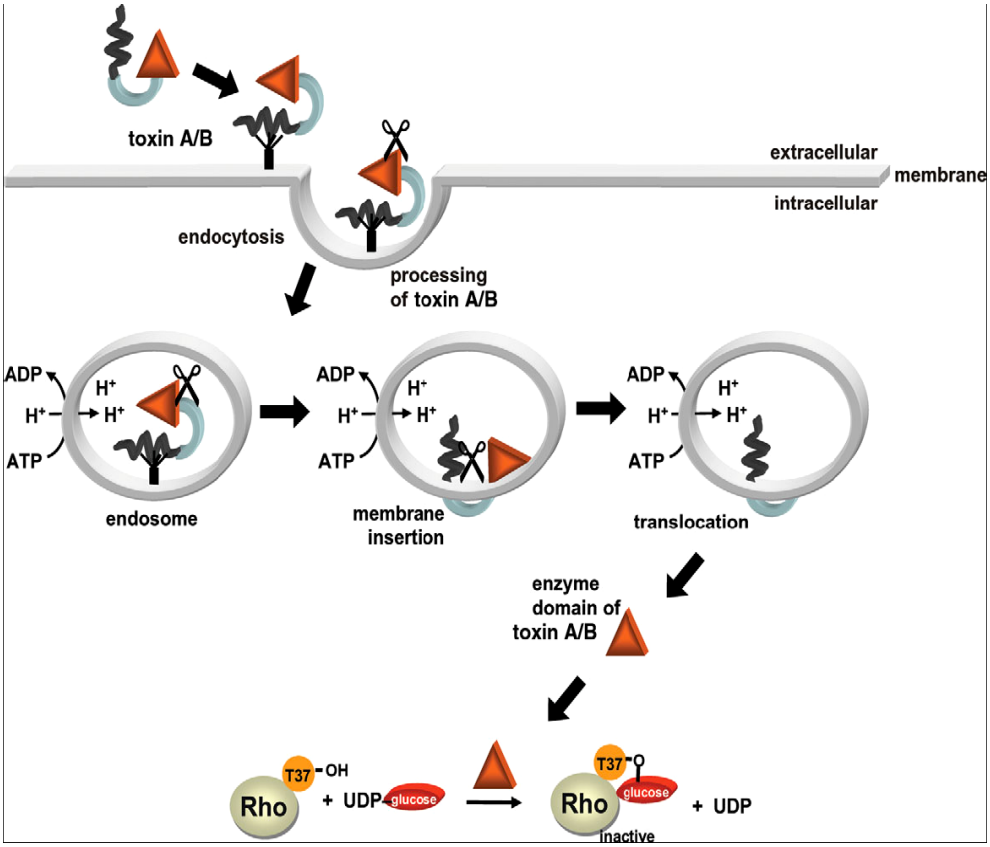

Figure 1.3. Model of the uptake of *C. difficile* toxins. The uptake of the toxins involves binding to receptors on the surface of target cells, subsequent endocytocis, cleavage of N-terminal catalytic domain with subsequent translocation from an acidic endosomal compartment into the cytosol. In the cytosol, the toxins glucosylate Rho proteins by using UDP-glucose as a cosubstrate. (from reference 63)

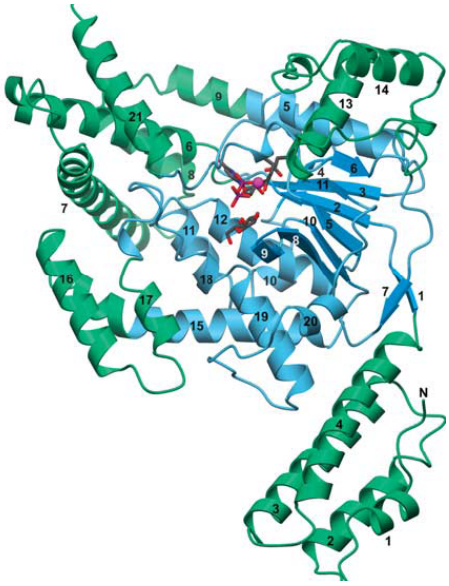

Figure 1.4. Stereoview of the N-terminal catalytic portion of toxin B. Structure is depicted as a ribbon plot with α-helices and ß-strands. (from reference 64)

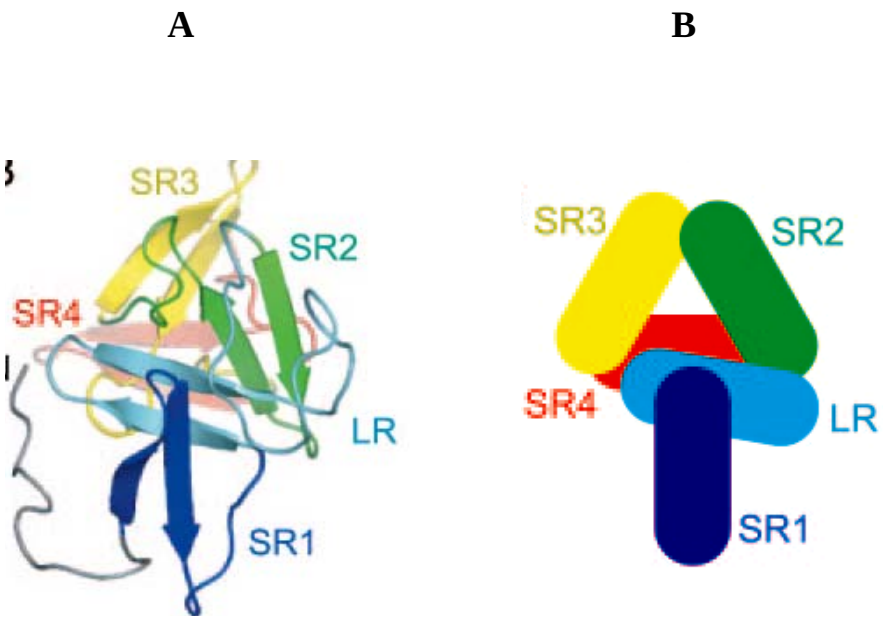

Figure 1.5. Stereoview of solenoid structure of C-therminal domain of toxin A. (A) ribbon representation and (B) schematic representation with rectangles. (from reference 59)

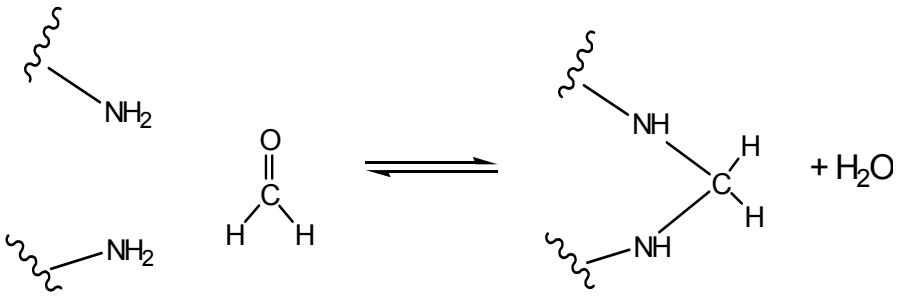

Scheme 1.1. Crosslinking of side chains containing primary amines with formaldehyde to form methylene bridges.

Chapter 2:

Physical Characterization of Clostridium difficile Toxins and Toxoids - Effect of the Formaldehyde Crosslinking on Thermal Stability.

2.1. Introduction

Clostridium difficile (*C. difficile*) is a gram-positive, endospore forming rod-shaped bacterium.[1] *C. difficile* has more than 150 ribotypes, 24 toxinotypes and produces two large toxins designated A (308 kDa, 2,710 amino acids) and B (260 kDa, 2,366 amino acids). The toxins are responsible for *C. difficile*-associated disease (CDAD), which manifests itself as nosocomial diarrhea and pseudomembranous colitis.[2-6] Unfortunately, treatment of CDAD with antimicrobial agents (metronidazole and vancomycin) leads to recurrence of the disease.[7-9] To induce immunity against CDAD both passive and active vaccination have been attempted, with the active vaccination being more effective.[10,11] Vaccination employing the administration of formaldehyde crosslinked (inactivated) toxoids A and B, has been shown to be effective in hamsters, healthy adults and patients with recurrent CDAD.[12-15]

C. difficile toxins A and B exhibit 49% amino acid identity and belong to the large clostrodial cytotoxin (LCT) family, which includes the *Clostridium sordelii* toxins and *Clostridium novyi* alpha toxin. Toxins A and B possess high molecular weight, an amino-terminal enzymatic domain (e.g. residues 1-543), a central hydrophobic region (e.g. residues 900-1,200) and a carboxy-terminal domain carrying carbohydrate recognition sequence repeats (e.g. residues 1,750-2,710 or 2,366).[4,16-20] It is thought that the carboxy-terminal part binds to cell surface carbohydrate containing receptors which leads to endocytosis of the toxin.[21,22] The central hydrophobic region then undergoes pH-induced conformational changes which

mediate formation of pores and translocation of the amino-terminal fragment from early endosomes to the cytoplasm.[23-25] In the cytosol, the amino-terminal enzymatic fragment catalyzes glycosylation of Rho/Ras proteins at Thr37/35 which leads to shutdown of essential cellular processes.[26] The structure of the amino-terminal domain of toxin B and the carboxy-terminus domain of toxin A are well characterized although the complete structure of the toxins is not yet available. The role of the hydrophobic region is especially poorly understood.[27] To explore the structural characteristics of both toxins under a range of conditions, this study elucidates the tertiary and secondary structure as well as aggregation behavior at pH 5.5-8.0 for toxin A and pH 5.0-7.5 for toxin B. In addition, the properties of the toxins were monitored as a function of temperature over the same pH interval.

Treatment of the toxins with formaldehyde leads to reaction with the N-terminal amino acid residues and the side chains of arginine, cysteine, histidine and lysine residues, and the subsequent formation of methylol groups and Schiff-bases as well as intramolecular methylene bridges with amine, phenol, imidazole or indole groups.[28-34] The intramolecular crosslinking of toxins with formaldehyde leads to their complete inactivation with at least partial retention of their immunogenicity. In addition, the crosslinking may result in changes in the toxin's shape and overall stabilization of structure.[35-38]

Since the formaldehyde crosslinked *C. difficile* toxoids A and B are candidates for vaccine development, a better understanding of their structures as a function of pH and temperature is of a great interest for the design of stable vaccine formulations. A

comparison of the toxins' and toxoids' behaviors was also performed to probe the effect of formaldehyde crosslinking on their structures and thermal stabilities, to further facilitate their use as vaccine agents.

2.2. Experimental methods

2.2.1. Materials

Toxins and toxoids A and B were produced in highly purified form by Acambis Inc. (Cambridge, MA). The production and purification of the material is described elsewhere.[15] The concentration of the proteins was determined by UV absorbance at 280 nm using extinction coefficients of 1.173 for toxin/toxoid A and 0.967 for toxin/toxoid B. All reagents used in these studies were of analytical grade and were purchased from Sigma (St. Louis, MO). MOPS/succinate (10 mM of each) buffers (pH 5.0, 5.5, 6.0, 6.5, 7.0, 7.5 and 8.0) containing 100 mM NaCl were used for characterization of the proteins over the entire pH range examined. Sodium phosphate buffer (5 mM) at pH 7.0 was used for assignment of secondary structure by CD. For buffer exchange, protein was dialyzed at refrigerator temperature using Slide-A-Lyzer® Dialysis Cassettes, 10 kDa MWCO (Pierce, Rockford, IL).

2.2.2. Characterization of physical stability

2.2.2.1. Sample preparation.

Protein solutions were studied at a concentration of 0.2 mg/ml for CD studies and 0.1 mg/ml for fluorescence and UV absorption analyses. No concentration dependence was seen over this concentration range. Toxin/toxoid A was studied at six pH values from 5.5 to 8.0 at half unit pH intervals. Toxin/toxoid B was studied at six pH values from 5.0 to 7.5 also at half unit pH intervals. The pH range selected was chosen to be above the theoretical isoelectric point for each toxin (5.50 for toxin A and 4.42 for toxin B). Each sample was evaluated in duplicate to ensure reproducibility of the measurements.

2.2.2.2. High-Resolution UV Absorbance Spectroscopy.

High-resolution UV absorbance spectra were acquired using an Agilent 8453 UV-visible spectrophotometer. The spectra were obtained every 2.5°C over the temperature range of 10 to 85°C with a 5 min incubation (sufficient for equilibrium to be reached) at each temperature. Aggregation of the proteins was studied by simultaneously monitoring optical density at 350 nm (OD 350 nm) as a function of temperature. Second derivatives of UV absorbance spectra in the near-UV region were used for construction of an initial empirical phase diagram (EPD). Details of this procedure are described elsewhere.[39,40] Spectral analysis was performed using Chemstation™ software from Agilent. Second derivative spectra were obtained by using a nine point filter and the Savitsky-Golay method to fit data to a third order polynomial. The spectra were smoothed using 99 interpolated points between each raw data point, permitting 0.01 nm resolution. Peak positions were determined from

the interpolated spectra using Microcal Origin^{TM} 6.0 software. This EPD is a measure of protein tertiary structure at each temperature/pH condition (construction of the EPD is discussed below).

2.2.2.3. Far-UV Circular Dichroism (CD) Spectroscopy.

CD spectra were acquired using a Jasco J-810 spectropolarimeter equipped with a 6-position Peltier temperature controller. CD spectra were obtained from 260-190 nm with a scanning speed of 20 nm/min, a 2 sec response time and an accumulation of 2. Assignment of secondary structure was performed with DICHROWEB software utilizing the CDSSTR (7) analysis algorithm.[41,42] A mean residue weight of 114 was used for toxin/toxoid A and 110 for toxin/toxoid B. To study thermal transitions (melting curves) of the proteins (in sealed cuvettes with a 0.1-cm pathlength), the CD signal at 208 nm was monitored every 0.5°C over the 10 to 85°C temperature range employing a temperature ramp of 15°C/hr. The CD signal was converted to molar elipticity by Jasco Spectral Manager software. The midpoint temperature of the thermal transition was obtained from a sigmoid fitting of the melting curves using Origin software.

2.2.2.4. Intrinsic Tryptophan (Trp) Fluorescence Spectroscopy.

Fluorescence spectra were acquired using a Photon Technology International (PTI) spectrofluorometer (Lawrenceville, NJ) equipped with a turreted 4-position Peltier-controlled cell holder. An excitation wavelength of 295 nm was used to excite Trp

and the emission spectra (>95% Trp emission) were collected from 305 to 450 nm with a step size of 0.5 nm and 0.5 sec integration time. Excitation and emission slits of 4 nm and a 1-cm pathlength quartz cuvette were used. Emission spectra were collected every 2.5°C with 5 min of equilibration over a temperature range of 10 to 85°C. A buffer baseline was subtracted from each raw emission spectrum. Peak positions of the emission spectra were obtained from polynomial fits using Origin software.

2.2.2.5. ANS Fluorescence Spectroscopy.

Accessibility of apolar sites on the proteins was monitored by fluorescence emission of the extrinsic probe 8-Anilino-1-naphthalene sulfonate (ANS). Each sample contained a 20-fold molar excess of ANS to protein. The ANS was excited at 372 nm and emission spectra were collected from 400 to 600 nm with a step size of 2 nm and a 1-sec integration time. Emission spectra were collected every 2.5°C with 5 min of equilibration over a temperature range of 10 to 85°C. The ANS-buffer baseline at each corresponding pH was subtracted from the raw emission spectra. Peak positions of the emission spectra were obtained from polynomial fits using Origin software.

2.2.2.6. Dynamic Light Scattering.

The mean hydrodynamic diameter of the proteins at pH 6.5 was analyzed using a dynamic light scattering instrument (Brookhaven Instrument Corp., Holtzille, NY) equipped with a 50 mW diode-pumped laser (λ = 532 nm). The scattered light was

monitored at 90° to the incident beam, and autocorrelation functions were generated using a digital auto-correlator (BI-9000AT). The hydrodynamic diameter was calculated from the diffusion coefficient by the Stokes-Einstein equation using the method of cumulants (lognormal number based). In addition, the data was fit to a non-negatively constrained least squares algorithm to yield multi-modal distributions (MSD). The instrument was equipped with a temperature-controlled circulating water bath RTE111 (Neslab, Newington, NH) and the hydrodynamic diameter was monitored over a temperature range of 10 to 85°C.

2.2.2.7. Empirical Phase Diagrams (EPDs).

Empirical phase diagrams were constructed as described previously.[40] CD molar elipticity at 208 nm, intrinsic Trp fluorescence intensity, ANS fluorescence intensity and optical density at 350 nm data sets were used for construction of each phase diagram. Near-UV second derivatives peak positions were also used for construction of separate EPDs to visualize changes in aromatic residue environments. All calculations were performed using Matlab software (The MathWorks, Natick, MA). Briefly, the experimental data sets were represented as n-dimensional vectors in n x n density matrices, where n is the number of variables (e.g. CD, fluorescence, OD 350 nm, etc) at each pH-temperature combination. The density matrices were used to derive n sets of eigenvalues and eigenvectors. The three eigenvectors which correspond to the highest eigenvalues were employed to re-expand the data into three dimensions, and each vector was assigned a color (red, green or blue). The resulting

multi-colored plots represent contributions of each vector at a given pH/temperature point. The regions of the EPDs with similar color indicate similar physical states of the protein. A detailed explanation of the calculations involved in construction of EPDs is presented elsewhere.[40]

2.3. Results

2.3.1. High-Resolution UV Absorbance Spectroscopy

Second derivative UV spectra of the toxins and toxoids revealed the presence of six negative peaks (Figure 2.1). The peaks are approximately positioned at the following wavelengths: 253 nm (Phe), 260 nm (Phe), 266 nm (Phe/Tyr), 277 nm (Tyr), 285 nm (Tyr/Trp) and 292 nm (Trp) at 10°C.[40] Changes in the position of 5 of the peaks are shown over the indicated temperature range for toxin/toxoid A (Figure 2.2) and toxin/toxoid B (Figure 2.3.).

In the case of toxin A, the peak positions first shifted to lower wavelength (blue shift) by 1-25 nm and then to higher wavelength (red shift) upon heating (Figure 2.2a). The onset and magnitude of the shifts were earlier and higher for protein at lower pH values. Blue shifts are generally indicative of changes in aromatic side chain environments towards more polar conditions and are consistent with unfolding of the protein. In contrast, red shifts are generally associated with more apolar environments and typically result from the formation of aggregated protein upon heating. Thus the observed shifts of the peak positions at about 45°C suggest that

toxin A undergoes partial unfolding with subsequent protein association and ultimately precipitation. In the case of toxoid A, the peak positions were red shifted by 1-6 nm upon heating to ~50°C, where the onset and magnitude of the shift was earlier and higher for protein at lower pH (Figure 2.2b). The red shift of the peak positions is consistent with formation of visually observed insoluble aggregates at higher temperatures and increased variability of the data. The absence of unfolding (blue shift) prior to precipitation and delayed onset of the thermal transition in toxoid A suggests that the formaldehyde crosslinking leads to tertiary structure with more pronounced thermal stability.

For toxin B, the peak positions shifted by 1-6 nm and the direction of the shifts was pH sensitive (Figure 2.3a). Toxin B at pH 5.0 and 5.5 demonstrated significant blue shifts in the peak positions at about 45°C, whereas at higher pH the peaks were slightly red shifted upon heating. The blue shifts in the peak positions at low pH are indicative of thermally induced unfolding and consistent with visually observed precipitation. The small shifts in peak position at higher pH suggest little or no change in the environment of the aromatic residues upon heating. The peak positions of toxoid B were red shifted by 0.1-1 nm upon heating to about 50°C (Figure 2.3b). The observed precipitation of toxoid B at pH 5.0 and 5.5 at elevated temperatures did not lead to significant shifts of the peak positions. These observations again suggest that the formaldehyde crosslinking of toxin B leads to tertiary structure with increased thermal stability.

The aromatic residue's peak positions as a function of pH and temperature are summarized in the form of empirical phase diagrams for toxins/toxoids A and B in Figure 4. In this case, the data for the corresponding toxin and toxoid was processed together as a single matrix permitting a direct comparison between the two proteins. The EPDs clearly show more pronounced changes in tertiary structure of toxin A compared to toxin B, and of toxins in general compared to their corresponding toxoids. In the cases of toxin A and toxin B (only at pH 5.0 and 5.5), the appearance of regions with clearly different color at elevated temperature indicates more dramatic changes in the aromatic residue's environment. The change in color at about 50°C seen for all proteins suggests a change in the proteins tertiary structure and correlates well with the actual observed changes in peak positions.

The tendency of the proteins to aggregate at elevated temperature was directly monitored employing the optical density at 350 nm (OD 350 nm) and is summarized in Figure 2.5. The turbidity of toxin/toxoid A increased at all pH values upon heating. The observed decrease of the OD 350 nm correlates directly with protein precipitation and adsorption to the walls of the cuvvette. Both toxin A and toxoid A displayed an increasing onset temperature of aggregation with increasing pH (Figure 2.5e). Toxoid A started to precipitate at higher temperature compared to its crosslinked homologue (Figure 2.5b). In addition, toxoid A had a greater pH sensitivity to aggregation with small changes in pH producing a significant delay in the onset of precipitation.

The elevated turbidity of toxin B at pH 5.0 and 5.5 indicates the presence of soluble aggregates (Figure 2.5c). Toxin B formed insoluble aggregates at ~ 45°C at

pH 5.0, ~ 70°C at pH 5.5 and ~ 75°C at pH 6.0. The temperature effect on the OD 350 nm was small at pH 6.5-7.5. The increased turbidity of toxoid B at pH 5.0 indicates the presence of soluble aggregates which started to precipitate at ~ 55°C (Figure 2.5d). Toxoid B at pH 5.5 formed insoluble aggregates at ~ 65°C. Toxoid B at pH 6.0-7.5 demonstrated only a small effect of temperature on OD 350 nm. Toxoid B at pH 6.0 did not appear to form insoluble aggregates. The onset of the toxoid's aggregation was delayed by ~10°C compared to the toxins. These observations once again support the greater stability of the toxoids against aggregation at elevated temperatures.

2.3.2. Far-UV Circular Dichroism (CD) Spectroscopy

The CD spectra of the toxins and toxoids at 10°C displayed double minima at approximately 208 and 222 nm (Figure 2.6). The spectra of the proteins in the absence of sodium chloride (which interferes with data collected in the far UV) showed a good fit to algorithm reconstructed data (DICHROWEB) and allowed us to estimate a secondary structure of ~35% α-helix, ~20% ß-sheet, ~ 20% turns and ~25% unordered regions for toxins/toxoids A and B (Table 2.1). Toxin/toxoid A at pH 5.5 and toxin B at pH 5.0 and 5.5 display lower molar ellipticity suggesting less ordered structure (Figure 2.6).

Changes in the CD signal at 208 nm upon heating were monitored for both toxins and toxoids (Figure 2.7). The CD signal at 208 nm decreased significantly for toxin and toxoid A indicating at least partial unfolding and perhaps protein

aggregation at higher temperature (Figure 2.7a,b). The midpoint of the thermal transitions (Tm) was pH dependent and occured at lower temperature for protein at low pH (Figure 2.7e). The Tm of toxoid A was increased by about 6°C at pH 5.5 and about 12°C at pH 8.0 compared to toxin A.

Toxin B displayed considerable precipitation at pH 5.0-6.0 upon heating and therefore produced a significant decrease of the signal at 208 nm (Figure 2.7c). This precipitation was preceded by a slight decrease of the signal at ~ 25°C at pH 5.0, ~30°C at pH 5.5 and ~ 35°C at pH 6.0. Heating of toxin B at pH 6.5-7.5 led to small changes in secondary structure corresponding to subtle thermally induced conformational changes in the protein at ~ 43°C at pH 6.5, ~ 45°C at pH 7.0 and ~ 47°C at pH 7.5. Toxoid B at pH 5.0 and 5.5 had a significant decrease of the signal at 208 nm due to thermally induced precipitation (Figure 2.7d). At pH 5.5 toxoid B showed a biphasic thermal transition presumably reflecting a secondary structure decrease at ~45°C and precipitation at ~65°C. Heating of toxoid B at pH 6.0-7.5 led to smaller changes in secondary structure. The anticipated increase in Tm with increased pH was seen here as well (Figure 2.7e). Reversibility of the toxin/toxoid B CD spectral changes at pH 6.5-7.5 was studied upon cooling the previously heated samples to 10°C. The structural changes were not reversible, however, the changes of the CD spectra were similar over the pH range examined (data not shown). Spectral changes for protein at pH 7.0 are illustrated in Figure 8. The secondary structure assignment of the previously heated protein (in buffer without NaCl) is summarized in Table 2.1. Toxin/toxoid B had increased ß-sheet and unordered character upon

heating which suggests that the heating induced partial unfolding leads to structural reorganization and possibly formation of soluble aggregates (supported by OD 350 nm data). The Tm of toxoid B was delayed by about 22°C at pH 5.0 and by about 14°C at pH 7.5 compared to unmodified toxin B. The toxins and toxoids had similar shapes to their thermal transitions although the toxoids had transitions at higher temperatures.

2.3.3. Intrinsic Trp Fluorescence Spectroscopy

The tertiary structure of the proteins as a function of temperature was also studied by measuring the intensity and peak position of their Trp emission (Figure 2.9). There are 25 Trp residues in toxin A and 16 in toxin B. Monitoring of Trp emission at elevated temperature was not possible for toxin/toxoid A at all pH values and toxin/toxoid B at pH 5.0-5.5 due to broadening of the emission peak by excessive light scattering caused by aggregating protein. The onset of emission peak broadening in toxin A occurred at ~ 47.5°C at pH 5.0-6.5 and ~ 50°C at pH 7.0-8.0 (Figure 2.9 a,e). The onset of emission peak broadening in toxoid A was pH dependent and occurred at ~ 47.5°C at pH 5.5, ~ 50°C at pH 6.0, ~ 53°C at pH 6.5, ~ 53°C at pH 7.0, ~ 55°C at pH 7.5 and ~60°C at pH 8.0 (Figure 2.9 b,f). Toxin and toxoid B displayed an onset of emission peak broadening at ~40°C at pH 5.0 and ~ 55°C at pH 5.5 (Figure 2.9 c-h). The emission intensity manifested a stepwise decrease at ~40°C for toxin B and at ~50°C for toxoid B at pH 6.0-7.5. Emission peak positions of toxin B were shifted to lower wavelength at ~30°C prior to a red shift at ~40°C. Toxoid B

produced red shifted emission peak positions at ~50°C. These red shifts of the emission peak position suggest movement of the indole side chains to a more polar environment upon heating. Toxin and toxoid B displayed similar changes in tertiary structure with temperature, with the toxoid showing transitions at about 10°C temperature (Figure 2.9 d,h) .

2.3.4. ANS Fluorescence

The tertiary structure of the proteins was further evaluated by the appearance of previously buried apolar regions using the ability of ANS to bind to more hydrophobic regions of proteins. Protein bound ANS typically displays less solvent-induced quenching of its fluorescence and therefore increased emission intensity and a blue shift of its peak position. ANS emission peak positions in the presence of four proteins at various pH values and temperatures are shown in Figure 2.10. The peak positions at 10°C were blue shifted at lower pH which suggests that the toxins and toxoids had more solvent exposed apolar regions and were partially unfolded at lower pH values. The unfolding of toxin A and exposure of ANS binding moieties upon heating to 40°C was manifested by increased ANS fluorescence intensity and a blue shift in its emission (Figure 2.10 a,e). Data could not be collected at temperatures above 55°C due to extensive emission peak broadening. Toxoid A manifested ANS binding events at about 50°C and the data could not be collected above 60°C (Figure 2.10 b,f). Toxin and toxoid B displayed a pH dependent temperature of transition with low temperature unfolding of protein at lower pH as shown in Figures 2.10 c-i.

The extensive broadening of the emission peek seen for the toxin/toxoid B at pH 5.0-6.0 is manifested by an absence of data at higher temperature. Toxoids A and B again displayed about a 10°C delay in their unfolding compared to the toxin.

2.3.5. Dynamic Light Scattering

The hydrodynamic diameter and polydispersity of the proteins at pH 6.5 and 10°C are summarized in Table 2.2. The theoretical diameter (calculated for a sphere with a partial specific volume of 0.75 ml/mg) is 9.2 nm for toxin A and 8.8 nm for toxin B. Toxin A manifests a significantly larger observed diameter compared to the calculated size. This can probably be explained by the presence of a small amount of high molecular weight aggregated toxin A.[43] The toxoids have smaller hydrodynamic diameters than their corresponding toxins. This presumably reflects a compaction of the toxins from the formaldehyde crosslinking process. The hydrodynamic diameter of toxin/toxoid A increased significantly upon heating, with toxin A displaying an onset of the thermal transition at about 50°C and toxoid A near 60°C (Figure 2.11 a,b). The hydrodynamic diameter of toxin B increased stepwise at about 60°C, whereas the diameter of toxoid B manifests a much smaller increase at about 70°C (Figure 2.11 c,d). Polydispersity of ~0.3 seen in the toxins and toxoids suggest that multiple populations are present in each protein.

2.3.6. Empirical Phase Diagrams (EPDs)

Structural characterization of *C. difficile* toxins and toxoids was performed with multiple techniques to understand both their aggregation tendencies, as well as any changes in secondary and tertiary structure induced by a wide range of pH and temperature conditions.

Toxin A displayed diverse structural behavior at different pH values including partial unfolding at pH 5.5, precipitation upon heating at 40-50°C (OD 350 nm), tertiary structure alteration near ~40-50°C (ANS binding and second derivative UV spectroscopy), and modification of its secondary structure above 50°C. Toxoid A precipitated upon heating at 50-70°C, altered its tertiary structure near 50°C and modified its secondary structure above 55-60°C. To better define the state of each protein as a function of pH and temperature, the OD 350 nm, Trp and ANS fluorescence, and CD data were mathematically processed[40] and visualized in the form of empirical phase diagrams (Figure 2.12). The distinct colors under each condition revealed four distinct regions in the phase diagrams. Consideration of the individual data allowed assignment of the various regions in the phase diagram to individual protein physical states. Based on this analysis, the following structural phases of toxin A are proposed: 1) partially unfolded at pH 5.5; 2) natively folded in the pH range 6-8; 3) a gradual transition between states in the temperature range 45 – 55°C and 4) formation of insoluble aggregates at approximately 55°C. The crosslinked toxoid A displayed the following structural states: 1) partially unfolded at pH 5.5; 2) folded in the pH range 6-8; 3) a transition in form between 50 and 65°C and 4) the presence of insoluble aggregates above 50 – 65°C.

Toxin B also manifested diverse structural characteristics as a function of pH partial unfolding at pH 5-5.5, precipitation at pH 5.0-6.0 upon heating to 45-75°C (OD 350 nm), changes in tertiary structure at ~40°C (Trp fluorescence, ANS binding and second derivative UV spectroscopy), and alterations in secondary structure between 25 and 45°C. Toxoid B precipitated at pH 5.0-5.5 upon heating to 50-65°C, altered its tertiary structure at ~50°C, and changed its secondary structure at from 50-60°C.

The color map for toxin B can than be interpreted as follows: 1) partially unfolded at pH 5.0-5.5; 2) unaltered in the pH range 6.0-7.5; 3) changing states within the temperature range 45-50°C; 4) becoming insoluble at pH 5.0-6.0 and at temperatures above of 45-60°C; and 5) forming soluble aggregates at pH 6.5-7.5 and at temperatures above 50°C. The corresponding phase diagram for toxoid B provides the related structural description: 1) partially unfolded at pH 5.0; 2) folded in the pH range 5.5-7.5; 3) transition at 50-65°C; 4) insoluble aggregate appearance at pH 5.0 and 5.5 and at temperatures above 55-60°C; and 5) soluble aggregate formation over the pH range 6-7.5 at temperatures above 60°C.

2.4. Disscussion

These biophysical studies of *C. difficile* toxins and toxoids A and B permitted their systematic characterization over a wide range of pH and temperature. This picture is summarized and visualized as EPDs in Figure 2.12. This work shows that

the A and B toxins are partially unfolded at low pH (5-5.5) and folded in a presumably native form at pH 6-8. These observations are consistent with previously reported pH-induced conformational changes of toxin B in early endosomes.[23-25] Circular dichroism studies of the two toxins demonstrate that they possess a complex secondary structure with significant helical, ß-sheet and unordered character. The observed CD spectra can be explained by the diverse structure of the toxins, in which each domain presents a unique contribution. The amino-terminal catalytic portion of toxin B consists of 543 residues which are arranged in a mixed α/ß-structure of 11 ß-strands in the core and 21 α-helices on the periphery.[26] The 39 repeats in the carboxy-terminal domain (960 residues) from toxin A are arranged in the form of a ß-selenoid fold.[22] The absence of information on the middle part of the toxins (~1207 residues) permits the extrapolation that the observed large overall helical character of the toxins appears to be a contribution from a combination of the amino-terminal domain and undefined middle parts of the proteins.

Even though the A and B toxins have 49% amino acid identity and possess a similar domain organization, they display some different properties and quite distinct thermal behavior. Toxin A displayed a hydrodynamic diameter twice that of toxin B although we presume this to be from the presence of a small amount of aggregates. In terms of thermal stability, toxin A possesses a tendency to precipitate upon heating at all pH values while toxin B only precipitated at pH 5-6 and formed soluble aggregates at pH 6.5-7.5. The observed dissimilarities between the toxins could be related to

differences in their structure (carboxy-terminal domain), mechanisms of action (enterotoxicity in animals) and their enzymatic activity (velocity and extent)[20].

Crosslinking of the two toxins with formaldehyde led to the formation of toxoids with slightly more compact hydrodynamic diameters but surprisingly similar properties. This is especially important in the use of the toxoids as vaccines since it is essential to maintain their structural identity as immunogenes. Toxoid A was subjected to the formation of insoluble aggregates at more elevated temperatures compared to toxin A. Unlike toxin B, toxoid B precipitated upon heating only at pH 5.0-5.5. The temperature induced secondary and tertiary structural changes in toxoid B were delayed by 10-15°C compared to toxin B. These observations suggest that formaldehyde crosslinking stabilizes the structure of the *C. difficile* toxoids. The observed superior thermal stability of *C. difficile* toxoids seen here is consistent with previously reported effects of crosslinking on diphtheria toxoid[35,38] and could be related to both a direct stabilizing effect of crosslinking on folding and inhibition of electrostatically driven unfolding (especially due to loss of charges on Lys residues).[44]

The studies indicate that at pH 6-7.5 below 50°C the toxoids are in a folded state. These results can be used to develop more physically stable formulations by selection of accelerated stability conditions for subsequent excipient screening studies as described in the following paper.[45]

2.5. Conclusions

This study of *C.difficile* toxins A and B demonstrates both similarities (secondary structure and low pH induced partial unfolding) and differences (stability and thermal behavior) between the two toxins. The superiority of the formaldehyde crosslinked toxoids' thermal stability illustrates the power and utility of this approach for vaccine development.

2.6. Bibliography

1. Todar K. 2005. Todar's online textbook of bacteriology. ed.: University of Wisconsin-Madison Department of Bacteriology.

2. Kuijper EJ, Coignard B, Tull P 2006. Emergence of Clostridium difficile-associated disease in North America and Europe. Clinical Microbiology and Infection 12(Suppl. 6):2-18.

3. Drudy D, Fanning S, Kyne L 2007. Toxin A-negative, toxin B-positive Clostridium difficile. Int. J. Infect. Dis. 11(1):5-10.

4. Warny M, Pepin J, Fang A, Killgore G, Thompson A, Brazier J, Frost E, McDonald LC 2005. Toxin production by an emerging strain of Clostridium difficile associated with outbreaks of severe disease in North America and Europe. Lancet 366(9491):1079-1084.

5. Dove CH, Wang SZ, Price SB, Phelps CJ, Lyerly DM, Wilkins TD, Johnson JL 1990. Molecular characterization of the Clostridium difficile toxin A gene. Infect Immun 58(2):480-488.

6. Barroso LA, Wang SZ, Phelps CJ, Johnson JL, Wilkins TD 1990. Nucleotide sequence of Clostridium difficile toxin B gene. Nucleic Acids Res 18(13):4004.

7. Jodlowski TZ, Oehler R, Kam LW, Melnychuk I 2006. Emerging therapies in the treatment of Clostridium difficile-associated disease. Ann Pharmacother 40(12):2164-2169.

8. Pepin J 2006. Improving the treatment of Clostridium difficile-associated disease: where should we start? Clin Infect Dis 43(5):553-555.

9. Kyne L, Kelly CP 2001. Recurrent Clostridium difficile diarrhoea. Gut 49(1):152-153.

10. Giannasca PJ, Warny M 2004. Active and passive immunisation against Clostridium difficile diarrhoea and colitis. Old Herborn University Seminar Monograph 17(Possibilities for Active and Passive Vaccination Against Opportunistic Infections):91-105.

11. Lyerly DM, Bostwick EF, Binion SB, Wilkins TD 1991. Passive immunization of hamsters against disease caused by Clostridium difficile by use of bovine immunoglobulin G concentrate. Infect Immun 59(6):2215-2218.

12. Sougioultzis S, Kyne L, Drudy D, Keates S, Maroo S, Pothoulakis C, Giannasca Paul J, Lee Cynthia K, Warny M, Monath Thomas P, Kelly Ciaran P. 2005. Clostridium difficile toxoid vaccine in recurrent C. difficile-associated diarrhea. ed., United States: Gastroenterology Division, Beth Israel Deaconess Medical Center, Harvard Medical School, Boston, Massachusetts, 02215,USA. p 764-770.

13. Torres JF, Thomas WD, Jr., Lyerly DM, Giel MA, Hill JE, Monath TP 1996. Clostridium difficile vaccine: influence of different adjuvants and routes of immunization on protective immunity in hamsters. Vaccine Research 5(3):149-162.

14. Torres JF, Lyerly DM, Hill JE, Monath TP 1995. Evaluation of formalin-inactivated Clostridium difficile vaccines administered by parenteral and mucosal routes of immunization in hamsters. Infect Immun 63(12):4619-4627.

15. Kotloff KL, Wasserman SS, Losonsky GA, Thomas W, Jr., Nichols R, Edelman R, Bridwell M, Monath TP 2001. Safety and immunogenicity of increasing doses of a Clostridium difficile toxoid vaccine administered to healthy adults. Infect Immun 69(2):988-995.

16. Just I, Gerhard R 2004. Large clostridial cytotoxins. Rev. Physiol. Biochem. Pharmacol. 152:23-47.

17. Just I, Gerhard R 2006. Clostridium difficile toxins A and B: modulation of intracellular signal cascades. Crossroads between Bacterial Protein Toxins and Host Cell Defences:43-56.

18. Just I, Selzer J, Wilm M, von Eichel-Streiber C, Mann M, Aktories K 1995. Glucosylation of Rho proteins by Clostridium difficile toxin B. Nature (Lond) 375(6531):500-503.

19. von Eichel-Streiber C, Boquet P, Sauerborn M, Thelestam M 1996. Large clostridial cytotoxins--a family of glycosyltransferases modifying small GTP-binding proteins. Trends Microbiol 4(10):375-382.

20. Warny M, Kelly CP 2003. Pathogenicity of Clostridium difficile toxins. Microbial Pathogenesis and the Intestinal Epithelial Cell:503-524.

21. Greco A, Ho JGS, Lin S-J, Palcic MM, Rupnik M, Ng KKS 2006. Carbohydrate recognition by Clostridium difficile toxin A. Nat. Struct. Mol. Biol. 13(5):460-461.

22. Ho JGS, Greco A, Rupnik M, Ng KKS 2005. Crystal structure of receptor-binding C-terminal repeats from Clostridium difficile toxin A. Proc Natl Acad Sci U S A 102(51):18373-18378.

23. Walev I, Bhakdi SC, Hofmann F, Djonder N, Valeva A, Aktories K, Bhakdi S 2001. Delivery of proteins into living cells by reversible membrane permeabilization with streptolysin-O. Proc Natl Acad Sci USA 98(6):3185-3190.

24. Barth H, Pfeifer G, Hofmann F, Maier E, Benz R, Aktories K 2001. Low pH-induced formation of ion channels by Clostridium difficile toxin B in target cells. J Biol Chem 276(14):10670-10676.

25. Qa'Dan M, Spyres LM, Ballard JD 2000. pH-induced conformational changes in Clostridium difficile toxin B. Infect Immun 68(5):2470-2474.

26. Reinert DJ, Jank T, Aktories K, Schulz GE 2005. Structural Basis for the Function of Clostridium difficile Toxin B. J Mol Biol 351(5):973-981.

27. Jank T, Giesemann T, Aktories K 2007. Rho-glucosylating Clostridium difficile toxins A and B: new insights into structure and function. Glycobiology 17(4):15-22R.

28. Metz B, Kersten GFA, Hoogerhout P, Brugghe HF, Timmermans HAM, de Jong A, Meiring H, ten Hove J, Hennink WE, Crommelin DJA, Jiskoot W 2004. Identification of Formaldehyde-induced Modifications in Proteins: Reactions with model peptides. J Biol Chem 279(8):6235-6243.

29. Fraenkel-Conrat HL, Cooper M, Olcott HS 1945. Reaction of CH2O with proteins. J Am Chem Soc 67:950-954.

30. Fraenkel-Conrat H, Brandon BA, Olcott HS 1947. The reaction of formaldehyde with proteins. IV. Participation of indole groups. Gramicidin. J Biol Chem 168:99-118.

31. Fraenkel-Conrat H, Olcott HS 1948. Reaction of formaldehyde with proteins. V. Cross-linking between amino and primary amide or guanidyl groups. J Am Chem Soc 70:2673-2684.

32. Fraenkel-Conrat H, Olcott HS 1948. Reaction of formaldehyde with proteins. VI. Cross-linking of amino groups with phenol, imidazole, or indole groups. J Biol Chem 174:827-843.

33. Martin CJ, Lam DP, Marini MA 1975. Reaction of formaldehyde with the histidine residues of proteins. Bioorg Chem 4(1):22-29.

34. Thaysen-Andersen M, Jorgensen SB, Wilhelmsen ES, Petersen JW, Hojrup P 2007. Investigation of the detoxification mechanism of formaldehyde-treated tetanus toxin. Vaccine 25(12):2213-2227.

35. Paliwal R, London E 1996. Comparison of the conformation, hydrophobicity, and model membrane interactions of diphtheria toxin to those of formaldehyde-treated toxin (diphtheria toxoid): formaldehyde stabilization of the native conformation inhibits changes that allow membrane insertion. Biochemistry 35(7):2374-2379.

36. Rappuoli R, Douce G, Dougan G, Pizza M 1995. Genetic detoxification of bacterial toxins: a new approach to vaccine development. Int Arch Allergy Immunol 108(4):327-333.

37. Rappuoli R 1994. Toxin inactivation and antigen stabilization: Two different uses of formaldehyde. Vaccine 12(7):579-581.

38. Kersten G, Jiskoot W, Hazendonk T, Spiekstra A, Westdijk J, Beuvery C 1999. Characterization of diphtheria toxoid. Pharmacy and Pharmacology Communications 5(1):27-31.

39. Fan H, Vitharana SN, Chen T, O'Keefe D, Middaugh CR 2007. Effects of pH and Polyanions on the Thermal Stability of Fibroblast Growth Factor 20. Mol. Pharm. 4(2):232-240.

40. Kueltzo LA, Ersoy B, Ralston JP, Middaugh CR 2003. Derivative absorbance spectroscopy and protein phase diagrams as tools for comprehensive protein characterization: A bGCSF case study. J. Pharm. Sci. 92(9):1805-1820.

41. Whitmore L, Wallace BA 2004. DICHROWEB, an online server for protein secondary structure analyses from circular dichroism spectroscopic data. Nucleic Acids Res 32(Web Server):W668-W673.

42. Lobley A, Whitmore L, Wallace BA 2002. DICHROWEB: an interactive web-site for the analysis of protein secondary structure from circular dichroism spectra. Bioinformatics 18(1):211-212.

43. Fiorentini C, Thelestam M 1991. Clostridium difficile toxin A and its effects on cells. Toxicon 29(6):543-567.

44. London E 1992. Diphtheria toxin: membrane interaction and membrane translocation. Biochim Biophys Acta FIELD Full Journal Title:Biochimica et biophysica acta 1113(1):25-51.

45. Salnikova M, S, Joshi S, B, Rytting J, Howard, Acambis cf, Middaugh C, Russell Preformulation Studies of Clostridium difficile Toxoids A and B. J. Pharm. Sci. in preparation.

FIGURES AND TABLES

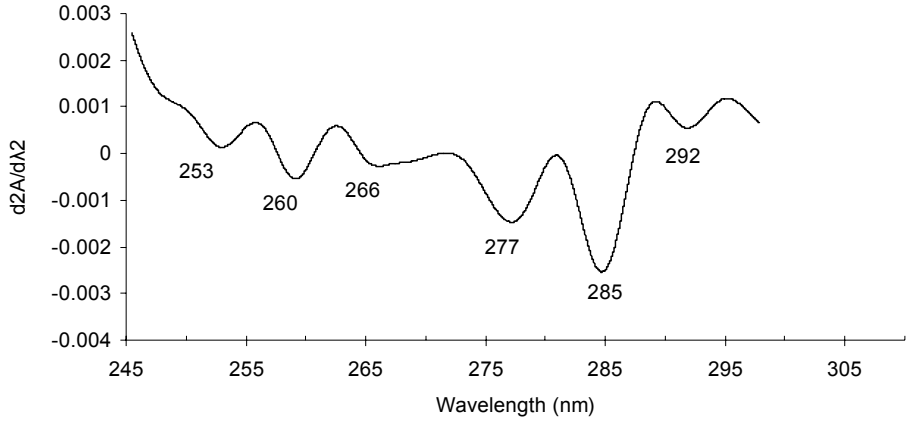

Figure 2.1. Second derivative near-UV absorbance spectrum for toxin/toxoid A and B at 10°C.

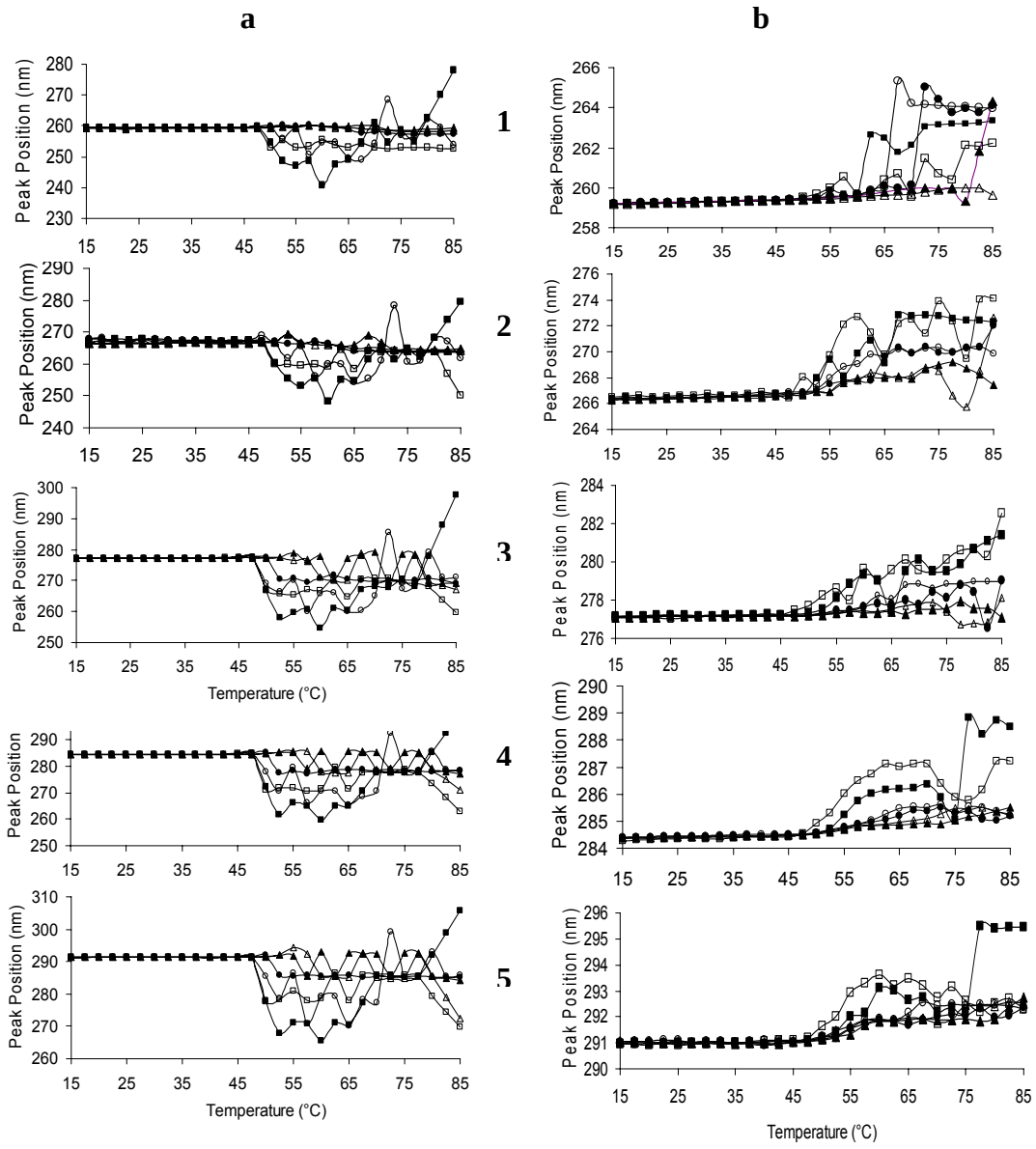

Figure 2.2. Shifts in second derivative UV absorption peak position as a function of temperature for toxin A (a) and toxoid A (b) at pH 5.5 (□), 6.0 (■), 6.5 (○), 7.0 (●), 7.5 (Δ), 8.0 (▲).The figures represent the following negative peaks: (1) 260 nm, Phe; (2) 266 nm, Phe/Tyr; (3) 277 nm, Tyr; (4) 285 nm, Tyr/Trp; (5) 293 nm, Trp. The thermal traces represent an average of two measurements, where each data point had standard error of less than 0.5. Peak position scale was adjusted to reflect the changes.

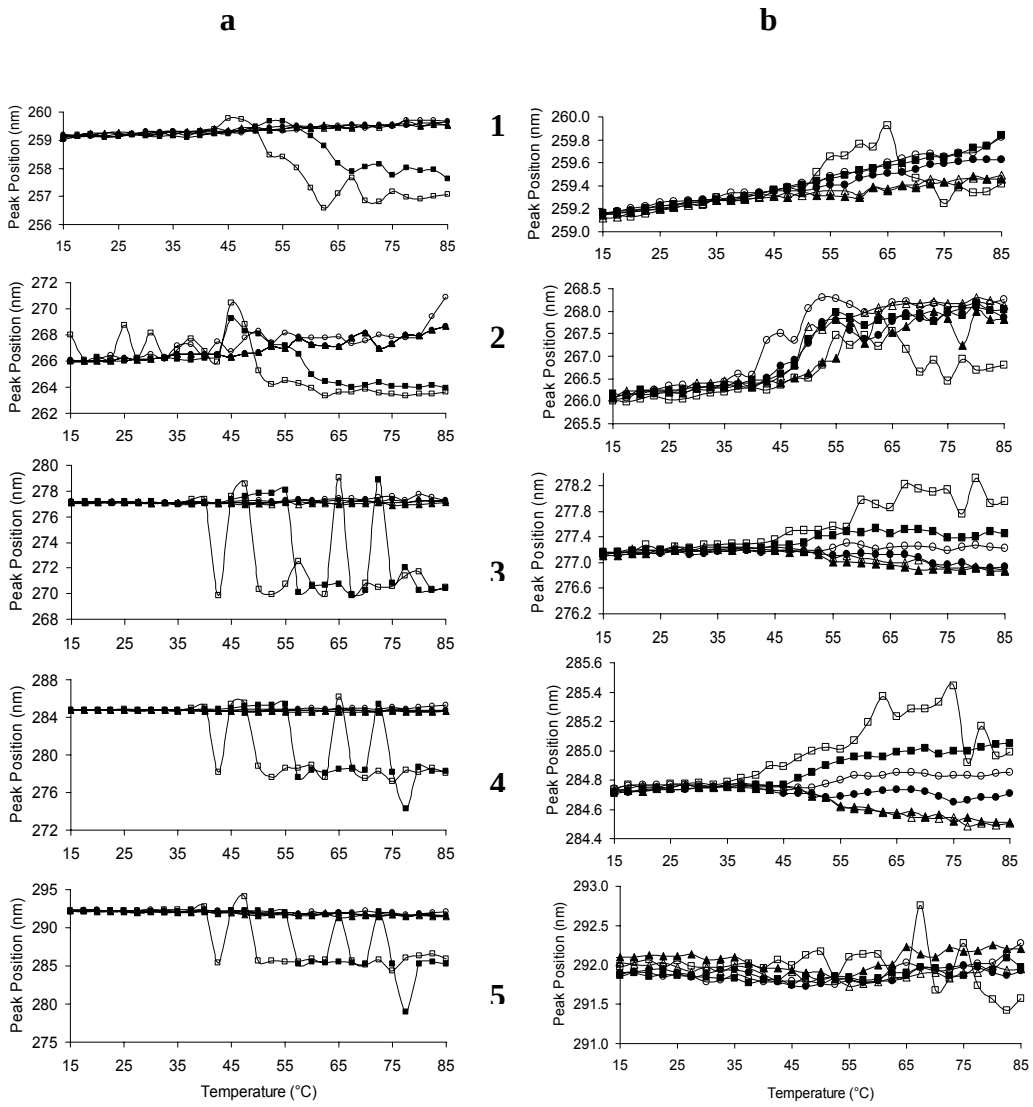

Figure 2.3. Shifts in second derivative UV absorption peak position as a function of temperature for toxin B (a) and toxoid B (b) at pH 5.0 (□), 5.5 (■), 6.0 (○), 6.5 (●), 7.0 (Δ), 7.5 (▲).The figures represent the following negative peaks: (1) 260 nm, Phe; (2) 266 nm, Phe/Tyr; (3) 277 nm, Tyr; (4) 285 nm, Tyr/Trp; (5) 293 nm, Trp. The thermal traces represent an average of two measurements, where each data point had standard error of less than 0.5. Peak position scale was adjusted to reflect the changes.

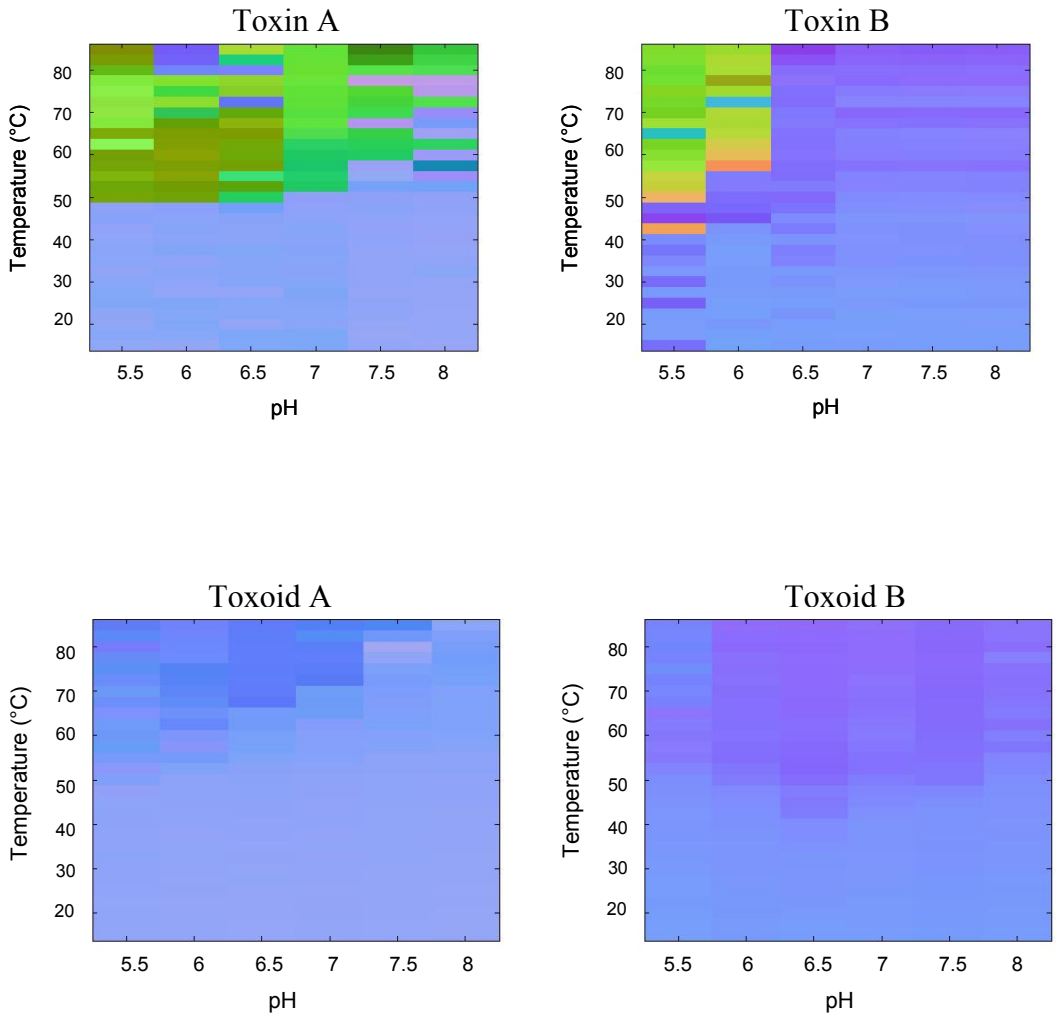

Figure 2.4. High resolution second derivative near UV spectroscopy peak positions based empirical phase diagrams for toxin/toxoid A and toxin/toxoid B (the data for the corresponding toxin and toxoid was normalized simultaneously).

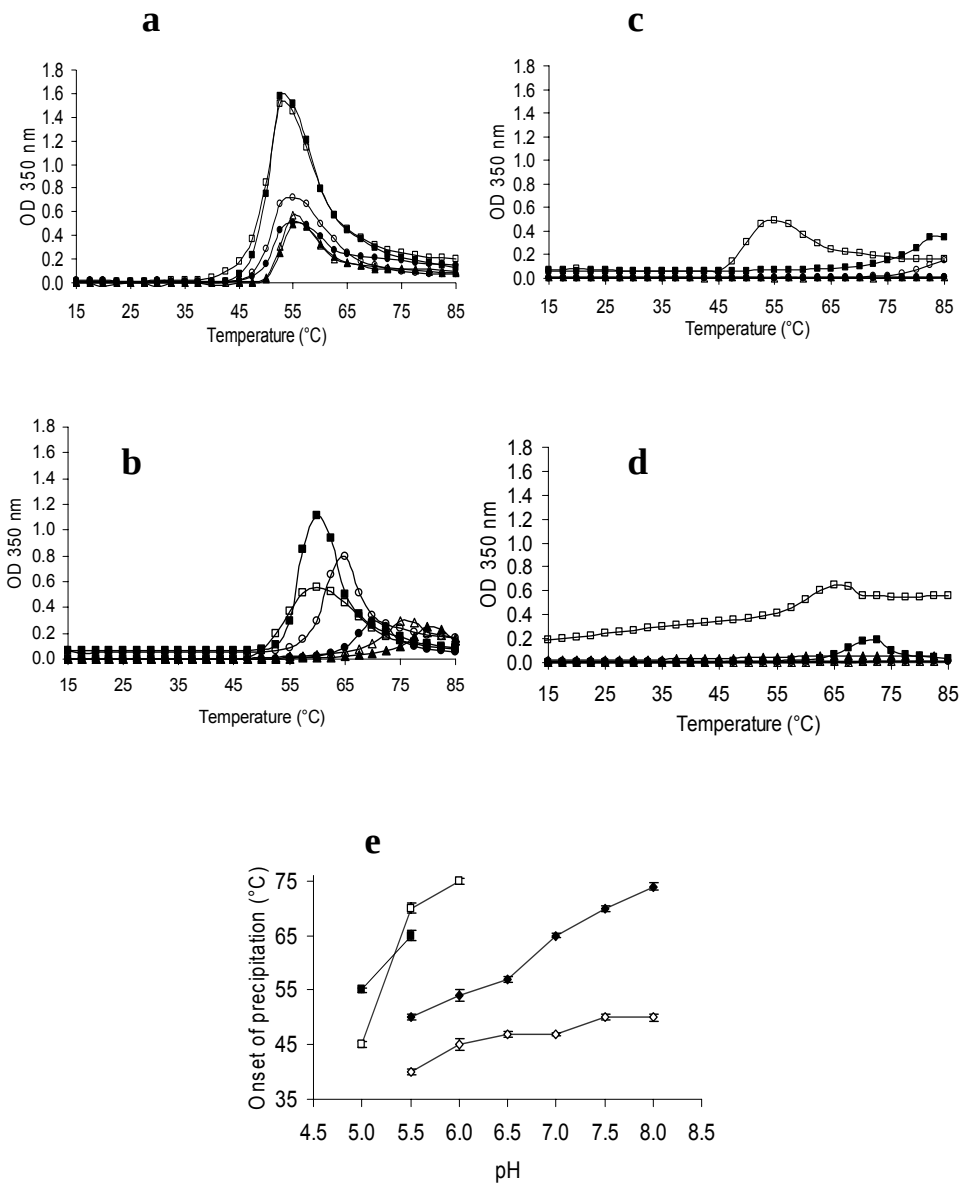

Figure 2.5. Traces of optical density at 350 nm as a function of temperature for toxin A (a) and toxoid A (b) at pH 5.5 (□), 6.0 (■), 6.5 (○), 7.0 (●), 7.5 (Δ), 8.0 (▲); and toxin B (c) and toxoid B (d) at pH 5.0 (□), 5.5 (■), 6.0 (○), 6.5 (●), 7.0 (Δ), 7.5 (▲).The thermal traces represent an average of two measurements, where each data point had standard error of less than 0.05. Onset of precipitation (e), where the temperature is encoded by rhomb for toxin A, filled rhomb for toxoid A, square for toxin B and filled square for toxoid B.

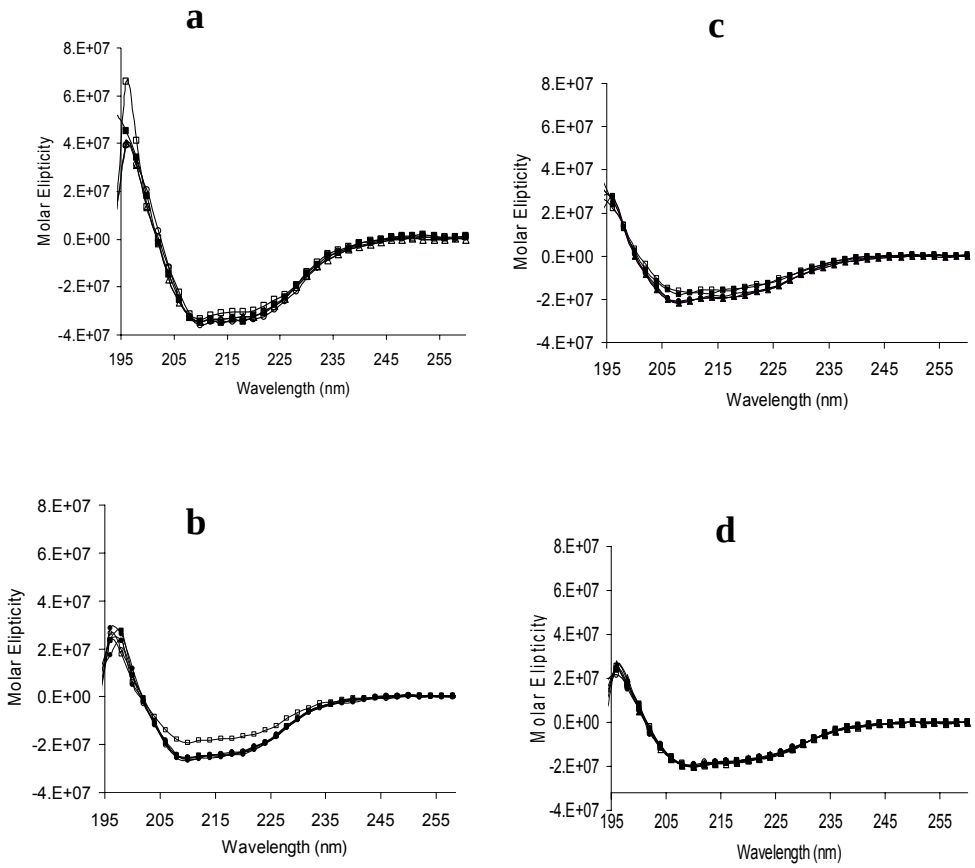

Figure 2.6. CD spectra at 10°C for toxin A (a) and toxoid A (b) at pH 5.5 (□), 6.0 (■), 6.5 (○), 7.0 (●), 7.5 (Δ), 8.0 (▲); and toxin B (c) and toxoid B (d) at pH 5.0 (□), 5.5 (■), 6.0 (○), 6.5 (●), 7.0 (Δ), 7.5 (▲).The thermal traces represent an average of two measurements, where each data point had standard error of less than 0.05.

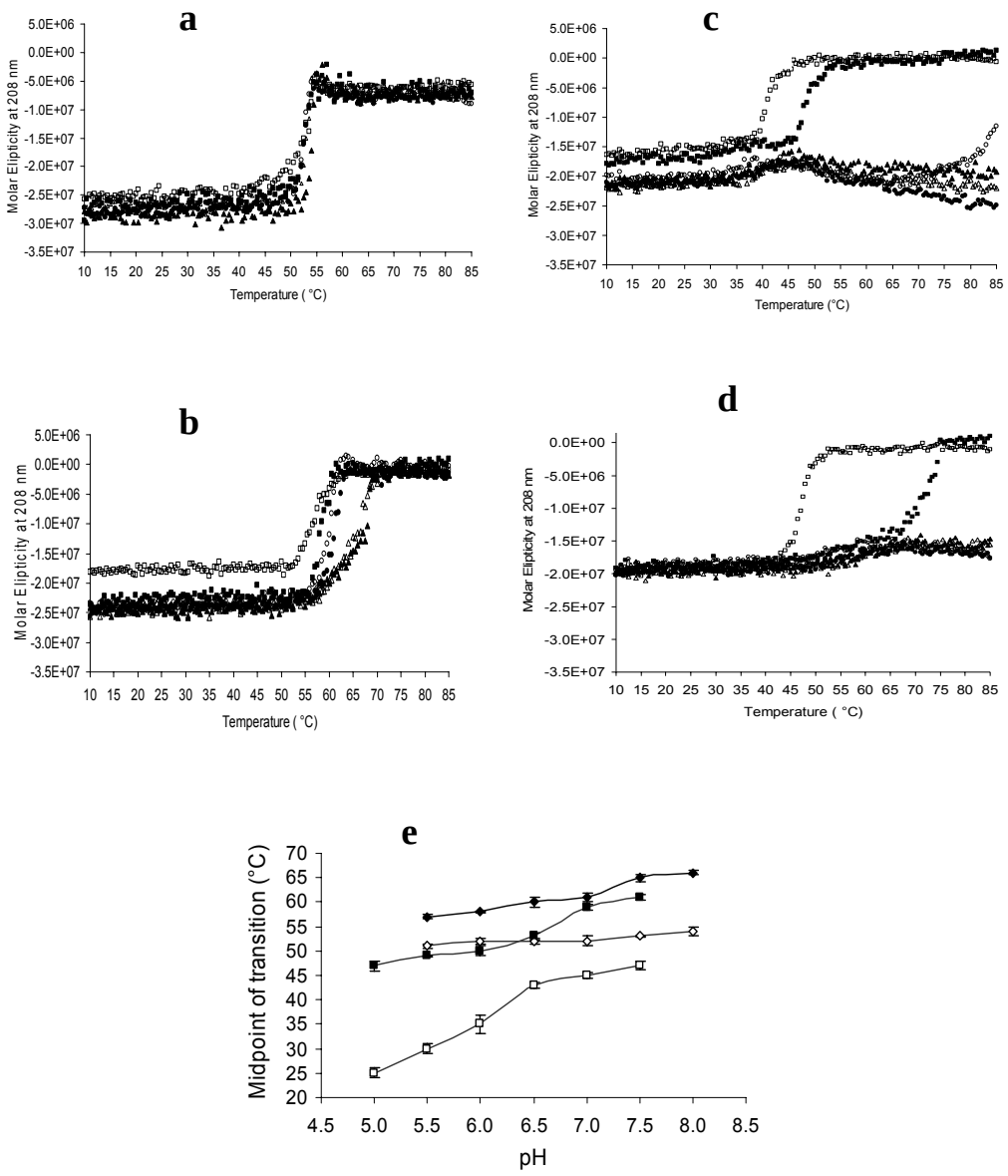

Figure 2.7. CD trace at 208 nm over the temperature range for toxin A (a) and toxoid A (b) at pH 5.5 (□), 6.0 (■), 6.5 (○), 7.0 (●), 7.5 (Δ), 8.0 (▲); and toxin B (c) and toxoid B (d) at pH 5.0 (□), 5.5 (■), 6.0 (○), 6.5 (●), 7.0 (Δ), 7.5 (▲).The thermal traces represent an average of two measurements, where each data point had standard error of less than 0.25. Midpoints of thermal transitions (e), where the temperature is encoded by rhomb for toxin A, filled rhomb for toxoid A, square for toxin B and filled square for toxoid B.

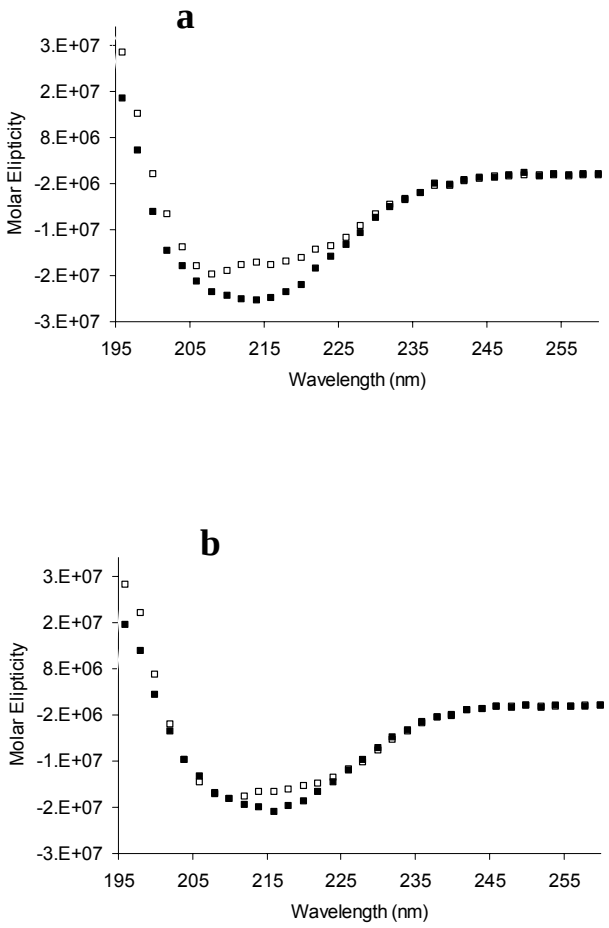

Figure 2.8. CD spectra at 10°C for toxin B (a) and toxoid B (b) at pH 7.0: before melt (□), after melt (■). Each spectrum represents an average of two measurements, where each data point had standard error of less than 0.05.

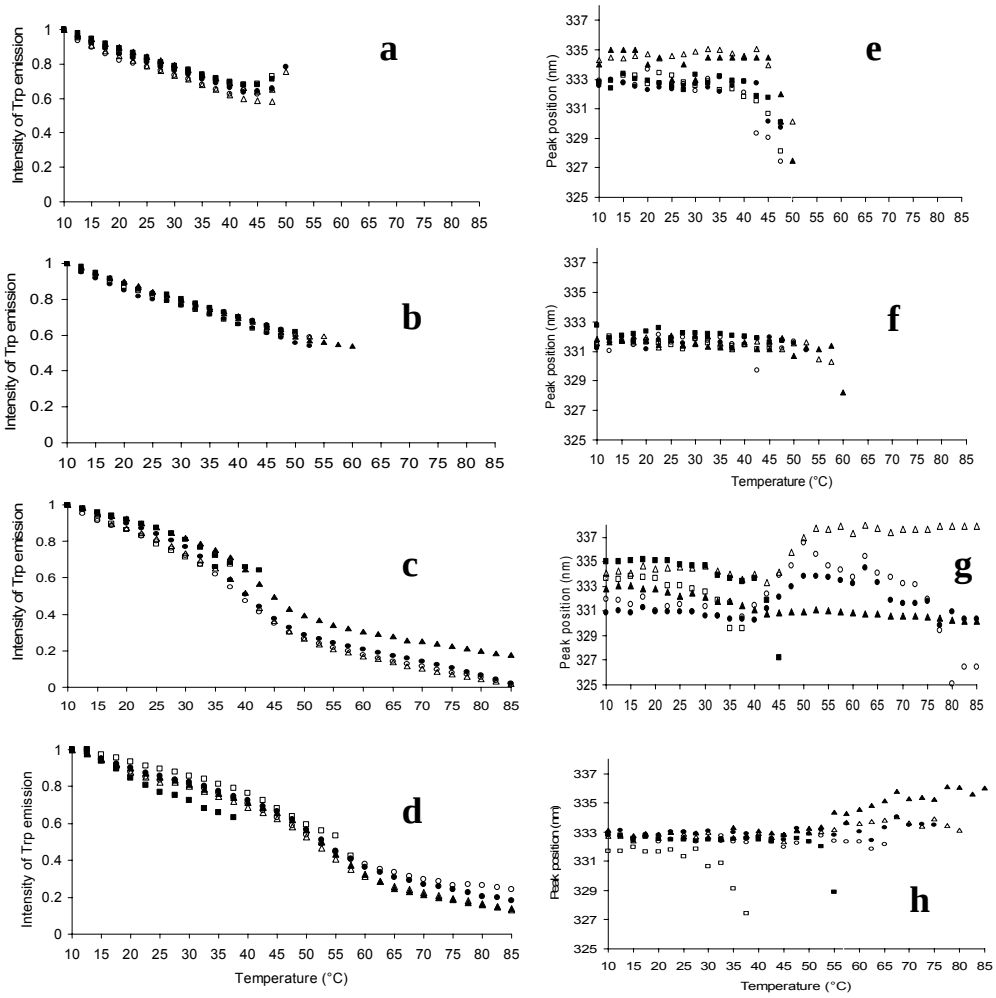

Figure 2.9. Trp fluorescence as a function of temperature: (a-d) normalized emission peak intensity change and (e-h) emission peak position change for toxin A (a,e) and toxoid A (b,f) at pH 5.5 (□), 6.0 (■), 6.5 (○), 7.0 (●), 7.5 (Δ), 8.0 (▲); and toxin B (c,g) and toxoid B (d,h) at pH 5.0 (□), 5.5 (■), 6.0 (○), 6.5 (●), 7.0 (Δ), 7.5 (▲). The thermal traces represent an average of two measurements, where each data point had standard error of less than 0.5.

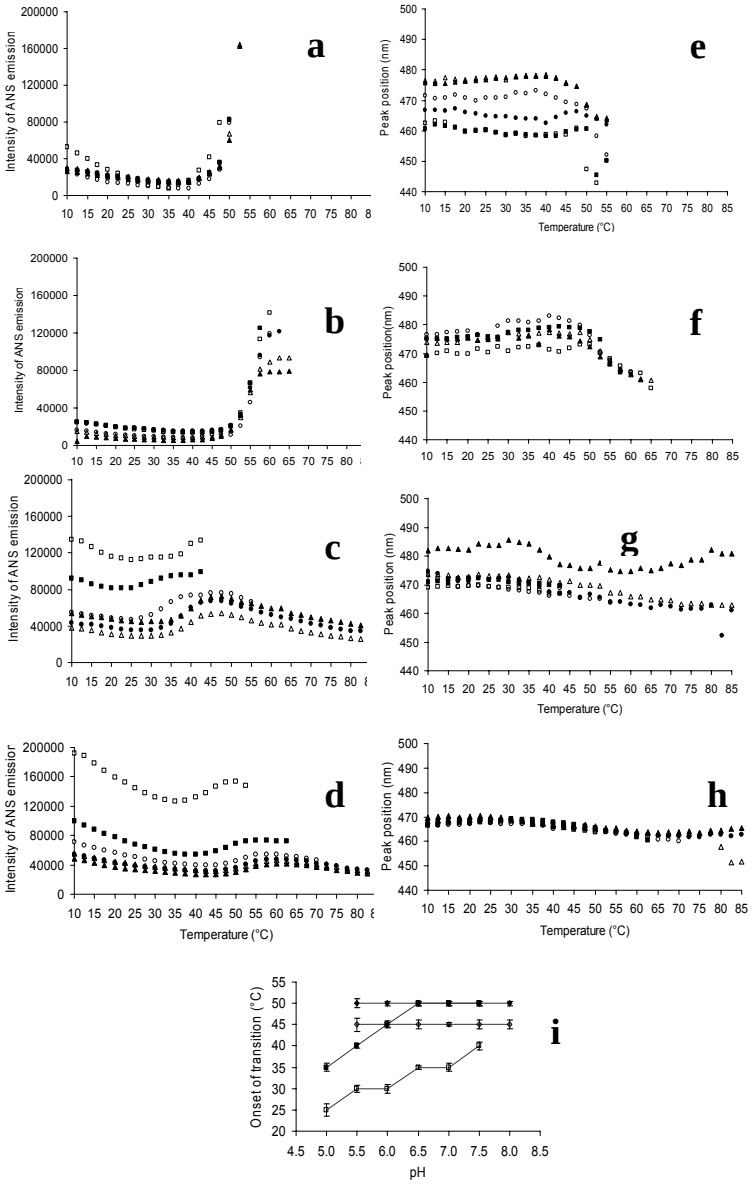

Figure 2.10. ANS fluorescence as a function of temperature: (a-d) emission peak intensity change and (e-h) emission peak position change for toxin A (a,e) and toxoid A (b,f) at pH 5.5 (□), 6.0 (■), 6.5 (○), 7.0 (●), 7.5 (Δ), 8.0 (▲); and toxin B (c,g) and toxoid B (d,h) at pH 5.0 (□), 5.5 (■), 6.0 (○), 6.5 (●), 7.0 (Δ), 7.5 (▲). The thermal traces represent an average of two measurements where each data point has standard error of less than 0.5. Onsets of thermal transitions (i), where the temperature is encoded by rhomb for toxin A, filled rhomb for toxoid A, square for toxin B and filled square for toxoid B.

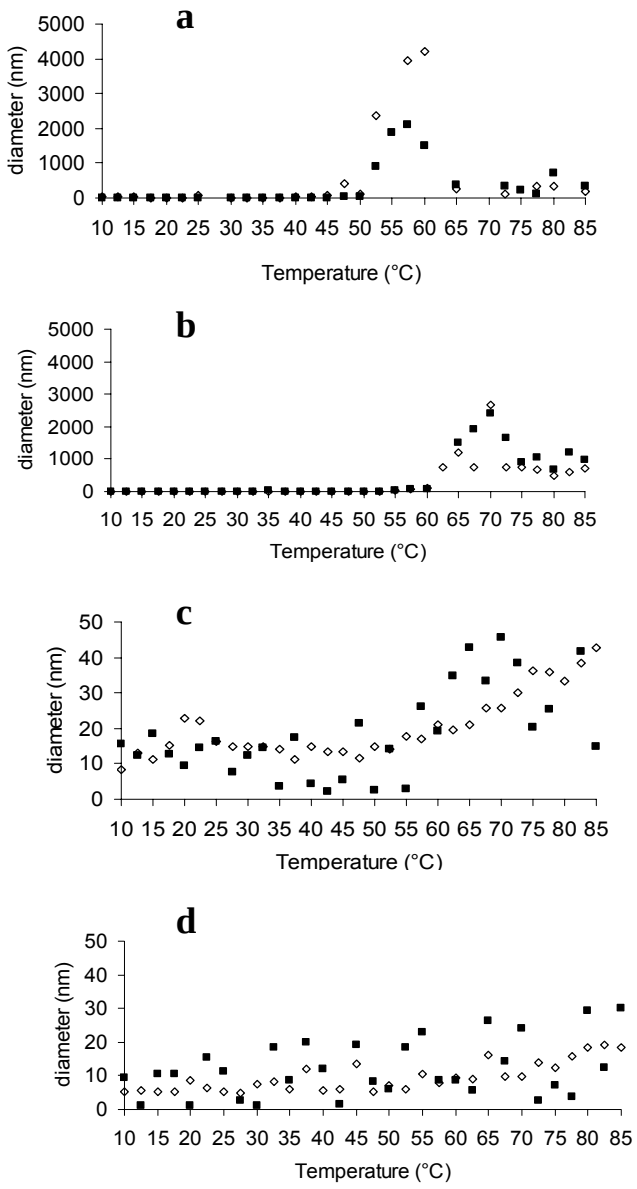

Figure 2.11. Hydrodynamic diameter as a function of temperature: for toxin A (a), toxoid A (b), toxin B (c) and toxoid B (d); MSD Number based(■) and Lognormal Number based (◊). The thermal traces represent an average of two measurements where each data point has standard error of less than 1.0. Note that in figure A and B sizes estimated above 1000 nm are not reliable.

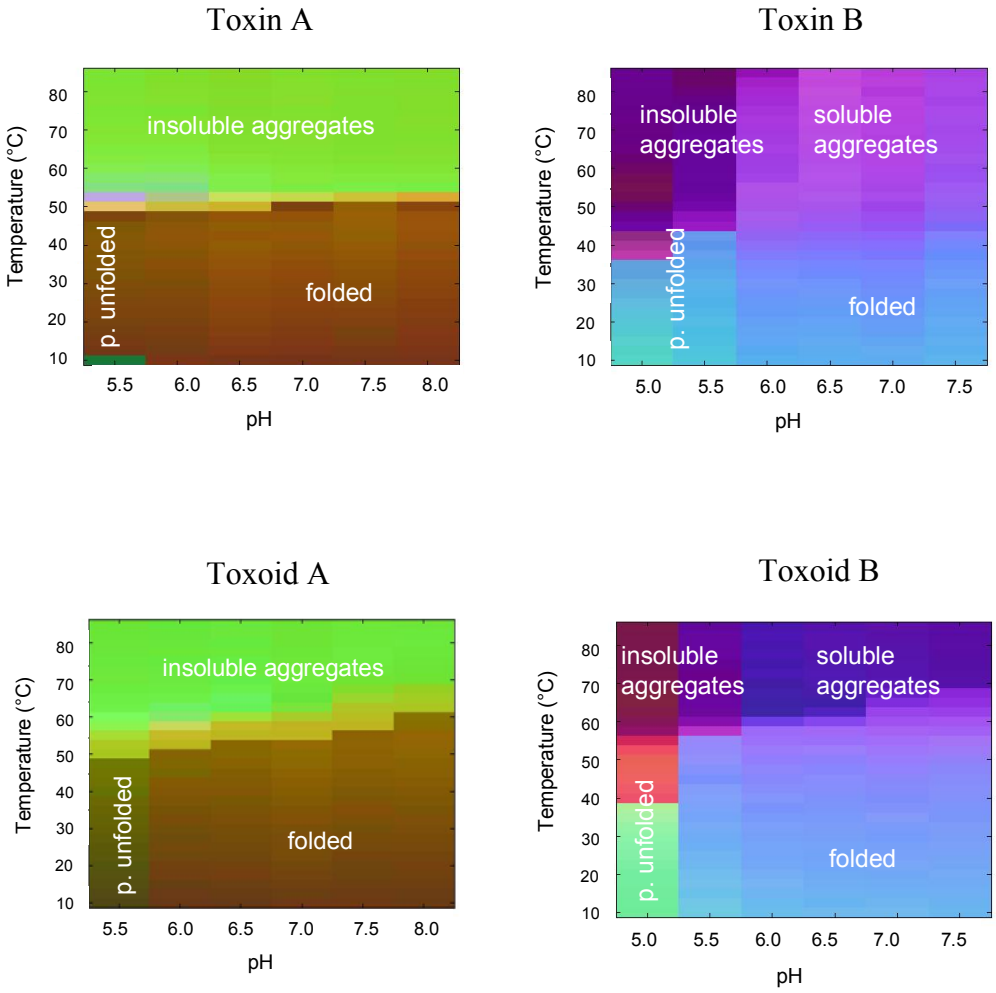

Figure 2.12. Empirical phase diagram created using OD 350, Trp and ANS fluorescence, and CD data for toxins/toxoids A and B (p.unfolded stands for partially unfolded). Data was normalized simultaneously for the corresponding toxin and toxoid.

Table 2.1. Secondary structure assignment with DICHROWEB (estimated error is ±2-3%). Note that CD measurements were performed on protein in 5 mM sodium phosphate buffer pH 7.0. *Assignment of secondary structure in previously heated protein.

	%			
	helix	sheet	turns	unordered
Toxin A	32	23	22	22
Toxoid A	32	25	19	24
Toxin B	36	21	18	25
Toxoid B	36	18	18	28
Toxin B*	8	35	23	33
Toxoid B*	7	34	25	33

Table 2.2. Lognormal Number based mean hydrodynamic diameter and polydispersity for toxins/toxoids A and B.

	Mean Diameter (nm)	Polydispesity
Toxin A	24.9 ±0.6	0.298 ±0.05
Toxoid A	9.6 ±0.7	0.206 ±0.06
Toxin B	8.4 ±0.5	0.315 ±0.02
Toxoid B	5.1 ±0.4	0.271 ±0.04

Chapter 3:

Preformulation Studies of *Clostridium difficile* Toxoids A and B.

3.1. Introduction

Clostridium difficile (*C. difficile*) toxins A and B are responsible for *C. difficile*-associated disease (CDAD), which manifests itself as nosocomial diarrhea and pseudomembranous colitis.[1-5] Treatment of the toxins with formaldehyde results in the corresponding toxoids A and B which are completely inactivated and possess at least partial retention of their immunogenicity.[6] It has been shown that vaccination employing both toxoids is effective in hamsters, healthy adults and patients with recurrent CDAD.[6-9] Additionally, the administration of both free and aluminum salt (adjuvant) bound toxoids leads to appropriate immune responses.[9,10] The administration of both toxoids simultaneously is more effective than administration of the individual proteins.[11]

Since both the A and B toxoids are current candidates for vaccine development, a comprehensive study of their structures as a function of pH and temperature has been reported earlier.[12] This study identified different physical states of the toxoids under the various conditions examined and established their superior thermal stability compared to the corresponding toxins. Even though the crosslinked toxoids reside in a presumably native-like folded state and exhibit some physical stability at pH 6-7.5, improvement of their conformational integrity and a reduction in their tendency to aggregate is clearly desirable to produce optimal storage stability.

In the previously indicated studies, a tendency for both of the toxoids to form aggregates at low pH and elevated temperatures was seen.[12] This appears to be the prevalent pathway of physical degradation of both toxoids. Thus, in this work an

aggregation assay was selected to screen for stabilizers. Approximately 30 GRAS (generally regarded as safe) compounds at various concentrations and in several combinations were examined for their ability to inhibit the aggregation of the toxoids. Compounds which effectively inhibited aggregation of both toxoids were further investigated for their ability to enhance the structural stability of the proteins. To identify stabilizing agents for adjuvant bound toxoids, selected exipients were further studied for their ability to enhance the thermal stability of adjuvant bound toxoids.

3.2. Experimental methods

3.2.1. Materials

Toxoids A and B were produced in highly purified form by Acambis Inc. (Cambridge, MA). The production and purification of this material is described elsewhere.[7] The concentration of the proteins was determined by UV absorbance at 280 nm using extinction coefficients of 1.173 for toxoid A and 0.967 for toxoid B. All reagents used were of analytical grade and were purchased from Sigma (St. Louis, MO). Sodium phosphate buffer (5 mM, pH 5.0, 5.5 and 6.5) containing 150 mM NaCl was used for the excipient screening studies. Sodium phosphate buffer (5 mM, pH 6.5) containing 150 mM NaCl was used for the agitation and adjuvant studies. For buffer exchange, protein was dialyzed at refrigerator temperature using Slide-A-Lyzer® Dialysis Cassettes, 10 kDa MWCO (Pierce, Rockford, IL).

3.2.2. Excipient Screening Studies

3.2.2.1. Aggregation Assay.

Approximately 30 GRAS (generally regarded as safe) compounds in 58 variations of concentration and in several combinations were screened for their ability to inhibit the aggregation of the toxoids. Aggregation of the protein was monitored by optical density measurements at 350 nm (OD 350 nm) using a 96-well plate reader (Spectra Max M5, Molecular Devices, Sunnyvale, CA). The aggregation assay was performed at pH 5.5 for toxoid A (1.2 mg/ml) and at pH 5.0 for toxoid B (0.5 mg/ml) at 55°C. These conditions were selected based upon the phase boundaries observed in the empirical phase diagrams reported previously.[12] Under these conditions, the proteins are partially unfolded and spontaneously associate. Thus, any stabilizing influence of the excipients that perturbs these two processes can be potentially detected. In a 96-well plate, the protein was added to wells containing excipient(s) at the corresponding pH and the samples were incubated at 55°C for 75 min in case of toxoid A and 55 min for toxoid B. The optical density of the solutions was monitored at 350 nm every 5 min. Controls of protein solutions without added compounds and buffer alone with excipient(s) were examined simultaneously. The measurements were corrected for intrinsic buffer-excipient behavior by subtracting the blanks prior to data analysis. Each sample was evaluated in triplicate. Percent inhibition of aggregation was calculated employing the following expression:

$$\%\text{inhibition of aggregation} = 100 - \left[\frac{\Delta OD_{350}\,(E)}{\Delta OD_{350}\,(C)} \times 100 \right]$$

Where ΔOD_{350} (E) represents the change in OD 350 nm of the protein in the presence of the excipient and ΔOD_{350} (C) the change in OD 350 nm of the protein without excipient.[13]

3.2.2.2. Structural Stability Studies.

Toxoid solutions were studied at a concentration of 0.2 mg/ml for CD measurements and 0.1 mg/ml for fluorescence and UV absorption analysis. No concentration dependence was seen over this range. Each sample was evaluated in duplicate to ensure reproducibility of the measurements.

3.2.2.2.1. Far-UV Circular Dichroism (CD) Spectroscopy.

CD spectra were acquired using a Jasco J-810 spectropolarimeter equipped with a 6-position Peltier temperature controller. CD spectra were obtained from 260-190 nm with a scanning speed of 20 nm/min, an accumulation of 2 scans and a 2 s response time. The CD signal at 208 nm was monitored every 0.5°C over a 10 to 85°C temperature range employing a temperature ramp of 15°C/hr to study thermal transitions (melting curves) of the proteins (in sealed cuvettes with 0.1 cm pathlength). The CD signal was converted to molar elipticity by Jasco Spectral

Manager software. The midpoint temperature of the thermal transition was obtained from a sigmoid fitting of the melting curves using Origin software.

3.2.2.2.2. ANS Fluorescence Spectroscopy.

Accessibility of apolar sites on the proteins was monitored by fluorescence emission of the extrinsic probe 8-Anilino-1-naphthalene sulfonate (ANS). Each sample contained a 20-fold molar excess of ANS to protein. The emission spectra were collected from 400 to 600 nm with a step size of 2 nm and a 1-s integration time after ANS excitation at 372 nm. Emission spectra were collected every 2.5°C with 5 min of equilibration over a temperature range of 10 to 85°C. The ANS-buffer baseline at each corresponding pH was subtracted from the raw emission spectra. Peak positions of the emission spectra were obtained from polynomial fits using Origin software.

3.2.2.2.3. High-Resolution UV Absorbance Spectroscopy.

High-resolution UV absorbance spectra were acquired using an Agilent 8453 UV-visible spectrophotometer. Aggregation of the proteins was studied by monitoring the OD at 350 nm every 2.5°C over the temperature range of 10 to 85°C with a 5 min incubation (sufficient for equilibrium to be reached) at each temperature.

3.2.2.2.4. Dynamic Light Scattering (DLS).

The mean hydrodynamic diameter of the proteins at pH 6.5 (alone and in presence of excipients) was analyzed using a dynamic light scattering instrument (Brookhaven

Instrument Corp., Holtzille, NY). The instrument was equipped with a 50 mW diode-pumped laser (λ = 532 nm) and the scattered light was monitored at 90° to the incident beam. The autocorrelation functions were generated using a digital auto-correlator (BI-9000AT). The hydrodynamic diameter was calculated from the diffusion coefficient by the Stokes-Einstein equation using the method of cumulants (lognormal number based). The data were fit to a non-negatively constrained least squares algorithm to yield multi-modal distributions (MSD). The instrument was equipped with a temperature-controlled circulating water bath RTE111 (Neslab, Newington, NH) and the hydrodynamic diameter was monitored over a temperature range of 10 to 85°C.

3.2.2.2.5. Differential Scanning Calorimetry (DSC).

DSC was performed using a MicroCal VPDSC with autosampler (MicroCal, LLC; Northampton, MA). Thermograms of toxoids (0.5 mg/ml) alone and in the presence of excipient(s) were obtained from 10-90°C using a scan rate of 60°C/hr. The filled cells were equilibrated for 15 min at 10°C before beginning each scan. Thermograms of the buffer alone were subtracted from each protein scan prior to analysis.

3.2.2.2.6. Agitation studies.

Toxoid solutions at a concentration of 0.4 mg/ml were studied in the presence and absence of the excipients. Protein samples (0.4 ml) were placed in 1.5 ml centrifuge tubes and shaken in a rotator (Thermomixer R, Eppendorf AG, Hamburg, Germany)

at 300 rpm for 72 hrs at a constant temperature of 4°C. The concentration of the protein and OD 350 nm were measured before and after the rotation to evaluate adsorption to vessel walls and aggregation. Samples were centrifuged for 10 min at a speed of 10,000xg at 4°C and the concentration and OD 350 nm of the supernatant were measured to detect formation of insoluble aggregates. The structure of the proteins was evaluated by CD. Each sample was measured in duplicate.

3.2.3. Adjuvant Studies

3.2.3.1. Adsorption to Aluminum Hydroxide (Alhydrogel®).

The ability of the toxoids to adsorb to Alhydrogel® (Brenntag Biosectror, Fredericksund, Denmark) at various concentrations (0.025 – 1 mg/ml) was determined by constructing a binding isotherm. The protein solutions in the presence of 0.4 mg/ml Alhydrogel® were tumbled in an end-over-end tube rotator at refrigerator temperature for 20 min. The samples were centrifuged at 14,000xg for 30 s to pellet the adjuvant. The value of the concentration of the protein remaining in the supernatants was used for the construction of binding curves. The ability of protein to bind to the Alhydrogel® in the presence of excipients was determined by the same procedure. In this case, the Alhydrogel® was added to the protein-excipient solution.

3.2.3.2. Desorption of toxoids from Alhydrogel®.

Desorption of the proteins from Alhydrogel® was evaluated in presence of 2 M NaCl. The toxoid Alhydrogel® pellets were prepared as described above. The pellets were washed with buffer (pH 6.5) to remove protein present in the supernatant prior to addition of the NaCl solution. The Alhydrogel® solutions were tumbled in an end-over-end tube rotator at refrigerator temperature for 20 min. The samples were centrifuged at 14,000xg for 30 s to pellet the adjuvant. The concentration of the protein in the supernatants was used for the construction of desorption isotherms.

3.2.3.3. Stability of Toxoids Bound to Alhydrogel®.

The thermal stability of the toxoids bound to Alhydrogel® was monitored with DSC using a MicroCal VP-AutoDSC (MicroCal, LLC, Northampton, MA). Toxoids at 0.5 mg/ml were bound to 0.4 mg/ml Alhydrogel® by the procedure described above. Thermorgams of the toxoids were obtained from 10 to 90°C with a scanning rate of 60°C/hr. The samples were equilibrated for 15 min at 10°C before each scan. Thermograms of the Alhydrogel® alone were subtracted from each protein/adjuvant scan prior to analysis.

3.3. Results and disscussion

3.3.1. Excipient Screening Studies

To investigate the ability of GRAS compounds to prevent/delay aggregation, toxoids were incubated alone and in presence of excipients under the stress conditions

(incubation at 55°C). Aggregation of the toxoids was monitored in a high-throughput fashion by monitoring changes in OD at 350 nm during the incubation time (75 min for toxoid A and 55 min for toxoid B). The turbidity changes were further used to calculate % of aggregation inhibition and are summarized in Table 3.1 for toxoid A and Table 3.2 for toxoid B.

High-throughput aggregation assays of toxoid A found that more than half of the excipients either delayed or prevented increases of OD 350 nm over time and led to inhibition of aggregation by 90% or more (Table 3.1). Among the excipients examined, 2.5% albumin, 2.5% α-cyclodextrin, 0.1% tween 80, 0.3 M histidine and 0.3 M lysine led to instantaneously high OD 350 nm values which suggests that the toxoid A is insoluble under this conditions. The aggregation of the toxoid A was also significantly enhanced in the presence of 16 other excipients, among which 25 and 50 mM arginine/glutamine mixture, 0.3 M arginine and 0.3 M proline were especially potent.

Inhibition of toxoid B aggregation by 90% or more occurred in presence of 15 excipients (Table 3.2). The presence of 0.3 M histidine or 0.2 M sodium citrate led to instantaneously high OD 350 nm. Another 20 compounds more gradually induced aggregation during the time monitored. Extremely high increases in OD 350 nm were observed in presence of 0.015 M calcium chloride, 0.15 M ascorbic acid and 0.3 M arginine.

In many cases, the aggregation of both toxoids was facilitated by the same excipients (Table 3.1 and 3.2). In contrast, 5% 2-OH propyl γ-CD, 0.01% and 0.1%

tween 20, 0.15M aspartic acid and 0.3M guanidine facilitated aggregation of toxoid B, but not toxoid A. In addition, aggregation in the presence of 0.015 M calcium chloride was much greater for toxoid B than toxoid A. This may be related to the known increased thermal stability of the toxin A C-terminal domain in the presence of calcium chloride.[14] The dissimilarities between the toxoids in their responses to solute induced aggregation is presumably related to structural differences between the corresponding toxins.[3,15] An absence of inositolphosphates among compounds studied suggests that the observed aggregation of the toxoids does not involve autocatalytic cleavage.[16] Most of the carbohydrates, detergents and cyclodextrins examined inhibited aggregation of the toxoids. The following excipients were found to efficiently inhibit aggregation of both of the toxoids: 20% trehalose, 20% sucrose, 10% sorbitol, 10% dextrose and 20% glycerol.

The above mentioned carbohydrates, sorbitol, glycerol and two surfactants (0.05% / 0.1% tween 80 and 0.1% pluronic F-68) were further studied for their ability to stabilize the protein's secondary and tertiary structure at pH 6.5 by monitoring ANS fluorescence, CD signal changes upon heating and DSC (Figure 3.1 and 3.2). Toxoid A in the presence of 20% sucrose and 20% trehalose produced an earlier onset of secondary structure change, whereas the rest of the excipients delayed the thermal transition by ~2°C (Figure 3.1a). Surprisingly, Toxoid B manifested an earlier onset of secondary structure change only in presence of 20% sucrose while the rest of the excipients delayed the thermal transition by ~1°C (Figure 3.2a). The early onset of the toxoids' secondary structure change in the presence of trehalose and/or sucrose

could be explained by stabilization of partially unfolded state(s) by the solutes. Additionally, the possibility that the toxoids are partially unfolded upon binding to their C-terminal carbohydrate recognition sequence repeats by polysaccharides[17] can not be ruled out. In the case of the structural destabilization by the second mechanism, the dissimilarity of the two toxoids behavior in the presence of trehalose could be related to structural differences between toxoids (the C-terminal domain possesses 30 repeats in toxoid A and 19 repeats in toxoid B)[15]. It is interesting to note that the monosaccharide (dextrose) had a stabilizing effect on the secondary stricture of both toxoids. Temperature-induced unfolding of both toxoids and associated binding of ANS was not influenced by the presence of the compounds (Figure 3.1b, 3.2b). The effect of the detergents on the temperature induced unfolding of the toxoids was monitored with DSC and did not appear to be significant (Figure 3.1c, 3.2c and table 3.3). These observations suggest that the excipients do not strongly stabilize the structure of the toxoids by the well described preferential exclusion mechanism[18,19], but rather inhibit their aggregation by other mechanisms, such as by direct blocking of the protein/protein interactions that are responsible for protein association.

To study the effect of a combination of the more active agents on secondary structure, the results from a mixture of sorbitol, dextrose and tween 80 was characterized by monitoring the toxoid's thermal transitions with CD and aggregation with OD 350 nm (Figures 3.3 and 3.4). The heating of solutions of tween 80 (0.05% or 0.1%) alone in the presence of sorbitol and/or dextrose lead to changes in its

micelle structure, which were manifested by a decrease in the CD signal and increased light scattering as monitored by OD 350 nm (Figure 3.5). The concentration of the excipients had an approximately linear effect on the temperature of the thermal transitions (Figure 3.6). This supports the hypothesis that the excipients prevent aggregation by directly inhibiting protein association. The effects of the excipients on the thermal transition are summarized in Table 3.4 and 3.5. The combination of 10% dextrose and 10% sorbitol in the presence or absence of 0.05% tween 80 tends to delay the midpoint of the thermal transition of both the toxoids to the greatest extent (~4°C for toxoid A and ~10°C for toxoid B) (Figure 3.3). This can be explained by either a synergistic effect and/or the higher total concentration of the stabilizing compounds. In the case of toxoid B, the onset temperature of the transition was not delayed in the presence of combinations of agents, but the midpoint of the thermal transition was significantly delayed. This could be related to a more gradual unfolding of toxoid B in the presence of the two or more excipients. Toxoid A manifested a significant delay of aggregation (monitored with OD 350 nm) in presence of stabilizing compounds (Figure 3.4a). The hydrodynamic diameter of the toxoids in the presence and absence of the excipients was also monitored by DLS (Figure 3.7). Toxoid A manifested a delayed onset of the previously observed hydrodynamic diameter increase in the presence of the excipients (Figure 3.7 a-c), whereas a smaller effect was seen with toxoid B (Figure 3.7 d-f). These observations suggest that the particular combination of potential vaccine excipients tested here stabilizes protein structure by both a preferential hydration mechanism and direct

inhibition of protein association. The use of such stabilizing compounds could potentially increase the physical stability of the toxoids during storage.

3.3.1.1. Agitation studies

The effect of agitation on toxoid physical stability was studied by monitoring protein adsorption to the walls of storage vials, formation of insoluble aggregates and changes in protein thermal stability. An insignificant change in protein concentration, OD 350 nm and in CD melts in the presence and absence of the excipients (not illustrated) indicated that the toxoids do not undergo major physical changes upon application of this agitation-based stress.

3.2.3. Adjuvant Studies

Adjuvant binding isotherms revealed that the toxoids efficiently bind to Alhydrogel® at low concentrations with binding saturated at higher protein concentration (Figure 3.8a). The toxoids at 0.5 mg/ml are 95% or more bound to Alhydrogel®, which allows use of DSC to directly monitor the stability of protein on the surface of the adjuvant. The absence of toxoids desorption upon addition of 2 M NaCl indicates that the interaction of toxoids with Alhydrogel® is not solely electrostatic as is often observed in protein/Aluminum hydroxide interactions[20-22] (Figure 3.8b).

Upon binding to Alhydrogel®, toxoid A manifests no detectable change in its thermal stability, whereas adjuvant bound toxoid B demonstrates a decrease of the

Tm by ~1.4°C. The fraction of Alhydrogel® bound toxoid is somewhat reduced in the presence of the most of the excipients (Table 3.6 and 3.7). This suggests that the excipients partially interfere with toxoid binding to Alhydrogel® perhaps by direct interaction with either the protein and/or adjuvant. The thermal stability of the proteins bound to Alhydrogel® in the presence and absence of the excipients is summarized in Table 3.6 for toxoid A and Table 3.7 for toxoid B. The presence of the excipients perturbed the thermal stability of adjuvant bound toxoids either by decreasing or increasing the transition temperature. A decrease of thermal stability was seen in both toxoids in presence of 10% sorbitol, whereas the presence of 10% sorbitol and 10% dextrose decreases the thermal stability of toxoid B alone. Additionally, tween 80 had a stabilizing effect only in case of adjuvant bound toxoid B. On the other hand, dextrose (10%) had a stabilizing effect on the thermal stability of both toxoids. Interestingly, the combination of the three excipients (10% sorbitol, 10% dextrose with 0.05% or 0.1% tween 80) tends to raise the thermal transition of both adjuvant bound toxoids by 3-4°C and might therefore be a candidate for further formulation development.

3.4. Conclusions

A systematic approach to stabilizer screening resulted in the identification of excipients which improved the thermal stability of both the A and B *Clostridium difficile* toxoids. Studies of Alhydrogel® bound toxoids in the presence of selected excipients identified conditions that produced improved physical stability of the adjuvant bound proteins. This study also generated information concerning the

toxoids physical behavior under a range of conditions (temperature, solute) that could be used to design formulations of enhanced storage stability.

3.5. Bibliography

1. Kuijper EJ, Coignard B, Tull P 2006. Emergence of *Clostridium difficile*-associated disease in North America and Europe. Clinical Microbiology and Infection 12(Suppl. 6):2-18.

2. Drudy D, Fanning S, Kyne L 2007. Toxin A-negative, toxin B-positive *Clostridium difficile*. Int J Infect Dis 11(1):5-10.

3. Warny M, Pepin J, Fang A, Killgore G, Thompson A, Brazier J, Frost E, McDonald LC 2005. Toxin production by an emerging strain of *Clostridium difficile* associated with outbreaks of severe disease in North America and Europe. Lancet 366(9491):1079-1084.

4. Dove CH, Wang SZ, Price SB, Phelps CJ, Lyerly DM, Wilkins TD, Johnson JL 1990. Molecular characterization of the *Clostridium difficile* toxin A gene. Infect Immun 58(2):480-488.

5. Barroso LA, Wang SZ, Phelps CJ, Johnson JL, Wilkins TD 1990. Nucleotide sequence of *Clostridium difficile* toxin B gene. Nucleic Acids Res 18(13):4004.

6. Torres JF, Lyerly DM, Hill JE, Monath TP 1995. Evaluation of formalin-inactivated *Clostridium difficile* vaccines administered by parenteral and mucosal routes of immunization in hamsters. Infect Immun 63(12):4619-4627.

7. Kotloff KL, Wasserman SS, Losonsky GA, Thomas W, Jr., Nichols R, Edelman R, Bridwell M, Monath TP 2001. Safety and immunogenicity of increasing doses of a *Clostridium difficile* toxoid vaccine administered to healthy adults. Infect Immun 69(2):988-995.

8. Sougioultzis S, Kyne L, Drudy D, Keates S, Maroo S, Pothoulakis C, Giannasca PJ, Lee CK, Warny M, Monath TP, Kelly CP. 2005. *Clostridium difficile* toxoid vaccine in recurrent *C. difficile*-associated diarrhea. Gastroenterology 128(3):764-770.

9. Torres JF, Thomas WD, Jr., Lyerly DM, Giel MA, Hill JE, Monath TP 1996. *Clostridium difficile* vaccine: influence of different adjuvants and routes of immunization on protective immunity in hamsters. Vaccine Res 5(3):149-162.

10. Giannasca PJ, Zhang Z-X, Lei W-D, Boden JA, Giel MA, Monath TP, Thomas WD, Jr. 1999. Serum antitoxin antibodies mediate systemic and mucosal protection from *Clostridium difficile* disease in hamsters. Infect Immun 67(2):527-538.

11. Kim PH, Iaconis JP, Rolfe RD 1987. Immunization of adult hamsters against *Clostridium difficile*-associated ileocecitis and transfer of protection to infant hamsters. Infect Immun 55(12):2984-2992.

12. Salnikova MS, Joshi SB, Rytting JH, Warny M, Middaugh CR *submitted*. Physical characterization of *Clostridium difficile* toxins and toxoids - effect of the formaldehyde crosslinking on thermal stability. J Pharm Sci.

13. Peek LJ, Brey RN, Middaugh CR 2006. A rapid, three-step process for the preformulation of a recombinant ricin toxin A-chain vaccine. J Pharm Sci 96(1):44-60.

14. Demarest SJ, Salbato J, Elia M, Zhong J, Morrow T, Holland T, Kline K, Woodnutt G, Kimmel BE, Hansen G 2005. Structural characterization of the cell wall binding domains of *Clostridium difficile* toxins A and B; Evidence that Ca2+ plays a role in toxin A cell surface association. J Mol Biol 346(5):1197-1206.

15. Just I, Gerhard R 2005. Large clostridial cytotoxins. Rev. Physiol. Biochem. Pharmacol. 152:23-47.

16. Reineke J, Tenzer S, Rupnik M, Koschinski A, Hasselmayer O, Schrattenholz A, Schild H, von Eichel-Streiber C 2007. Autocatalytic cleavage of *Clostridium difficile* toxin B. Nature (London) 446(7134):415-419.

17. Greco A, Ho JGS, Lin S-J, Palcic MM, Rupnik M, Ng KKS 2006. Carbohydrate recognition by *Clostridium difficile* toxin A. Nat Struct Mol Biol 13(5):460-461.

18. Timasheff SN 2002. Protein-solvent preferential interactions, protein hydration, and the modulation of biochemical reactions by solvent components. Proc Natl Acad Sci USA 99(15):9721-9726.

19. Timasheff SN 1998. Control of protein stability and reactions by weakly interacting cosolvents: the simplicity of the complicated. Adv Protein Chem 51:355-432.

20. Gupta RK, Rost BE, Relyveld E, Siber GR 1995. Adjuvant properties of aluminum and calcium compounds. Pharm Biotechnol 6:229-248.

21. Seeber SJ, White JL, Hem SL 1991. Predicting the adsorption of proteins by aluminium-containing adjuvants. Vaccine 9(3):201-203.

22. White JL, Hem SL 2000. Characterization of aluminium-containing adjuvants. Dev Biol 103:217-228.

FIGURES AND TABLES

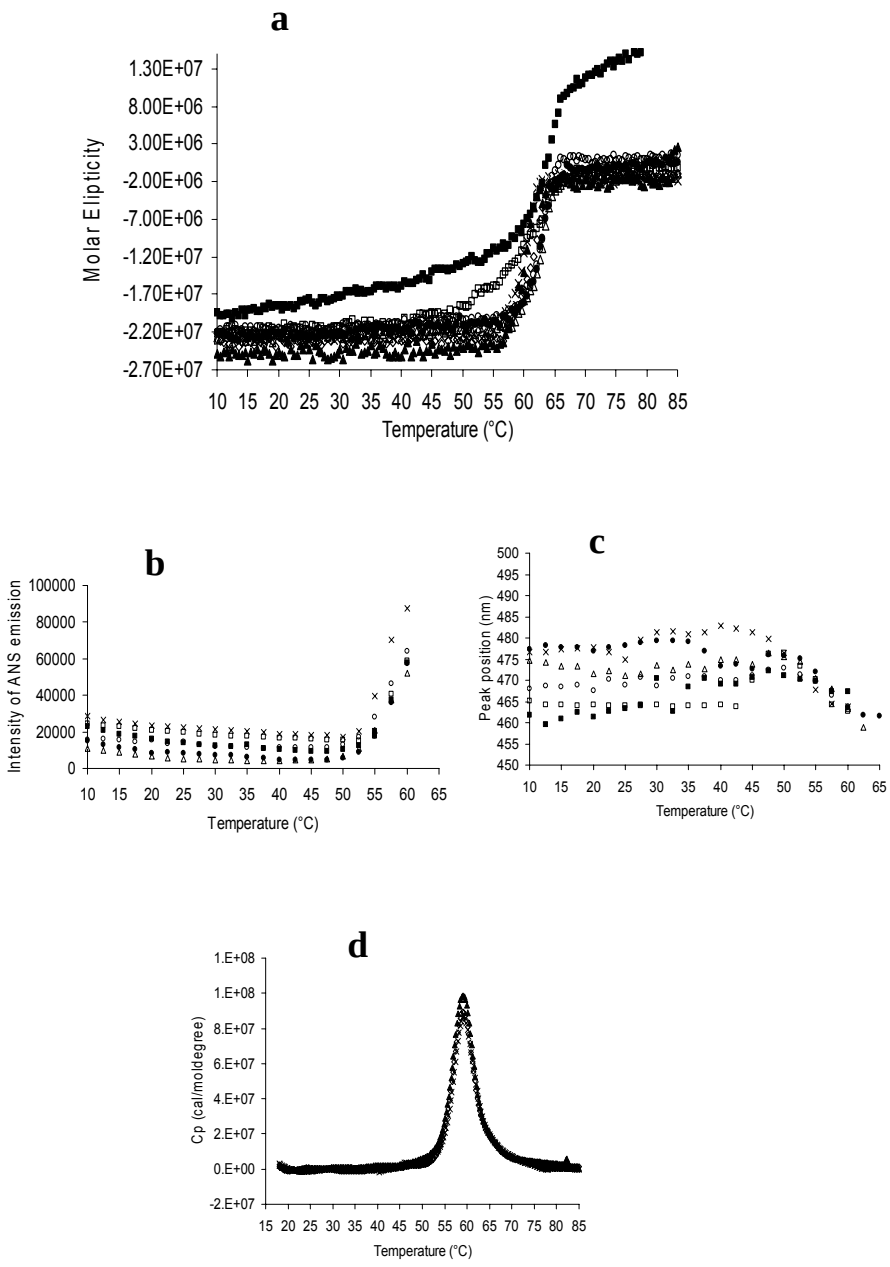

Figure 3.1. Studies of solute effects on the structural stability of toxoid A (x) in presence of 20% trehalose (□), 20% sucrose (■), 10% sorbitol (○), 10% dextrose (●), 20% glycerol (Δ), 0.05% tween 80 (▲), 0.1% pluronic F68 (◊): (a) CD signal at 208 nm; (c) ANS emission intensity (d) ANS emission peak position and (b) DSC thermogram. The thermal traces represent an average of 2 measurements, where each data point had a standard error of less than 0.5.

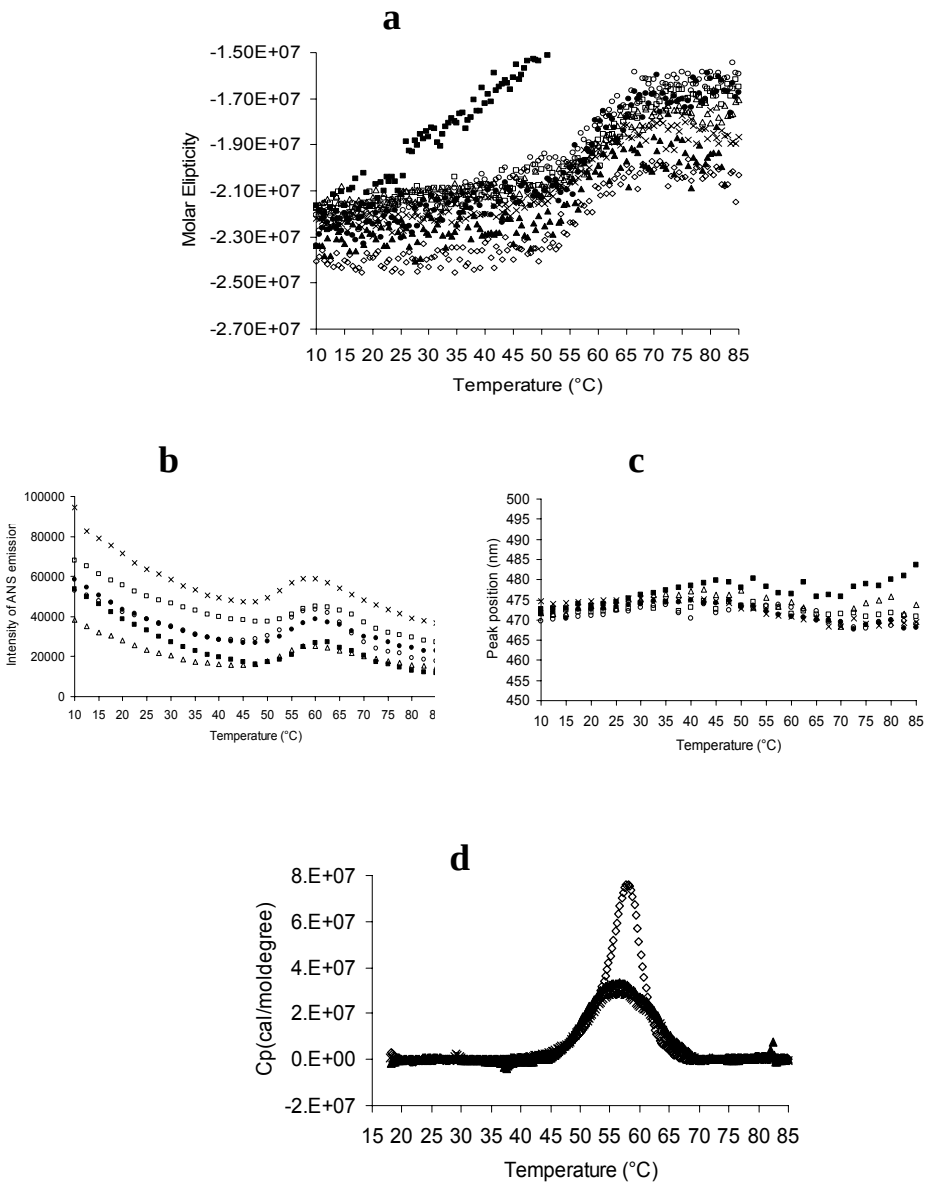

Figure 3.2. Studies of solute effects on the structural stability of toxoid B (x) in presence of 20% trehalose (□), 20% sucrose (■), 10% sorbitol (○), 10% dextrose (●), 20% glycerol (Δ), 0.05% tween 80 (▲), 0.1% pluronic F68 (◊): (a) CD signal at 208 nm; (c) ANS emission intensity (d) ANS emission peak position and (b) DSC thermograms. The thermal traces represent an average of 2 measurements. Each data point had a standard error of less than 0.5.

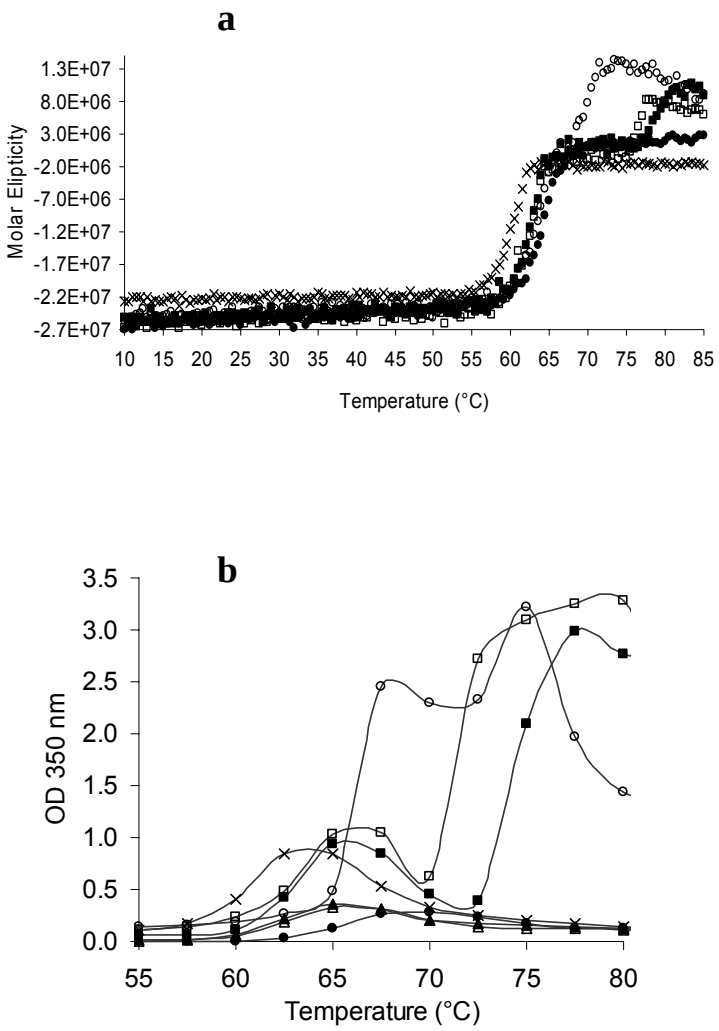

Figure 3.3. Studies of the effect of combinations of solutes on the thermal stability of toxoid A (x) in presence of 10% sorbitol and 0.05% tween 80 (□), 10% dextrose and 0.05% tween 80 (■), 10% sorbitol, 10% dextrose and 0.05% tween 80 (○), 10% dextrose and 10% sorbitol (●): (a) monitored by the CD signal at 208 nm and (b) OD 350 nm. The thermal traces represent an average of 2 measurements, in which each data point had a standard error of less than 0.05.

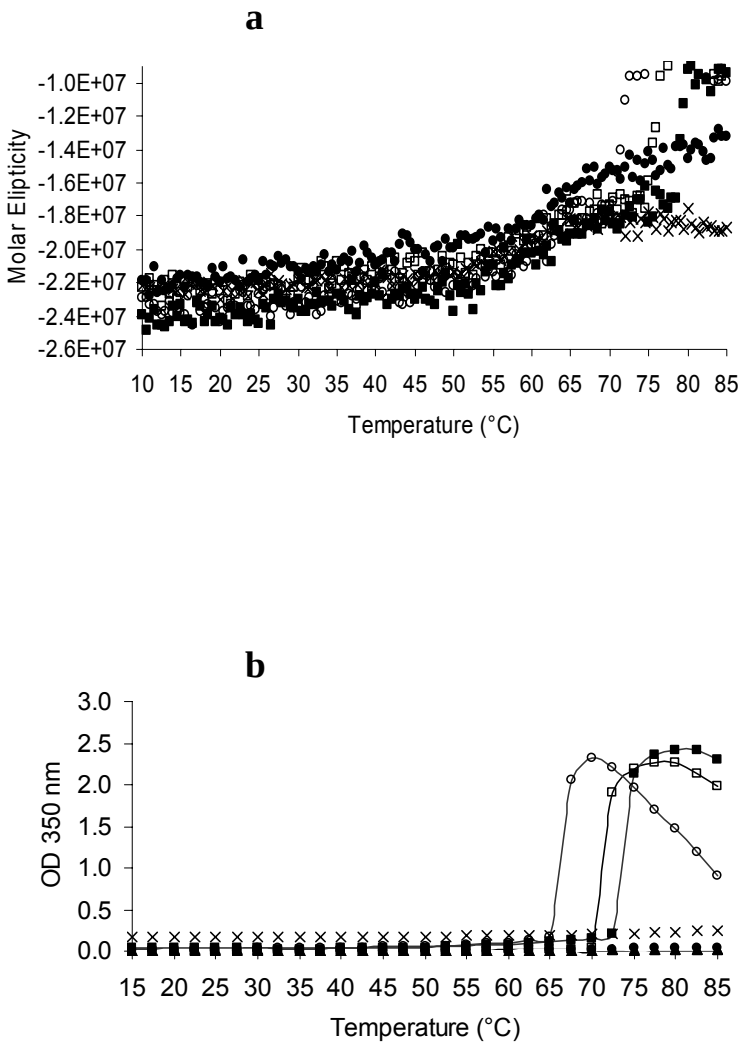

Figure 3.4. Studies of combinations of solutes and their effect on the thermal stability of toxoid B (x) in presence of 10% sorbitol and 0.05% tween 80 (□), 10% dextrose and 0.05% tween 80 (■), 10% sorbitol, 10% dextrose and 0.05% tween 80 (○), 10% dextrose and 10% sorbitol (●): (a) monitored by CD signal at 208 nm and (b) OD 350 nm. The thermal traces represent an average of 2 measurements, where each data point had standard error of less than 0.05.

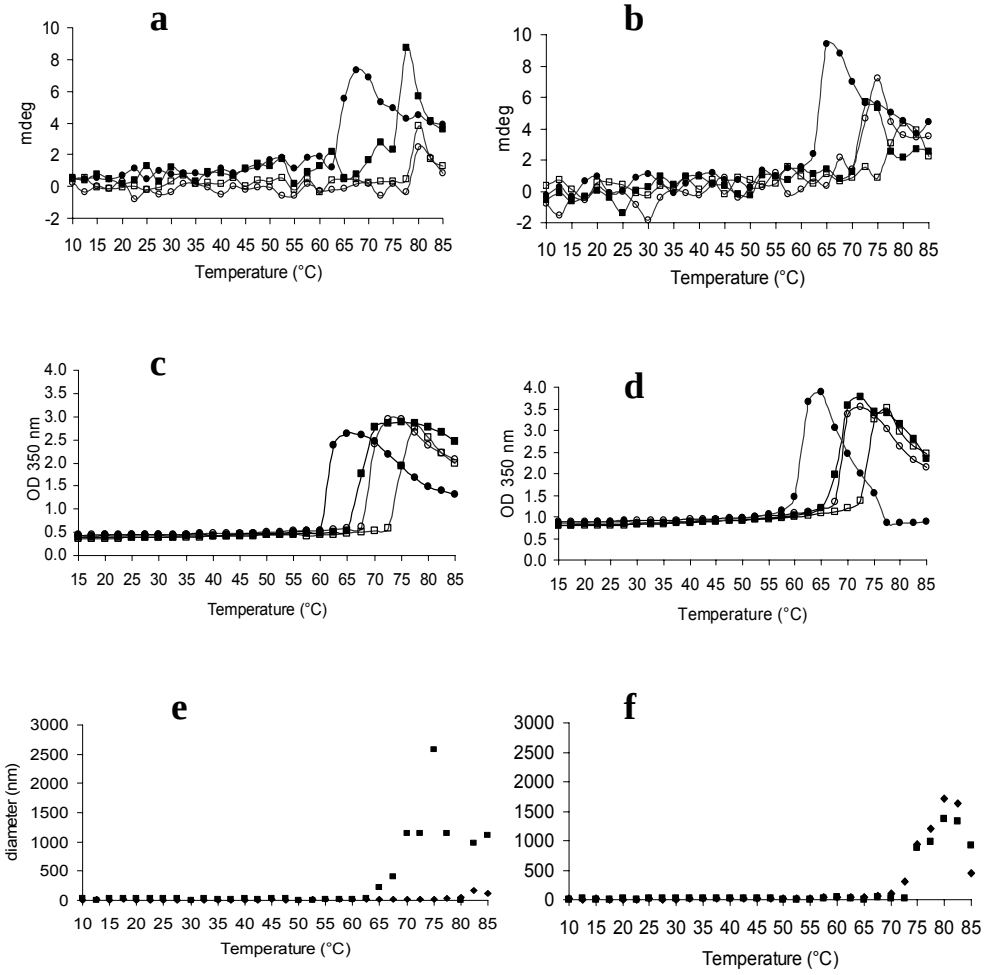

Figure 3.5. Studies of the properties of the tween 80 (□) in presence of 10% dextrose (■), 10% sorbitol (○), 10% dextrose and 10% sorbitol (●) as a function of temperature: 208 nm CD signal of 0.05% tween 80 (a) and 0.1% tween 80 (b); OD 350 nm for 0.05% tween 80 (c) and 0.1% tween 80 (d); hydrodynamic diameter MSD Number based (filled square) and Lognormal Number based (filled rhomb) for 0.05% tween 80 (e) and 0.1% tween 80 (f). Sizes of > 1μm are not accurate given the nature of DLS measurements. The thermal traces represent an average of 2 measurements, where each data point had standard error of less than 0.5.

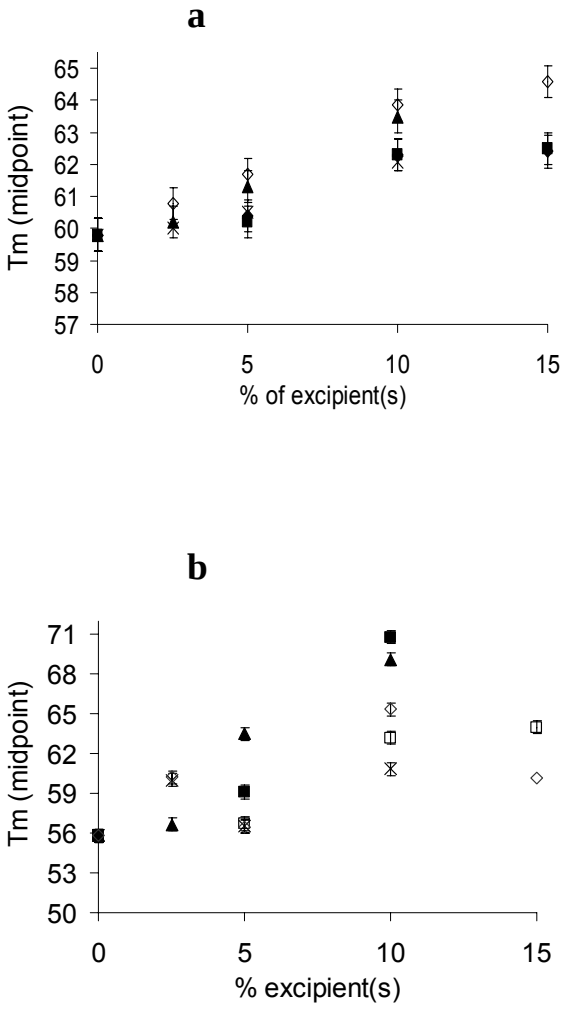

Figure 3.6. Studies of the effect of solute concentration on the midpoint of the thermal transition (Tm) monitored with CD 208 nm signal for toxoid A (a) and toxoid B (b) in presence of sorbitol and 0.05% tween 80 (♦), dextrose and 0.05% tween 80 (■), sorbitol, dextrose and 0.05% tween 80 (▲), sorbitol, dextrose and 0.1% tween 80 (x), sorbitol and dextrose (◊).

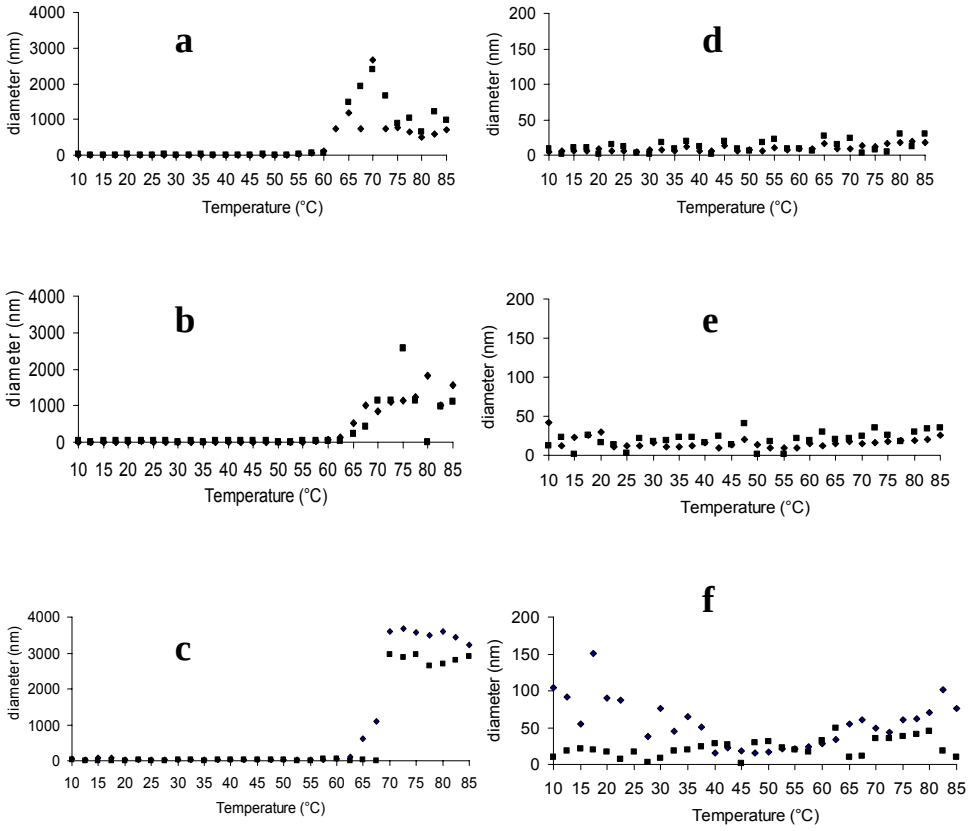

Figure 3.7. The hydrodynamic diameter as a function of temperature for toxoid A (a-c) and toxoid B (d-f) where the filled squares represent MSD number based diameter and filled rhomboids represent the lognormal number based diameter. Sizes of > 1 μm are not accurate given the nature of DLS measurements. (a,d) protein alone; (b,e) protein in presence of 10% sorbitol and 10% dextrose; (c,f) protein in presence of 10% sorbitol, 10% dextrose and 0.05% tween 80. The thermal traces represent an average of 2 measurements, where each data point had a standard error of less than 0.5

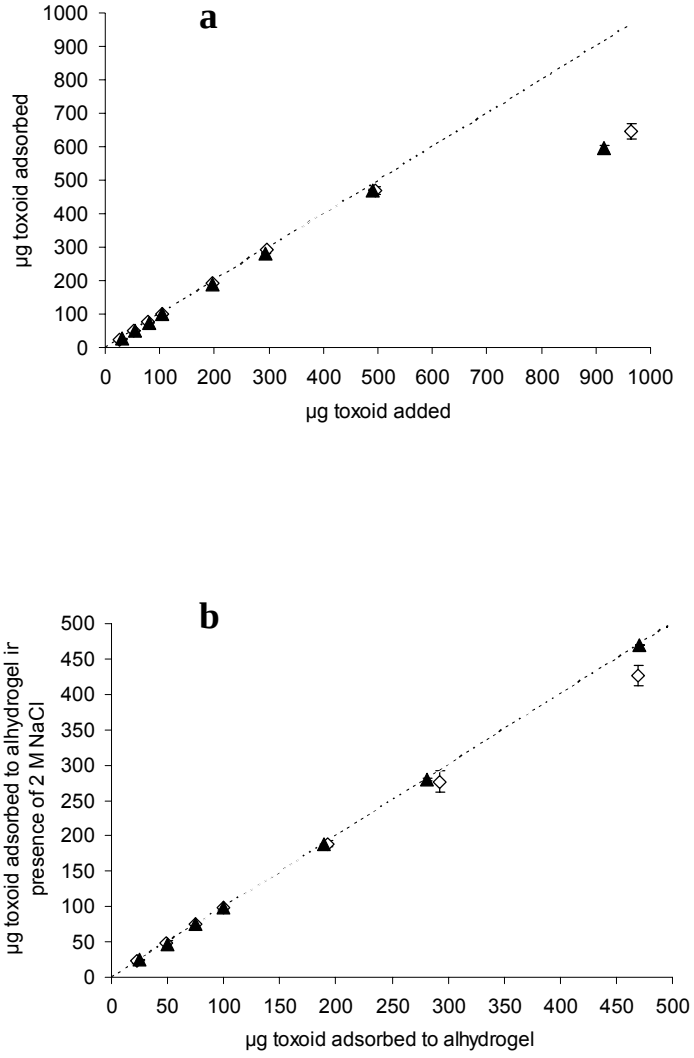

Figure 3.8. Alhydrogel® binding studies: (a) sorption isotherm and (b) desorption isotherm in presence of 2M NaCl for toxoid A (◊) and toxoid B (▲).

Table 3.1. Effect of GRAS excipients on toxoid A aggregation. Compounds which delay/prevent aggregation have positive % of aggregation inhibition values; compounds which induce aggregation have negative % of aggregation inhibition values.

Excipient Concentration	% Inhibition of aggregation	Excipient Concentration	% Inhibition of aggregation
Albumin 2.5%	103*	Glycerol 10%	88
α Cyclodextrin 2.5%	101*	2-OH propyl γ-CD 10%	81
Tween 80 - 0.1%	100*	Tween 20 - 0.05%	73
Dietanolamine 0.3M	100	Tween 80 - 0.05%	67
Sodium Citrate 0.1M	100	Aspartic Acid 0.15M	65
Sorbitol 10%	100	Tween 20 - 0.1%	64
Histidine 0.3M	100*	Pluronic F-68 0.05%	50
Sucrose 10%	100	Tween 20 - 0.01%	37
Trehalose 10%	100	Dextran Sulfate 0.04 mg/ml	30
Guanidine 0.3M	99	Brij 35 0.05%	26
Sorbitol 20%	99	Dextran Sulfate 0.004 mg/ml	16
Dextrose 20%	99	2-OH propyl γ-CD 5%	10
Dextrose 10%	99	Albumin 5%	9
Trehalose 20%	99	Brij 35 0.01%	-2
Sodium Citrate 0.2M	99	Calcium Chloride 0.015M	-7
Glycerol 20%	98	Pluronic F-68 0.01%	-14
Tween 80 - 0.01%	98	Gelatin 5%	-46
Albumin 1%	98	Malic Acid 0.15M	-52
Lactose 20%	98	Lactic Acid 0.15M	-72
Mannitol 10%	97	Gelatin 2.5%	-74
Sucrose 20%	97	Glutamic Acid 0.15M	-77
Pluronic F-68 0.1%	96	Dextran T40 0.003 mg/ml	-87
2-OH propyl ß-CD 10%	96	Glycine 0.3M	-88
2-OH propyl ß-CD 5%	96	Dextran Sulfate 0.1 mg/ml	-88
Dextran T40 0.08 mg/ml	95	Ascorbic Acid 0.15M	-99
Brij 35 0.1%	95	Proline 0.3M	-112
Dextran T40 0.03 mg/ml	93	Arginine 0.3M	-265
Lactose 10%	92	Arg/Glu 50mM each	-426
Lysine 0.3M	89*	Arg/Glu 25mM each	-463

Uncertainties are on the order of ±1%. *High initial OD 350 nm.

Table 3.2. Effect of GRAS excipients on toxoid B aggregation. Compounds which delay/prevent aggregation have positive % of aggregation inhibition values; compounds which induce aggregation have negative % of aggregation inhibition values.

Excipient Concentration	% Inhibition of aggregation	Excipient Concentration	% Inhibition of aggregation
α Cyclodextrin 2.5%	100	Dextran T40 0.03 mg/ml	35
Histidine 0.3M	100*	Dextran T40 0.08 mg/ml	25
Tween 80 - 0.1%	100	2-OH propyl γ-CD 10%	12
Tween 80 - 0.05%	100	Brij 35 0.05%	10
Albumin 1%	99	Pluronic F-68 0.05%	6
Dextrose 20%	99	Glycerol 10%	4
Albumin 5%	98	Dextran Sulfate 0.04 mg/ml	3
Sodium Citrate 0.2M	98*	Dextran Sulfate 0.004 mg/ml	2
Trehalose 20%	98	Tween 20 - 0.05%	0
Sodium Citrate 0.1M	97	2-OH propyl γ-CD 5%	-5
Sorbitol 20%	97	Tween 20 - 0.01%	-5
Sucrose 20%	96	Pluronic F-68 0.01%	-8
Dietanolamine 0.3M	96	Tween 20 - 0.1%	-13
Dextrose 10%	95	Brij 35 0.01%	-25
Sorbitol 10%	92	Glycine 0.3M	-26
Albumin 2.5%	87	Gelatin 2.5%	-36
2-OH propyl ß-CD 5%	79	Dextran Sulfate 0.1 mg/ml	-38
2-OH propyl ß-CD 10%	78	Arg/Glu 50mM each	-39
Mannitol 10%	76	Glutamic Acid 0.15M	-41
Sucrose 10%	71	Arg/Glu 25mM each	-42
Glycerol 20%	71	Aspartic Acid 0.15M	-50
Trehalose 10%	69	Gelatin 5%	-56
Pluronic F-68 0.1%	68	Proline 0.3M	-57
Brij 35 0.1%	63	Dextran T40 0.003 mg/ml	-59
Lactose 20%	52	Lactic Acid 0.15M	-80
Malic Acid 0.15M	44	Guanidine 0.3M	-96
Tween 80 - 0.01%	40	Calcium Chloride 0.015M	-141
Lactose 10%	39	Ascorbic Acid 0.15M	-223
Lysine 0.3M	37	Arginine 0.3M	-280

Uncertainties are on the order of ±1%. *High initial OD 350 nm.

Table 3.3. Effect of solutes (detergents) on the thermal stability of toxoid A and B. The thermal stability (Tm) was monitored by DSC. The Tm is the temperature corresponding to the maximum peak position of the thermal transition.

Protein	Tm (°C)
Toxoid A	59.8 ± 0.0
Toxoid A + 0.05% tween 80	59.1 ± 0.4
Toxoid A + 0.1%pluronic F68	59.1 ± 0.4
Toxoid B	55.8 ± 0.0
Toxoid B + 0.05% tween 80	56.1 ± 0.3
Toxoid B + 0.1%pluronic F68	58.0 ± 0.3

Table 3.4. Effect of excipients on the toxoid A midpoint of the thermal transition temperature (Tm). The thermal transition was monitored by the CD signal at 208 nm as a function of temperature. Each measurement was conducted in duplicate and has ~0.5°C of uncertainty.

Toxoid A in presence of excipient(s)	Tm	Tm difference
Toxoid A	59.8	0.0
20% trehalose	59.4	-0.5
20% sucrose	63.1	3.3
20% glycerol	62.4	2.6
0.1% pluronic F68	61.1	1.3
10% sorbitol	62.4	2.6
10% dextrose	62.4	2.6
0.05% Tween 80	59.9	0.0
5% sorbitol + 0.05% Tween 80	60.4	0.6
10% sorbitol + 0.05% Tween 80	62.3	2.5
15% sorbitol + 0.05% Tween 80	62.4	2.6
5% dextrose + 0.05% Tween 80	60.2	0.4
10% dextrose + 0.05% Tween 80	62.3	2.5
15% dextrose + 0.05% Tween 80	62.5	2.7
2.5% sorbitol + 2.5% dextrose + 0.05% Tween 80	60.2	0.4
5% sorbitol + 5% dextrose + 0.05% Tween 80	61.3	1.5
10% sorbitol + 10% dextrose + 0.05% Tween 80	63.5	3.7
0.1% Tween 80	59.0	-0.8
10% sorbitol + 0.1% Tween 80	60.6	0.7
10% dextrose + 0.1% Tween 80	61.5	1.7
2.5% sorbitol + 2.5% dextrose + 0.1% Tween 80	60.0	0.2
5% sorbitol + 5% dextrose + 0.1% Tween 80	60.5	0.7
10% sorbitol + 10% dextrose + 0.1% Tween 80	62.1	2.3
2.5% sorbitol + 2.5% dextrose	60.8	0.9
5% sorbitol + 5% dextrose	61.7	1.8
10% sorbitol + 10% dextrose	63.9	4.0
15% sorbitol + 15% dextrose	64.6	4.8
20% sorbitol + 20% dextrose	66.6	6.7
20% sorbitol + 10% dextrose	64.9	5.1
10% sorbitol + 20% dextrose	50.1	-9.7

Table 3.5. Effect of excipients on the toxoid B midpoint of thermal transition temperature (Tm). The thermal transition was monitored by the CD signal at 208 nm as a function of temperature. Each measurement was conducted in duplicate and has ~0.5°C of uncertainty.

Toxoid B in presence of excipient(s)	Tm	Tm difference
Toxoid B	55.8	0.0
20% trehalose	60.3	4.5
20% sucrose	-	-
20% glycerol	58.6	2.8
0.1% pluronic F68	56.2	0.4
10% sorbitol	56.6	0.8
10% dextrose	57.3	1.6
0.05% Tween 80	55.1	-0.7
5% sorbitol + 0.05% Tween 80	56.7	0.9
10% sorbitol + 0.05% Tween 80	63.2	7.4
15% sorbitol + 0.05% Tween 80	64.0	8.2
5% dextrose + 0.05% Tween 80	59.1	3.3
10% dextrose + 0.05% Tween 80	70.8	15.0
2.5% sorbitol + 2.5% dextrose + 0.05% Tween 80	56.7	0.9
5% sorbitol + 5% dextrose + 0.05% Tween 80	63.5	7.7
10% sorbitol + 10% dextrose + 0.05% Tween 80	69.1	13.3
0.1% Tween 80	53.6	-2.2
10% sorbitol + 0.1% Tween80	58.5	2.7
10% dextrose + 0.1% Tween80	62.6	6.9
2.5% sorbitol + 2.5% dextrose + 0.1% Tween 80	60.0	4.2
5% sorbitol + 5% dextrose + 0.1% Tween 80	56.5	0.8
10% sorbitol + 10% dextrose + 0.1% Tween 80	60.8	5.1
5% sorbitol + 5% dextrose	56.5	0.7
10% sorbitol + 10% dextrose	65.3	9.6
15% sorbitol + 15% dextrose	60.1	4.4
20% sorbitol + 20% dextrose	63.1	7.3
20% sorbitol + 10% dextrose	38.0	-17.8
10% sorbitol + 20% dextrose	61.2	5.5

Table 3.6. Thermal stability of toxoid A bound to Alhydrogel in the presence and absence of excipient(s) (unless specified otherwise). The thermal stability (Tm) was monitored by DSC, with the Tm indicating the temperature corresponding to the peak position of the thermal transition. The percent of toxoid bound to adjuvant was measured in each condition with an uncertainty of 1%. Each condition was studied in duplicate.

Toxoid A bound to Alhydrogel in the presence of solutes	% of bound protein	Tm	Tm differe-nce
Toxoid A not bound	-	58.8 ± 0.4	0.1
Toxoid A	96	58.7 ± 0.3	-
10% sorbitol	81	52.4 ± 1.5	-6.2
10% dextrose	86	60.6 ± 0.5	2.0
0.05% Tween 80	93	58.7 ± 0.1	0.0
10% sorbitol + 10% dextrose	77	62.9 ± 0.0	4.2
10% sorbitol + 10% dextrose + 0.05% Tween 80	81	63.1 ± 1.2	4.2
10% sorbitol + 10% dextrose + 0.1% Ttween 80	74	62.0 ± 1.3	3.3
10% sorbitol + 0.05% Tween 80	86	59.3 ± 0.8	0.7
10% dextrose + 0.05% Tween 80	85	59.5 ± 1.1	0.8

Table 3.7. The thermal stability of toxoid B bound to Alhydrogel in the presence and absence of solute(s) (unless specified otherwise). The thermal stability (Tm) was monitored by DSC. The Tm indicates the temperature corresponding to the peak position of the thermal transition. The percent of protein bound to adjuvant was measured under each condition with an uncertainty of 1%. Each condition was studied in duplicate.

Toxoid B bound to Alhydrogel in the presence of solute(s)	% of bound protein	Tm	Tm differe-nce
Toxoid B not bound	-	56.2 ± 0.4	1.4
Toxoid B	99	54.8 ± 0.5	-
10% sorbitol	92	52.5 ± 1.4	-2.2
10% dextrose	96	57.9 ± 0.2	3.1
0.05% Tween 80	96	58.2 ± 0.6	3.4
10% sorbitol + 10% dextrose	95	54.2 ± 0.9	-0.5
10% sorbitol + 10% dextrose + 0.05% Tween 80	99	58.0 ± 2.8	3.3
10% sorbitol + 10% dextrose + 0.1% Tween 80	77	58.7 ± 1.0	3.9
10% sorbitol + 0.05% Tween 80	96	58.5 ± 1.0	3.8
10% dextrose + 0.05% Tween 80	92	55.8 ± 2.5	1.1

Chapter 4:

Stability of Human Growth Hormone in Lyophilized Formulations – Effect of Protein-Excipient Interactions and Molecular Mobility

4.1. Introduction

Studies of lyophilized protein formulations have suggested that excipients able to hydrogen bond (H-bond) to proteins can enhance their stabilities. Excipients are thought to H-bond to proteins during secondary drying which leads to the preservation of protein structure and ultimately enhancement of stability during storage.[1] Although, studies have shown that some H-bonding excipients produce better protein stability than others,[2] to the best of our knowledge there are no systematic studies that establish direct relationship between the magnitude of protein-excipient interactions, structural relaxation of the dry amorphous matrix and the stability of a protein. A better understanding of the relationships between the physical characteristics of amorphous matrices and the stability of proteins in solid formulations may aid in development of more stable formulations and therefore be of significant interest.

To better understand the influence of the extent of protein-excipient interactions and molecular relaxation of any accompanying matrix on chemical (e.g. deamidation, oxidation, etc.) and physical (e.g. conformational integrity, formation of soluble and insoluble aggregates, etc.) protein stability, a model system was selected. The protein, human growth hormone (hGH), in the presence of two carbohydrates commonly used for lyophilization (sucrose and trehalose) was formulated in a 1:2 protein to excipient weight ratio. It has been shown previously that the 1:2 hGH to excipient weight ratio is effective in stabilizing the protein and prohibits crystallization of the excipients during storage.[3] Sucrose and trehalose are

structural isomers (possessing the same molecular formula but different topological structures) and contain equal numbers of H-bond donors and acceptors. In addition, sucrose forms an amorphous matrix with a lower glass transition temperature (Tg) and has a tendency to form more homogeneous mixtures with polymers compared to trehalose.[4] These similarities and differences make sucrose and trehalose ideal candidates for obtaining a better understanding of the role of protein-excipient interactions as they are related to amorphous/amorphous phase separations and structural relaxation of amorphous matrices.

The extent of interaction between hGH and excipient were measured using a number of different techniques including ISC, DSC, WSA and FTIR. The use of these methods to characterize protein solids is descried in detail elsewhere.[2,4-8] The fragility of the amorphous matrix was determined from the dependence of the glass transition temperature on scanning rate (utilizing DSC) and was used to calculate initial relaxation times employing the Vogel–Tammann–Fulcher (VTF) equation.[9] Additionally, solutions of hGH with and without sucrose and trehalose were characterized by a variety of techniques to see to what extent solution properties might be predictive of the protein in the lyophilized solid state.

4.2. Experimental methods

4.2.1. Materials

Human growth hormone (hGH) was provided by Genentech Inc. (South San Francisco, CA) in highly purified form. All reagents were of analytical grade and were purchased from Sigma (St. Louis, MO). The protein was dialyzed into potassium phosphate buffer (5 mM) at pH 7.4 using sulfur and heavy metal free Spectra/Por dialysis membranes (7) with MWCO of 10 kDa at refrigerator temperature. Subsequently, concentration of the protein to 12 mg/ml resulted in a stock solution which was diluted with buffer containing the excipient (sucrose or trehalose) to obtain solutions with the desired protein concentration. As shown in previous studies of hGH in lyophilized formulations,[10] solutions at pH of 7.4 lead to adequate stability of the protein in the solid state and therefore were selected for these studies.

4.2.1.1. Lyophilization Procedure

Lyophilization vials (5 cc Fisher brand amber glass with linerless screw tops) were filled with 1 ml of solution containing hGH and sucrose or trehalose in a 1:2 weight ratio (each vial contained 1 mg/ml of protein and 2 mg/ml of excipient). Protein or sugar alone was lyophilized under the same conditions (e.g. concentration and volume) to obtain a lyophilized solid with one component. Lyophilization was performed in a Virtis Advantage Lyophilizer (Gardiner, NY). The vials were loaded at ambient temperature and a shelf temperature of -40°C was maintained for 2 h. A chamber pressure of 60 mTorr was applied and the shelf temperature was maintained at -40°C for additional 5 h. The temperature was ramped to -35°C over 5 h and was

held at -35°C for 2 h, ramped to -10°C over 25 min and held at -10°C for 10 h. The initial steps of primary drying were performed at temperatures below Tg' (-28.5°C ± 0.3 for hGH/sucrose and -28.0°C ± 0.4 for hGH/trehalose). The Tg' values (onsets of the thermal transition) were measured with a Q100-DSC (TA instruments Inc., New Castle, DE). Approximately 20μL samples in hermetically sealed aluminum pans were frozen to -60°C and subsequently heated to 0°C at 10°C/min. Secondary drying was performed by increasing the shelf temperature to 15°C over 30 min, holding it for 3 h with a subsequent ramp to 30°C over 5 min and a hold at 30°C for 6 h. This lyophilization cycle resulted in visually elegant amorphous lyo-cakes with less than 1% residual moisture. The absence of crystallization was confirmed with powder X-ray diffraction (D8 Advance, Bruker AXS) and the moisture content was measured by a Karl-Fischer coulometric titration method[11] (DL36 KF Coulometer, Columbus, OH). Vials with lyophilized solids were placed in a glove box (Labconco), purged with Argon for 2 hours, parafilm caped and stored in desiccators to assure absence of oxygen in the headspace to minimize oxidative degradation of hGH.

4.2.2. Extent of protein-excipient interaction

4.2.2.1. Isoperibol Solution Calorimetry (ISC).

The enthalpies of dissolution of hGH/excipient physical mixtures and colyophilized samples were measured utilizing a Hart Scientific isoperibol solution calorimeter

(Model 4285). Measurements of dissolution enthalpies and calculation of the protein-excipient enthalpy of interaction are described in detail elsewhere.[8,12]

4.2.2.2. Water Sorption Analysis (WSA).

Hydration isotherms of the samples were monitored with a SGA-100 symmetric vapor sorption analyzer (VTI Corporation, Hialeah, FL). Prior to each measurement, the samples were dried in vacuum for 24 h. Water uptake by the lyophilized hGH/sugar mixture and the single component (protein or sugar) solids was measured during a stepwise increase of water partial pressure by 3% over a hydration range of 10-90% at 25°C. The humidity level was equilibrated for 5 min at each step. Interaction parameters were calculated over the range of 10-40% relative humidity (RH) based on theoretical and observed hydration isotherms as described previously.[5,6]

4.2.2.3. Differential Scanning Calorimetry (DSC).

The Tg values (onsets of the thermal transition) were measured with Q100-DSC (TA instruments Inc., New Castle, DE). Samples (2-5 mg) were sealed in aluminum pans (TA instruments) and were equilibrated for 5 min at -20°C. The temperature was modulated by ± 0.5°C every 100s while ramped to 200°C at a rate of 1°C/min. The theoretical Tg values for hGH/excipient (sucrose or trehalose) formulations were predicted employing the Gordon-Taylor equation.[4,7]

$$Tg_{12} = \frac{w_1 Tg_1 + K w_2 Tg_2}{w_1 + K w_2}$$

where Tg_{12} is a Tg of a mixture, w_1 and w_2 are the mass fractions of each component, and Tg_1 and Tg_2 are the respective glass transition temperatures. Calculation of the constant K was performed according to the Simha-Boyer rule with an assumption that the density of each component (ρ) is 1 g/cm^3.

$$K \approx \frac{Tg_1 \rho_1}{Tg_2 \rho_2}$$

4.2.2.4. Fourier Transform Infrared Spectroscopy (FTIR).

Deuterium oxide exchanged samples were prepared as reported previously[2] employing the lyophilization cycle described above. Approximately 0.5 mg of solid sample was used in diffuse reflectance (DRIFT) infrared measurement.[13] A diffuse reflectance accessory Graseby Specac Minidiff™ PN 4500 (Graseby Specac Inc., Faifield) was utilized in all measurements. Infrared spectra were recorded with a Nicolet Magna 560 ESP spectrometer (Nicolet Instrument, Madison, WI). For each spectrum, a 256-scan interferogram was collected in single beam mode with 4 cm^{-1} resolution. For the aqueous samples, native hGH (20 mg/ml in D_2O solution) was placed onto a ZnSe attenuated total reflectance (ATR) crystal (Spectra-Tech, Shelton,

CT). The exchange into D_2O was performed by lyophilization of the protein and resuspension in D_2O.

The analysis of the spectra and calculation of the predicted moisture content is described in detail elsewhere.[2] Briefly, each spectrum was corrected for scattering with Kubelka-Munk correction utilizing GRAMS/AI (7.0) software (Thermo Galactic). The amide I second derivative spectrum was area normalized. The area of the carboxylate peak at 1580 cm^{-1} was expressed as the fraction of the carboxylate band area measured for the native protein in solution and was utilized to calculate the predicted moisture content. The assumption that the moisture content of a sample with a relative carboxylate band area between 0 and 1 would fall between 0 and 12% moisture was utilized.

4.2.3. Conformational Characterization of Freeze-Dried Protein

Infrared spectra were recorded using a Nicolet Magna 560 ESP spectrometer (Nicolet Instrument, Madison, WI) in a DRIFT mode.[13] A diffuse reflectance accessory Graseby Specac Minidiff™ PN 4500 (Graseby Specac Inc., Faifield) was utilized in the measurement of a solid sample. For each spectrum, a 256-scan interferogram was collected in the single beam mode with 4 cm^{-1} resolution. The analysis of spectra and the calculation of the correlation coefficient is described in detail elsewhere.[14-17] Briefly, the amide I region of each spectrum was corrected for scattering with a Kubelka-Munk correction and the area normalized second derivative spectra were utilized to calculate a correlation coefficient (r).

$$r = \frac{\sum(x_i y_i)}{\sqrt{\sum x_i^2 \sum y_i^2}}$$

where x_i is the intensity of the spectrum for solid sample and y_i is the intensity of the spectrum of protein in solution at a wavenumber (i).

An aqueous sample (20 mg/ml in H_2O solution) was placed onto a ZnSe attenuated total reflectance (ATR) crystal (Spectra-Tech, Shelton, CT) and the spectra were recorded as described above.

4.2.4. Structural Mobility Measurements

The Tg values (onsets of the thermal transition) were measured with the Q100-DSC (TA instruments Inc., New Castle, DE) at heating rates of 2, 5, 10, 15 and 20°C/min. Indium was used to calibrate the temperature and cell constant. The average onset temperature of three measurements was reported as the glass transition temperature. The slope of the glass transition temperature changes as a function of scanning rate was used to calculate a fragility factor (m), which was further utilized for calculation of the parameters D and T_0. The parameters were utilized to estimate molecular relaxation time (τ) employing the Vogel–Tammann–Fulcher (VTF) equation.[9]

$$\tau = \tau_0 \exp\left(\frac{DT_0}{T - T_0}\right)$$

where τ_0 (~10^{-14}s) is the relaxation time at the high temperature, D is a parameter related to the fragility of material, and T_0 is the temperature at which the relaxation time tends towards infinity.

4.2.5. Stability Studies

Lyophilized samples were placed in an incubator (Precision scientific, Chicago, IL) at 50 ± 1°C for 7 months. At different storage times, the samples were reconstituted with 1 ml of water. To assure reproducibility, 2 samples were assayed at each time point. Deamidation of the hGH was monitored by reverse phase (RP) - HPLC using a method developed previously.[18] Shimadzu LC instrument (Kyoto, Japan) was equipped with a LC6A pump, SPD-6A UV detector, SCL-613 system controller and SIL-10AXL auto-injector. A Vydac C4 column with a mobile phase of 29% *n*-propanol and 71% 0.005 M Tris buffer at pH 7.5 was utilized for isocratic separation with UV detection at 220 nm. The stability data were fitted to a first order rate equation to obtain the rate constants.[19] Formation of hGH soluble aggregates was monitored by SEC-HPLC as reported earlier[10,20] and an equation describing "square root of time" kinetics[19,21] was used to fit the data. A TSK G3000SW column (Toyo Soda) with mobile phase containing 0.025 M ammonium bicarbonate at a flow rate of 1 ml/min was utilized for size exclusion separation and UV detection at 220 nm. Formation of hGH insoluble aggregates was studied by measuring the differences in concentration before and after filtration through a 0.22μm filter[3] and the data were fitted to "square root of time" kinetics.[19,21]

4.2.6. Studies of Solution Protein Formulations Before Lyophilization

4.2.6.1. High-Resolution UV Absorbance Spectroscopy.

Aggregation of hGH alone and in solution containing sucrose or trehalose was studied using an Agilent 8453 UV-visible spectrophotometer by monitoring optical density at 350 nm (OD 350 nm) every 2.5°C over the temperature range of 10 to 85°C. A 5 min incubation period (sufficient for equilibrium to be reached) was employed at each temperature point.

4.2.6.2. Dynamic Light Scattering (DLS).

The mean hydrodynamic diameter of the hGH in solution with and without excipient was analyzed with a dynamic light scattering instrument (Brookhaven Instrument Corp., Holtzille, NY). The instrument was equipped with a 50 mW diode-pumped laser (λ = 532 nm) and the scattered light was monitored at 90° to the incident beam. Autocorrelation functions were generated using a digital auto-correlator (BI-9000AT). The hydrodynamic diameter was calculated from the diffusion coefficient by the Stokes-Einstein equation using the method of cumulants (lognormal number based).

4.2.6.3. Differential Scanning Calorimetry.

Solution DSC was performed using a MicroCal VP-DSC with autosampler (MicroCal, LLC; Northampton, MA). Thermograms of hGH (1 mg/ml) alone and in the presence of excipient were obtained from 10-90°C using a scan rate of 60°C/hr. The filled cells were equilibrated for 15 min at 10°C before beginning each scan. Thermograms of the buffer alone were subtracted from each protein scan prior to analysis.

4.3. Results and disscussion

4.3.1. Extent of protein-excipient interactions

The extent of interaction between hGH and sucrose or trehalose was studied with ISC, DSC, WSA and FTIR measurements. Comparison of the theoretical and measured Tg values for the hGH/sugar formulations is shown in Figure 4.1. The measured Tg (371.5 ± 0.4 K for hGH/sucrose and 400.1 ± 0.4 K for hGH/trehalose) was significantly lower than the theoretical value (398 K for GH/sucrose and 422 K for GH/trehalose) in both the formulations. The larger difference between the theoretical and observed Tg in the case of hGH/sucrose formulation suggests that this mixture is more homogeneous and has a greater extent of interaction between the protein and sugar.

ISC studies showed that both hGH/sucrose and hGH/trehalose mixtures had exothermic enthalpies of dissolution (Figure 4.2). The dissolution of the hGH/excipient colyophilized mixture was less exothermic than the physical mixture

in both the formulations. The enthalpy of interaction (the difference of the enthalpy of dissolution between the colyophilized and physical mixtures) was almost twice as much in the case of hGH/sucrose (2.1 ± 0.1 kcal/g) compared to hGH/trehalose (1.3 ± 0.1 kcal/g) formulation. This suggests that both sugar containing formulations had detectable levels of intermolecular interactions and that the hGH/sucrose formulation had a greater extent of such interactions in agreement with the DSC results.

The WSA based interaction parameter was also much higher in case of hGH/sucrose compared to the trehalose containing formulation over the range of 10-40% RH (Figure 4.3). Surprisingly, the moisture content based on the FTIR carboxylate band area was lower than the actual moisture content in both formulations (Table 4.1). Thus, the FTIR based approach does not appear to be appropriate to measure the extent of the protein-excipient interactions in the case studied here.

DSC, ISC and WSA based evaluations of the extent of protein-excipient interactions demonstrate that hGH formulations containing sucrose and trehalose possess detectable extents of interaction between sugar and protein. In addition, the hGH/sucrose formulation displays a greater extent of interactions compared to the hGH/trehalose mixture. The latter observation probably is related to the presence of a more chemically-homogeneous mixture and/or more favorable spatial arrangement of the H-bonding groups in case of sucrose. It has been suggested that partial phase separation in protein/excipient formulations can lead to physical separation of the components.[22]

4.3.2. Structural Mobility Measurements

The slope from the dependence of the glass transition temperature on scanning rate was utilized to calculate initial relaxation times employing the Vogel–Tammann–Fulcher equation.[9] The initial relaxation time at 50°C was $4x10^{10}$s for hGH/trehalose and $6.4x10^{5}$s for the hGH/sucrose formulation. The much smaller relaxation time seen in the sucrose formulation suggests a correspondingly rapid structural relaxation. Thus, the hGH/trehalose seems to possess a more rigid matrix and slower molecular mobility at 50°C. Similar observations that trehalose/protein mixtures display slower structural relaxation than sucrose/protein formulations has been reported previously.[23]

4.3.3. Conformational Characterization of Freeze-Dried Protein

Lyophilization of hGH in the absence of sugars led to a significant perturbation of its secondary structure as shown in Figure 4.4. The correlation coefficient describes structural differences between the native protein in solution and the protein in the lyophilized state. The correlation coefficient close to 1.00 corresponds to a protein with unperturbed by lyophilization secondary structure. The correlation coefficient for the lyophilized sugarless hGH was 0.77, whereas addition of an excipient (sucrose or trehalose) led to preservation of secondary structure and a high correlation coefficient (~0.98). Both the hGH/sucrose and hGH/trehalose formulations had similar correlation coefficients.

4.3.4. Stability Studies

Both the hGH/sucrose and hGH/trehalose formulations had similar rates of deamidation and insoluble aggregate formation (Figures 4.5 and 4.6, and Table 4.2). It is important to note, however, that the stability of the lyophilized hGH in the absence of any lyo-protectants was significantly decreased. The hGH/sucrose displayed significantly less insoluble aggregates immediately after lyophilization (Figure 4.7, Tables 4.2 and 4.3). This suggests that sucrose serves as an efficient lyo- and cryo- protectant against lyophilization induced stresses that lead to formation of the insoluble protein. Moreover, the greater extent of protein-excipient interactions seen in hGH/sucrose formulation supports the hypothesis that the presence of sucrose leads to the formation of a more homogeneous mixture with a decreased extent of aggregation. In contrast, the rate of insoluble aggregate formation was much slower in the hGH/trehalose formulation (Table 4.2). This decreased rate of aggregation may be related to the slower structural relaxation (molecular mobility) of the trehalose containing matrix.

4.3.5. Studies of Protein Formulations before Lyophilization

hGH was also characterized in solution with and without trehalose or sucrose. The mean hydrodynamic diameter of hGH (~5 nm) remained unchanged despite the presence or absence of the sugars. Thermally induced unfolding of hGH was monitored with solution DSC and did not reveal any differences in behavior (Table 4.4). The thermally induced aggregation of hGH had the same onset temperature in

all formulations. The midpoint temperature of thermally induced aggregation, however, was delayed by 2-6°C in the presence of the sugars. Sucrose was more effective in delaying the midpoint temperature of the observed aggregation. The tendency of sucrose to alter the pattern of the thermally induced aggregation of hGH may be related to its ability to serve as a potent cryo- and lyo- protectant as seen in reduced insoluble aggregate formation upon lyophilization.

4.4. Summary and conclusions

hGH formulations containing sucrose demonstrated greater protein-excipient interactions and faster initial relaxation times than formulations containing trehalose. Although both formulations had similar rates of deamidation and soluble aggregate formation, the extent and rate of insoluble aggregate formation was different. The hGH/sucrose formulation demonstrated a higher rate and lower extent of insoluble aggregate formation. The decreased amount of higher order aggregate seen in the sucrose formulations can be correlated with the greater extent of the hGH-excipient interactions and the presence of a more homogeneous matrix. In contrast, the higher rate of insoluble aggregate formation in the sucrose formulation may be related to the greater molecular mobility of its amorphous matrix. Additionally, the characteristics of the protein in the presence of the sugar(s) may be related to the cryo- and lyo-protective properties of the excipient(s). Relationships between the extent of protein-excipient interactions, structural relaxation of the matrix and protein stability are

evident and can potentially serve as a basis for developing of stable lyophilized formulations.

4.5. Bibliography

1. Liao Y-H, Brown MB, Quader A, Martin GP 2002. Protective Mechanism of Stabilizing Excipients Against Dehydration in the Freeze-Drying of Proteins. Pharm. Res 19(12):1854-1861.

2. Allison SD, Chang B, Randolph TW, Carpenter JF 1999. Hydrogen bonding between sugar and protein is responsible for inhibition of dehydration-induced protein unfolding. Arch Biochem Biophys 365(2):289-298.

3. Costantino HR, Carrasquillo KG, Cordero RA, Mumenthaler M, Hsu CC, Griebenow K 1998. Effect of Excipients on the Stability and Structure of Lyophilized Recombinant Human Growth Hormone. J Pharm Sci 87(11):1412-1420.

4. Taylor LS, Zografi G 1998. Sugar-Polymer Hydrogen Bond Interactions in Lyophilized Amorphous Mixtures. J Pharm Sci 87(12):1615-1621.

5. Lopez-Diez EC, Bone S 2000. An investigation of the water-binding properties of protein + sugar systems. Physics in medicine and biology 45(12):3577-3588.

6. Lopez-Diez EC, Bone S 2004. The interaction of trypsin with trehalose: an investigation of protein preservation mechanisms. Biochimica et Biophysica Acta, 1673(3):139-148.

7. Shamblin SL, Taylor LS, Zografi G 1998. Mixing Behavior of Colyophilized Binary Systems. J Pharm Sci 87(6):694-701.

8. Souillac PO, Costantino HR, Middaugh CR, Rytting JH 2002. Investigation of protein/carbohydrate interactions in the dried state. 1. Calorimetric studies. J Pharm Sci 91(1):206-216.

9. Qiu Z, Stowell JG, Morris KR, Byrn SR, Pinal R 2005. Kinetic study of the Maillard reaction between metoclopramide hydrochloride and lactose. Int J Pharm 303(1-2):20-30.

10. Pikal MJ, Dellerman KM, Roy ML, Riggin RM 1991. The effects of formulation variables on the stability of freeze-dried human growth hormone. Pharm Res 8(4):427-436.

11. May JC, Grim E, Wheeler RM, West J 1982. Determination of residual moisture in freeze-dried viral vaccines: Karl Fischer gravimetric and thermogravimetric methodologies. J Biol Stand 10(3):249-259.

12. Souillac PO. 2000. Calorimetric and spectroscopic evaluation of protein/carbohydrate and protein/protein interactions. Ph.D. dissertation.

13. Souillac PO, Middaugh CR, Rytting JH 2002. Investigation of protein/carbohydrate interactions in the dried state. 2. Diffuse reflectance FTIR studies. Int J Pharm 235(1-2):207-218.

14. Nielsen L, Frokjaer S, Carpenter JF, Brange J 2001. Studies of the structure of insulin fibrils by Fourier transform infrared (FTIR) spectroscopy and electron microscopy. J Pharm Sci 90(1):29-37.

15. Dong A, Meyer JD, Brown JL, Manning MC, Carpenter JF 2000. Comparative fourier transform infrared and circular dichroism spectroscopic analysis of alpha1-proteinase inhibitor and ovalbumin in aqueous solution. Arch Biochem Biophys 383(1):148-155.

16. Dong A, Matsuura J, Manning MC, Carpenter JF 1998. Intermolecular beta-sheet results from trifluoroethanol-induced nonnative alpha-helical structure in beta-sheet predominant proteins: infrared and circular dichroism spectroscopic study. Arch Biochem Biophys 355(2):275-281.

17. Dong A, Prestrelski SJ, Allison SD, Carpenter JF 1995. Infrared spectroscopic studies of lyophilization- and temperature-induced protein aggregation. J Pharm Sci 84(4):415-424.

18. Riggin RM, Dorulla GK, Miner DJ 1987. A reversed-phase high-performance liquid chromatographic method for characterization of biosynthetic human growth hormone. Anal Biochem 167(1):199-209.

19. Chang L, Shepherd D, Sun J, Ouellette D, Grant KL, Tang X, Pikal MJ 2005. Mechanism of protein stabilization by sugars during freeze-drying and storage: Native structure preservation, specific interaction, and/or immobilization in a glassy matrix? J Pharm Sci 94(7):1427-1444.

20. Riggin RM, Shaar CJ, Dorulla GK, Lefeber DS, Miner DJ 1988. High-performance size-exclusion chromatographic determination of the potency of

biosynthetic human growth hormone products. Journal of Chromatography 435(2):307-318.

21. Chang L, Shepherd D, Sun J, Tang X, Pikal MJ 2005. Effect of sorbitol and residual moisture on the stability of lyophilized antibodies: Implications for the mechanism of protein stabilization in the solid state. J Pharm Sci 94(7):1445-1455.

22. Pikal MJ 1994. Freeze-drying of proteins: process, formulation, and stability. ACS Symposium Series 567 (Formulation and Delivery of Proteins and Peptides):120-133.

23. Duddu SP, Zhang G, Dal Monte PR 1997. The relationship between protein aggregation and molecular mobility below the glass transition temperature of lyophilized formulations containing a monoclonal antibody. Pharm Res 14(5):596-600.

FIGURES AND TABLES

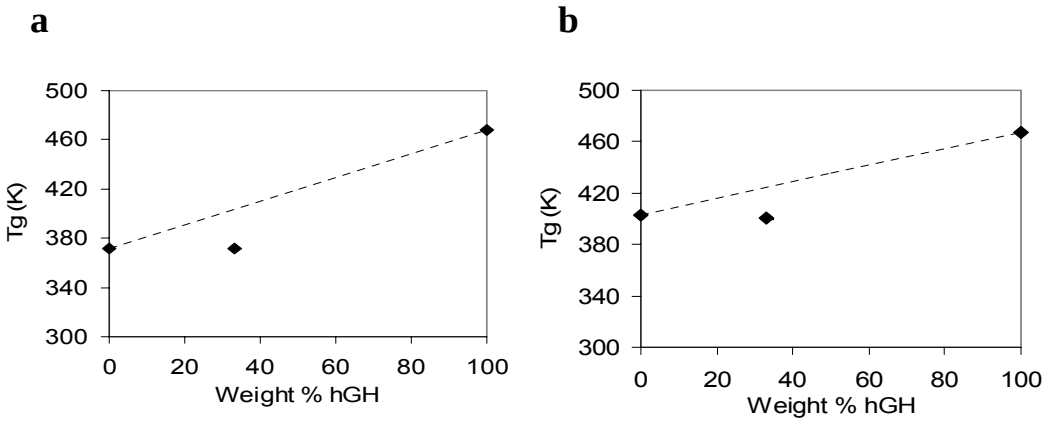

Figure 4.1. Tg values of colyophilized a) hGH/sucrose, and b) hGH/trehalose formulations as a function of composition. Measured Tg values are represented as symbols and the prediction by Gordon-Taylor equation is represented by the dotted line. Each measurement was conducted in duplicate and has a s.d. of 0.5.

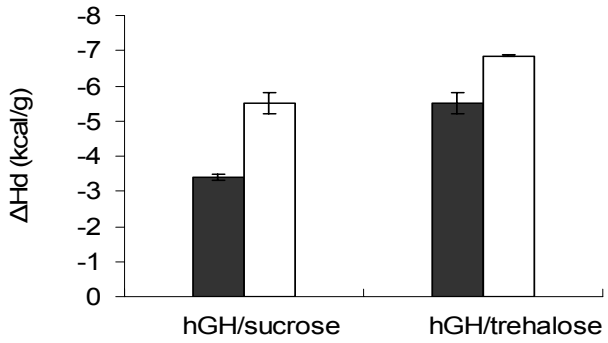

Figure 4.2. Enthalpy of dissolution for colyophilized (dark bars) and physical (white bars) mixtures of hGH in the presence of sugars.

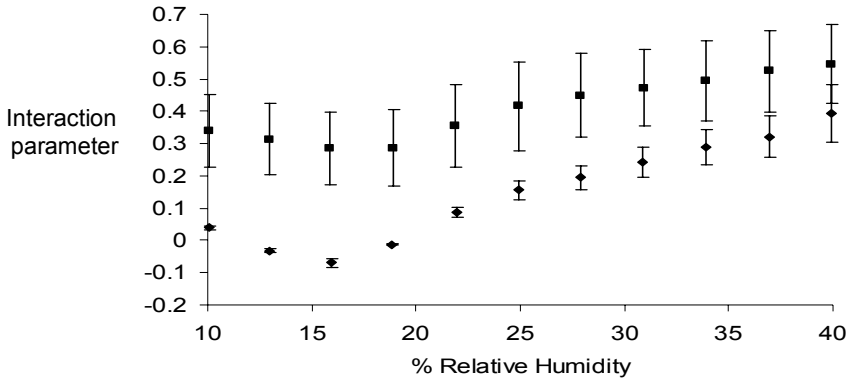

Figure 4.3. WSA-based interaction parameters for colyophilized hGH/sucrose (■) and hGH/trehalose (♦) mixtures as a function of RH.

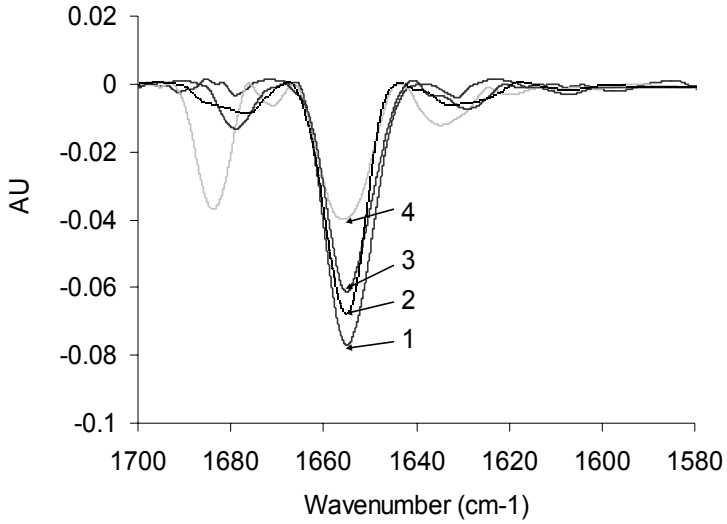

Figure 4.4. Second derivative amide I FTIR spectra of native hGH in solution (1), hGH in a lyophilized formulation with sucrose (2), trehalose (3) and dried protein alone (4).

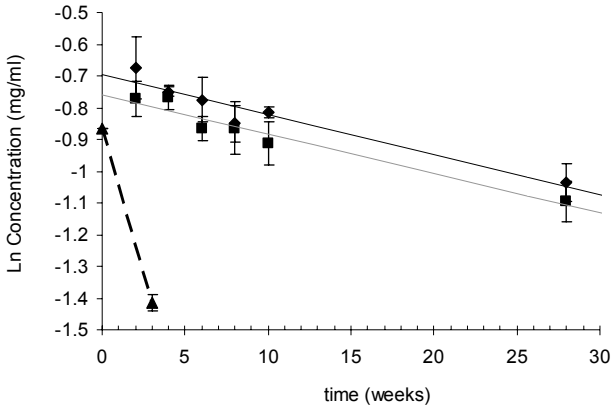

Figure 4.5. The kinetics of hGH deamidation in lyophilized formulations containing hGH alone (▲ and dotted line), hGH with sucrose (♦ and solid black line) and hGH with trehalose (■and solid grey line).

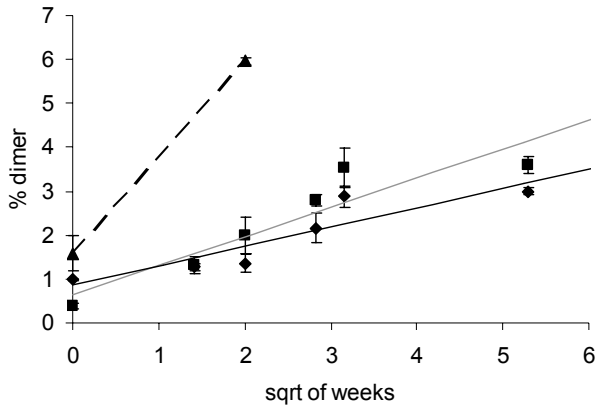

Figure 4.6. The kinetics of soluble aggregate formation in lyophilized formulations containing hGH alone (▲and dotted line), hGH with sucrose (♦ and solid black line) and hGH with trehalose (■ and solid grey line).

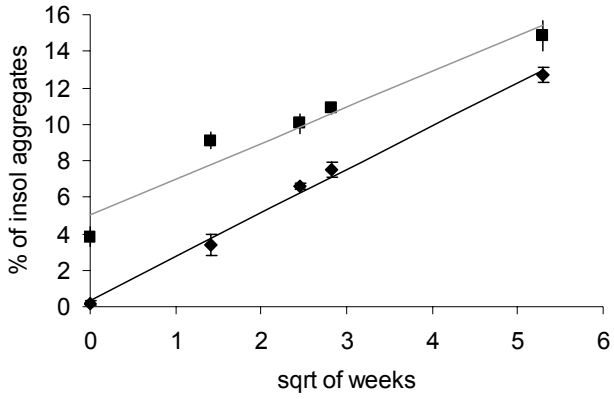

Figure 4.7. The kinetics of insoluble aggregate formation in lyophilized mixtures containing hGH with sucrose (♦ and solid black line) and hGH with trehalose (■ and solid grey line).

Table 4.1. Predicted and actual moisture content for hGH/excipient formulations. The prediction of moisture content was based on the area of the carboxilate band at 1580 cm^{-1} from FTIR measurements.

Formulation	Sample moisture (%)	Carboxylate band area	Relative carboxylate band area	Predicted moisture (%)
hGH/sucrose	1.76 ± 0.14	0.00455	0.095	1.14
hGH/trehalose	2.37 ± 0.23	0.0066	0.138	1.66

Table 4.2. Degradation rate constants for lyophilized hGH formulations.

Formulation	Deamidation rate constant (mg/ml-week)	Rate of soluble aggregates formation (%dimer/sqrtweek)	Rate of insoluble aggregate formation (% insoluble aggregate/sqrtweek)
hGH/sucrose	0.019 ± 0.01	0.4 ± 0.2	2.38 ± 0.01
hGH/trehalose	0.021 ± 0.01	0.7 ± 0.1	1.97 ± 0.06
hGH	-	2.1 ± 0.1	-

Table 4.3. Percent insoluble aggregate formed immediately after lyophilization and after 28 weeks of storage at 50°C.

Formulation	% insoluble aggregate	
	initial	after 28 weeks
hGH/sucrose	0.35 ± 0.04	12.0 ± 0.2
hGH/trehalose	5.0 ± 0.2	15.0 ± 0.2

Table 4.4. Midpoint transition temperature (Tm) for hGH in solutions with and without sugar. The Tm was monitored with solution DSC. The midpoint of the temperature of thermal aggregation was monitored by the OD at 350 nm.

	Tm	
Formulation	DSC	OD at 350 nm
hGH	79.0 ± 0.1	74.5 ± 0.6
hGH/sucrose	79.0 ± 0.2	76.2 ± 0.1
hGH/trehalose	79.1 ± 0.1	80.4 ± 1.1

Chapter 5:

Summary, Conclusions and Future Directions.

5.1. Solution protein formulations

5.1.1. Summary and conclusions

Chapters 2 and 3 describe studies directed towards physical characterization of *Clostridium difficile* (*C. difficile*) toxins, understanding the effects of formaldehyde crosslinking on the toxoids' thermal stability as well as preformulation studies of free and bound (to adjuvant) toxoids. The *C. difficile* toxins are responsible for *C. difficile*-associated disease (CDAD), which might be prevented by vaccination with formaldehyde crosslinked (inactivated) toxoids A and B.[1-5, 6-9] Since the A and B toxoids are current candidates for vaccine development, a better understanding of toxin and toxoid structure as a function of pH and temperature as well as identification of stabilizing compounds is potentially of a significant interest.

Our stepwise approach permitted the rational design of a study which generated critical information for eventual vaccine formulation. As described in Chapter 2, *C. difficile* toxins were characterized at pH 5-8 over the temperature range of 10-85°C. Structural changes and aggregation behavior were monitored with circular dichroism, intrinsic and extrinsic (ANS) fluorescence spectroscopy, turbidity measurements, high resolution UV absorbance spectroscopy and dynamic light scattering. The two toxins had similar secondary structure displaying a combination of helical, ß-sheet and unordered character. The absence of information on the middle part of the toxins (~1207 residues)[10,11] permitted the extrapolation that the

observed large overall helical content of the toxins' appears to arise from contributions from a combination of the amino-terminal domain and undefined middle parts of the proteins. It was seen that the A and B toxins are partially unfolded at low pH (5-5.5) and folded in a presumably native form at pH 6-8. These observations are consistent with previously reported pH-induced conformational changes of toxin B in early endosomes and proposed mechanisms of toxins entry into cells.[12-14]

The A and B *Clostrodial* toxins displayed some variation in properties and quite distinct thermal behavior. Toxin A possesses an apparent hydrodynamic diameter twice that of toxin B and tends to precipitate upon heating at all pH values. In contrast, toxin B only precipitated at pH 5-6 and formed soluble aggregates at pH 6.5-7.5. It was proposed that the observed dissimilarities between the toxins could be related to differences in their structure (specifically, the carboxy-terminal domain), their mechanisms of action (enterotoxicity in animals) and their enzymatic activity (velocity and extent)[15].

The combined results were mathematically analyzed to produce eigenvectors and eigenvalues which were visualized in empirical phase diagrams as described previously.[16] This showed that upon heating, toxin A at all pH values partially unfolded at ~45°C and formed insoluble aggregates at ~50°C. Toxin B partially unfolded at ~40°C, and upon heating to ~50°C precipitated at pH 5.0-6.0 and formed soluble aggregates at pH 6.5-7.5. The thermal stability of the toxins was pH dependent with the proteins more thermally stable at higher pH.

Similar studies of the formaldehyde crosslinked A and B toxoids revealed enhanced thermal stability compared to their corresponding toxins, in which secondary and tertiary structure changes as well as aggregation were delayed by about 10°C. The toxoid A displayed the following structural states: 1) partially unfolded at pH 5.5; 2) folded in the pH range 6-8; 3) a transition in form between 50 and 65°C and 4) the presence of insoluble aggregates above 50 – 65°C. The corresponding phase diagram for toxoid B provides the related structural description: 1) partially unfolded at pH 5.0; 2) folded in the pH range 5.5-7.5; 3) transition at 50-65°C; 4) insoluble aggregate appearance at pH 5.0 and 5.5 and at temperatures above 55-60°C; and 5) soluble aggregate formation over the pH range 6-7.5 at temperatures above 60°C.

These studies clearly demonstrated the stabilizing effect of formaldehyde crosslinking on the thermal stability of their corresponding toxoids. The effect of the formaldehyde crosslinking observed in our studies is consistent with previously reported favorable effects of intramolecular crosslinking on a variety of toxins with formaldehyde.[17-20]

Further studies with the goal of enhancing the physical stability of the two *Clostridium difficile* toxoids are described in Chapter 3. Screening for stabilizing compounds was performed by studying effect of 30 GRAS compounds at various concentrations and in several combinations on the behavior of the proteins. The screening was conducted in two parts. First, a high-throughput aggregation assay was used to screen for compounds which delayed or prevented aggregation of the toxoids

under stress conditions (pH 5-5.5 and 55°C). It was observed that 20% trehalose, 20% sucrose, 10% sorbitol, 10% dextrose and 20% glycerol efficiently inhibited aggregation of both of the toxoids. In the second part of the screening, these excipient and two surfactants (0.05% or 0.1% tween 80 and 0.1% pluronic F-68) were further studied for their ability to stabilize the protein's secondary and tertiary structure at pH 6.5. Monitoring CD signal changes upon heating revealed that some disaccharides (20% sucrose and/or 20% trehalose) produced an earlier onset of secondary structure change in both the toxoids. The rest of the excipients delayed the thermal transition by ~2°C. The early onset of the toxoids' secondary structure change in the presence of trehalose and/or sucrose was explained by stabilization of partially unfolded state(s) by the solutes. The possibility that the toxoids are partially unfolded upon binding to their C-terminal carbohydrate recognition sequence repeats by the polysaccharides[21] was not ruled out. It was proposed that the excipients do not strongly stabilize the structure of the toxoids by the well described preferential exclusion mechanism[22,23] but rather inhibit their aggregation by other mechanisms, such as direct blocking of the protein/protein interaction that are responsible for protein association.

The effect of a combination of the more active agents (sorbitol, dextrose and tween 80) on secondary structure was characterized by monitoring the toxoid's thermal transitions with CD and aggregation with OD 350 nm measurements. The concentration of the excipients had an approximately linear effect on the temperature of the thermal transitions. The combination of 10% dextrose and 10% sorbitol in the

presence or absence of 0.05% tween 80 delayed the midpoint of the thermal transition of both of the toxoids to a significant extent (~4°C for toxoid A and ~10°C for toxoid B), due to either a synergistic effect and/or the higher total concentration of the stabilizing compounds. These studies suggested that this particular combination of potential vaccine excipients stabilizes the toxoid's structure by both a preferential hydration mechanism and direct inhibition of protein association. The use of such stabilizing compounds could potentially increase the physical stability of the toxoids during storage.

Adjuvant binding isotherms revealed that the toxoids efficiently bind to Alhydrogel® at low concentrations and that their binding is saturated at higher protein concentration (~1 mg/ml). Desorption studies in the presence of 2 M NaCl indicated that the interaction of toxoids with Alhydrogel® was not solely electrostatic as is often observed in protein/Aluminum hydroxide interactions[24-26]. Interestingly, upon binding to Alhydrogel®, toxoid A manifests no detectable change in its thermal stability. In contrast, adjuvant bound toxoid B demonstrates a decrease of its Tm by ~1.4°C. The fraction of Alhydrogel® bound toxoid was reduced in the presence of most of such compunds suggesting that such compunds partially interfere with toxoid binding to Alhydrogel®. Finally, DSC studies of Alhydrogel® bound toxoids in the presence of selected excipients identified conditions (10% sorbitol, 10% dextrose with 0.05% or 0.1% tween 80) that produced improved physical stability of the adjuvant bound proteins.

This study of *C.difficile* toxins A and B demonstrated both similarities (secondary structure and low pH induced partial unfolding) and differences (stability and thermal behavior) between the two toxins. The superiority of the formaldehyde crosslinked toxoids' thermal stability illustrates the power and utility of this approach for vaccine development. The systematic approach to stabilizer screening resulted in the identification of excipients which improved the thermal stability of both *C. difficile* toxoids. Studies of Alhydrogel® bound toxoids in the presence of selected excipients identified conditions that produced improved physical stability of the adjuvant bound proteins. This information concerning the toxoids physical behavior under a range of conditions (temperature, solute) should be useful in the design of pharmaceutical formulations of enhanced storage stability.

5.1.2. Future directions

To select appropriate conditions for the optimum storage of *C. difficile* vaccines, it is important to perform expanded preformulation/formulation studies of the toxoids. To this end accelerated and long term storage stability studies are required. Such accelerated stability studies are usually performed at 3-4 different temperatures conditions (in this case 4, 15, 25, 35 and 40°C might be appropriate) and analyzed for presence of degradation products and biological activity at various time points. Even though Arrhenius behavior is often not observed in macromolecules, the accelerated stability studies are usually employed to provide critical information about protein behavior under different conditions (e.g. pH, concentration, solutes). Accelerated stability studies may result in the more rapid identification of conditions ultimately leading to appropriate protein stability during long term storage. Although prediction of degradation rates may not be possible, such studies are expected to reveal the presence of relevant degradation pathways. This, in turn, will provide the information necessary to select appropriate assays. Final long term stability studies employing these assays are performed under the selected storage conditions (usually refrigerator temperature) over the desired storage period (1-3 years).[27-29]

Since the administration of both toxoids simultaneously is favored to trigger the appropriate immune responses, it is desired to formulate both the A and B toxoids in a single formulation. A formulation containing two toxoids, however, may present a problem since it would be necessary to monitor the physical and chemical stability

of the individual protein during the stability studies. To permit the study of the individual protein in such a binary mixture, it would be necessary to utilize advanced methodologies of separation and analysis that are beyond the scope of this discussion.

Additionally, to increase level of toxoid-induced immune responses, the proteins must almost certainly be administered bound to aluminum salt (or some other) adjuvants. Thus, further optimization in terms of toxoid/adjuvant interactions will be necessary. Furthermore, studies of formulation containing adjuvant adsorbed toxoids will require a desorption step prior to analysis that must be developed. Alternatively, development of analytical technique capable of studying the stability of surface adsorbed protein would be necessary.

Formulation of vaccines is an extremely complex process which requires a thorough understanding of an antigen's properties, stability and activity over a wide range of conditions. Clearly, there is room for further improvements in this process.

5.2. Solid protein formulations

5.2.1. Summary and conclusions of chapter 4

To better understand the influence of the extent of protein/excipient interactions and molecular relaxation of the accompanying matrix on chemical (e.g. deamidation, oxidation, etc.) and physical (e.g. conformational integrity, formation of soluble and insoluble aggregates, etc.) protein stability, a model system containing human growth hormone (hGH) in the presence of two carbohydrates (sucrose and trehalose) was studied. Immediately after lyophilization, the extent of interactions between hGH and the sugars was measured with a number of different techniques including ISC, DSC, WSA and FTIR.[30-35] The fragility of the amorphous matrix was determined from the dependence of its glass transition temperature on scanning rate (employing DSC). This was used to calculate initial relaxation times employing the Vogel–Tammann–Fulcher (VTF) equation.[36] Additionally, hGH with and without sucrose and trehalose was characterized by a variety of techniques in solution to see to what extent solution properties might be predictive of the protein in the lyophilized solid. The physical and chemical stability of lyophilized hGH formulations during storage at 50°C for seven month was monitored by RP-HPLC, SEC-HPLC and UV. The hGH formulations containing sucrose demonstrated greater protein/excipient interactions and faster initial relaxation times compared to trehalose formulations. Although both formulations had similar chemical stability (rate of

deamidation), their physical stabilities (degree of aggregation) were different. The hGH/sucrose formulation manifested a higher rate and lower extent of insoluble aggregate formation. The decreased amount of aggregation in the sucrose formulations could be correlated with a greater extent of protein/excipient interaction and the presence of a more homogeneous mixture. In contrast, the higher rate of aggregation seen in the sucrose formulation could be directly correlated with the higher molecular mobility of the matrix. Additionally, characteristics of the protein in the presence of sugar(s) may be related to the cryo- and lyo- protective properties of the excipient(s). Relationships between the extent of protein/excipient interactions, structural relaxation of the matrix and protein stability are evident and can potentially serve as a basis for the development of more stable lyophilized formulations.

5.2.2. Future directions

Development of a solid protein formulation requires optimization of lyophilization process and consideration of the properties of the lyophilized solid. Optimization of the lyophilization process usually involves adjustment of freezing, primary drying and secondary drying steps to result in a lyocake with the desired properties. The properties of the lyocake such as residual moisture content, preservation of protein secondary structure, structural relaxation of matrix, and homogeneity of protein/excipient mixtures are usually evaluated. Numerous studies tried to correlate the properties of the lyophilized formulations with the short and long term stability of proteins. Unfortunately, most of the published results can be related only to the particular system studied and each protein formulation requires a different approach due to the unique characteristics of the individual protein.[37-39]

Recent studies showed that the preservation of protein native structure in solid formulations is directly related to long term stability of some proteins. In contrast, the molecular mobility of amorphous matrix (long range motions) poorly correlates with the stability. It was proposed that the specific interaction between stabilizer and protein might be responsible for the preservation of protein native structure and that short range motions of the amorphous matrix might influence the protein stability.[40,41]

The results of the study of the model system containing hGH and two isomeric sugars supported the importance of the protein/excipient interactions and the homogeneity of the amorphous mixture in the stability of the protein formulation

during accelerated stability studies. The clear correlation of protein stability with the extent of protein/excipient interactions and structural relaxation of matrix seen in this study with hGH may not necessarily be seen in other systems. Therefore, a study of a diverse library of proteins and excipients is required to test the consistency of our observations. Moreover, it would be of a great interest to study such formulations with a greater variety of isomeric stabilizer pairs at different ratios at the conditions of the accelerated and long term storage. A better understanding of the role and influence of each excipient in a mixture could potentially result in lyophilized formulations with significantly improved stability.

Additionally, evaluation of protein tertiary structure in solid formulation, monitoring of protein motions as well as short range mobility of an amorphous matrix in general and more in depth understanding of the specific interactions between protein and excipient will lead to a better understanding of the amorphous matrices and may result in improved stability of lyophilized protein formulations.

5.3. Bibliography

1. Kuijper EJ, Coignard B, Tull P 2006. Emergence of Clostridium difficile-associated disease in North America and Europe. Clinical Microbiology and Infection 12(Suppl. 6):2-18.

2. Drudy D, Fanning S, Kyne L 2007. Toxin A-negative, toxin B-positive Clostridium difficile. Int. J. Infect. Dis. 11(1):5-10.

3. Warny M, Pepin J, Fang A, Killgore G, Thompson A, Brazier J, Frost E, McDonald LC 2005. Toxin production by an emerging strain of Clostridium difficile associated with outbreaks of severe disease in North America and Europe. Lancet 366(9491):1079-1084.

4. Dove CH, Wang SZ, Price SB, Phelps CJ, Lyerly DM, Wilkins TD, Johnson JL 1990. Molecular characterization of the Clostridium difficile toxin A gene. Infect Immun 58(2):480-488.

5. Barroso LA, Wang SZ, Phelps CJ, Johnson JL, Wilkins TD 1990. Nucleotide sequence of Clostridium difficile toxin B gene. Nucleic Acids Res 18(13):4004.

6. Sougioultzis S, Kyne L, Drudy D, Keates S, Maroo S, Pothoulakis C, Giannasca Paul J, Lee Cynthia K, Warny M, Monath Thomas P, Kelly Ciaran P. 2005. Clostridium difficile toxoid vaccine in recurrent C. difficile-associated diarrhea. ed., United States: Gastroenterology Division, Beth Israel

Deaconess Medical Center, Harvard Medical School, Boston, Massachusetts, 02215,USA. p 764-770.

7. Torres JF, Thomas WD, Jr., Lyerly DM, Giel MA, Hill JE, Monath TP 1996. Clostridium difficile vaccine: influence of different adjuvants and routes of immunization on protective immunity in hamsters. Vaccine Research 5(3):149-162.

8. Torres JF, Lyerly DM, Hill JE, Monath TP 1995. Evaluation of formalin-inactivated Clostridium difficile vaccines administered by parenteral and mucosal routes of immunization in hamsters. Infect Immun 63(12):4619-4627.

9. Kotloff KL, Wasserman SS, Losonsky GA, Thomas W, Jr., Nichols R, Edelman R, Bridwell M, Monath TP 2001. Safety and immunogenicity of increasing doses of a Clostridium difficile toxoid vaccine administered to healthy adults. Infect Immun 69(2):988-995.

10. Reinert DJ, Jank T, Aktories K, Schulz GE 2005. Structural Basis for the Function of Clostridium difficile Toxin B. J Mol Biol 351(5):973-981.

11. Ho JGS, Greco A, Rupnik M, Ng KKS 2005. Crystal structure of receptor-binding C-terminal repeats from Clostridium difficile toxin A. Proc Natl Acad Sci U S A 102(51):18373-18378.

12. Walev I, Bhakdi SC, Hofmann F, Djonder N, Valeva A, Aktories K, Bhakdi S 2001. Delivery of proteins into living cells by reversible membrane

permeabilization with streptolysin-O. Proc Natl Acad Sci U S A 98(6):3185-3190.

13. Barth H, Pfeifer G, Hofmann F, Maier E, Benz R, Aktories K 2001. Low pH-induced formation of ion channels by Clostridium difficile toxin B in target cells. J Biol Chem 276(14):10670-10676.

14. Qa'Dan M, Spyres LM, Ballard JD 2000. pH-induced conformational changes in Clostridium difficile toxin B. Infect Immun 68(5):2470-2474.

15. Warny M, Kelly CP 2003. Pathogenicity of Clostridium difficile toxins. Microbial Pathogenesis and the Intestinal Epithelial Cell:503-524.

16. Kueltzo LA, Ersoy B, Ralston JP, Middaugh CR 2003. Derivative absorbance spectroscopy and protein phase diagrams as tools for comprehensive protein characterization: A bGCSF case study. J. Pharm. Sci. 92(9):1805-1820.

17. Paliwal R, London E 1996. Comparison of the conformation, hydrophobicity, and model membrane interactions of diphtheria toxin to those of formaldehyde-treated toxin (diphtheria toxoid): formaldehyde stabilization of the native conformation inhibits changes that allow membrane insertion. Biochemistry 35(7):2374-2379.

18. Rappuoli R, Douce G, Dougan G, Pizza M 1995. Genetic detoxification of bacterial toxins: a new approach to vaccine development. Int Arch Allergy Immunol 108(4):327-333.

19. Rappuoli R 1994. Toxin inactivation and antigen stabilization: Two different uses of formaldehyde. Vaccine 12(7):579-581.

20. Kersten G, Jiskoot W, Hazendonk T, Spiekstra A, Westdijk J, Beuvery C 1999. Characterization of diphtheria toxoid. Pharmacy and Pharmacology Communications 5(1):27-31.

21. Greco A, Ho JGS, Lin S-J, Palcic MM, Rupnik M, Ng KKS 2006. Carbohydrate recognition by Clostridium difficile toxin A. Nat. Struct. Mol. Biol. 13(5):460-461.

22. Timasheff SN 2002. Protein-solvent preferential interactions, protein hydration, and the modulation of biochemical reactions by solvent components. Proc Natl Acad Sci U S A 99(15):9721-9726.

23. Timasheff SN 1998. Control of protein stability and reactions by weakly interacting cosolvents: the simplicity of the complicated. Adv Protein Chem 51(Linkage Thermodynamics of Macromolecular Interactions):355-432.

24. Gupta RK, Rost BE, Relyveld E, Siber GR 1995. Adjuvant properties of aluminum and calcium compounds. Pharm. Biotechnol. 6:229-248.

25. Seeber SJ, White JL, Hem SL 1991. Predicting the adsorption of proteins by aluminium-containing adjuvants. Vaccine 9(3):201-203.

26. White JL, Hem SL 2000. Characterization of aluminium-containing adjuvants. Dev. Biol. (Basel, Switz.) 103(Physico-Chemical Procedures for the Characterization of Vaccines):217-228.

27. Cleland JL, Powell MF, Shire SJ 1993. The development of stable protein formulations: a close look at protein aggregation, deamidation, and oxidation. Crit Rev Ther Drug Carrier Syst 10(4):307-377.

28. Roberts CJ, Darrington RT, Whitley MB 2003. Irreversible aggregation of recombinant bovine granulocyte-colony stimulating factor (bG-CSF) and implications for predicting protein shelf life. J. Pharm. Sci. 92(5):1095-1111.

29. Roberts CJ 2003. Kinetics of Irreversible Protein Aggregation: Analysis of Extended Lumry-Eyring Models and Implications for Predicting Protein Shelf Life. J. Phys. Chem. B 107(5):1194-1207.

30. Allison SD, Chang B, Randolph TW, Carpenter JF 1999. Hydrogen bonding between sugar and protein is responsible for inhibition of dehydration-induced protein unfolding. Arch Biochem Biophys FIELD Full Journal Title:Archives of biochemistry and biophysics 365(2):289-298.

31. Lopez-Diez EC, Bone S 2000. An investigation of the water-binding properties of protein + sugar systems. Phys Med Biol FIELD Full Journal Title:Physics in medicine and biology 45(12):3577-3588.

32. Lopez-Diez EC, Bone S 2004. The interaction of trypsin with trehalose: an investigation of protein preservation mechanisms. Biochimica et Biophysica Acta, General Subjects 1673(3):139-148.

33. Shamblin SL, Taylor LS, Zografi G 1998. Mixing Behavior of Colyophilized Binary Systems. J Pharm Sci 87(6):694-701.

34. Souillac PO, Costantino HR, Middaugh CR, Rytting JH 2002. Investigation of protein/carbohydrate interactions in the dried state. 1. Calorimetric studies. J Pharm Sci 91(1):206-216.

35. Taylor LS, Zografi G 1998. Sugar-Polymer Hydrogen Bond Interactions in Lyophilized Amorphous Mixtures. J Pharm Sci 87(12):1615-1621.

36. Qiu Z, Stowell JG, Morris KR, Byrn SR, Pinal R 2005. Kinetic study of the Maillard reaction between metoclopramide hydrochloride and lactose. Int. J. Pharm. 303(1-2):20-30.

37. Hill JJ, Shalaev EY, Zografi G 2005. Thermodynamic and dynamic factors involved in the stability of native protein structure in amorphous solids in relation to levels of hydration. J. Pharm. Sci. 94(8):1636-1667.

38. Allison SD, Chang B, Randolph TW, Carpenter JF 1999. Hydrogen bonding between sugar and protein is responsible for inhibition of dehydration-induced protein unfolding. Arch Biochem Biophys 365(2):289-298.

39. Carpenter JF, Izutsu K-I, Randolph TW 1999. Freezing- and drying-induced perturbations of protein structure and mechanisms of protein protection by stabilizing additives. Drugs Pharm Sci 96(Freeze-Drying/Lyophilization of Pharmaceutical and Biological Products):123-160.

40. Chang L, Shepherd D, Sun J, Ouellette D, Grant KL, Tang X, Pikal MJ 2005. Mechanism of protein stabilization by sugars during freeze-drying and

storage: Native structure preservation, specific interaction, and/or immobilization in a glassy matrix? J. Pharm. Sci. 94(7):1427-1444.

41. Chang L, Shepherd D, Sun J, Tang X, Pikal MJ 2005. Effect of sorbitol and residual moisture on the stability of lyophilized antibodies: Implications for the mechanism of protein stabilization in the solid state. J. Pharm. Sci. 94(7):1445-1455.